Supporting Information for:

Reconstitution and substrate specificity of the thioether-forming radical *S*-adenosylmethionine enzyme in freyrasin biosynthesis

Timothy W. Precord,[†,‡] Nilkamal Mahanta,[†,‡,§] and Douglas A. Mitchell[†,‡*]

†Department of Chemistry, [‡]Carl R. Woese Institute for Genomic Biology, University of Illinois at Urbana-Champaign, Urbana, Illinois 61801, USA.
§Department of Chemistry, Indian Institute of Technology, Dharwad, Karnataka, India, 580011

* Corresponding author:
Douglas A. Mitchell (douglasm@illinois.edu), phone: 1-217-333-1345, fax: 1-217-333-0508

Table of Contents:

Experimental Methods

General materials and methods. Materials and reagents were purchased from Gold Biotechnology, Fisher Scientific, or Sigma-Aldrich unless otherwise noted. Yeast extract and tryptone were purchased from Dot Scientific. Molecular biology reagents for cloning (e.g. restriction enzymes, Q5 polymerase, T4 DNA ligase, and deoxynucleotides) were purchased from New England Biolabs. Oligonucleotide primers were obtained from Integrated DNA Technologies. DNA spin columns were purchased from Epoch Life Sciences. Sanger sequencing was performed by the Roy J. Carver Biotechnology Center (University of Illinois at Urbana-Champaign). Polymerase chain reactions were performed using a Bio-Rad S1000 thermal cycler. *Escherichia coli* DH5α and BL21(DE3) strains were used for plasmid maintenance and protein overexpression, respectively. Matrix-assisted laser desorption/ionization time-of-flight (MALDI-TOF-MS) analysis was performed using a Bruker UltrafleXtreme MALDI-TOF mass spectrometer (Bruker Daltonics) in reflector positive mode at the University of Illinois School of Chemical Sciences Mass Spectrometry Laboratory.

Molecular biology techniques. A pETDuet-1 vector was recently described for the co-expression of the freyrasin precursor peptide and the radical S-adenosylmethionine (SAM) enzyme PapB (WP_019688962.1) in which the precursor peptide (PapA) is fused to the C-terminus of maltose-binding protein (MBP) tag with a tobacco etch virus (TEV) protease-cleavage site N-terminal to the precursor sequence in the first multiple cloning site.[1] PapB was cloned into the second multiple cloning site and was untagged. This vector was used for all heterologous co-expression experiments. PapB was additionally cloned into a pET28 vector fused to the C-terminus of MBP. This vector was used for purified enzyme reconstitution assays as well as generation of the MBP-PapB-RRE (RiPP precursor peptide recognition element) construct for rescue assay *in trans*. PapA was similarly cloned into pETDuet-1 with an N-terminal MBP tag and an empty second multiple cloning site. This vector was used for purification of unmodified freyrasin precursor for *in vitro* assays. Site-directed mutagenesis (SDM) was performed using the QuikChange method (Agilent) as per the manufacturer's instructions using PfuTurbo DNA polymerase. The primers used to create each mutant are listed in **Table S2**.

Preparation of modified freyrasin and freyrasin variants. *E. coli* BL21-RIPL (DE3) cells were transformed with pETDuet_MBP-PapA_PapB or the point mutant being analyzed (*e.g.* pETDuet_MBP-PapA D6E_PapB) and streaked onto LB agar plates supplemented with 100 μg/mL ampicillin and 34 μg/mL chloramphenicol. A single colony was used to inoculate a 5 mL culture of Lysogeny Broth (LB) with the same antibiotics. After overnight growth at 37 °C, 2 L of Terrific Broth (TB) in a 4 L flat bottom flask was inoculated and grown to ~1.2 OD_{600}. At this density, cultures were cooled at 4 °C for 30 min and then expression was induced with 0.5 mM isopropyl β-D-1-thiogalactopyranoside (IPTG). The culture was shaken at 90 rpm for 16 h at room temperature. The cells were harvested by centrifugation at 4,000 × g for 15 min. Cell pellets were frozen at -20 °C until purification.

When ready for purification, harvested cells were resuspended in ice cold lysis buffer [50 mM Tris pH 7.5, 500 mM NaCl, 2.5% (*v/v*) glycerol, 0.1% (*v/v*) Triton X-100] supplemented with 3 mg/mL lysozyme and a 0.5 mL of a protease inhibitor cocktail [16 mg/mL benzamidine HCl, 6 mM phenylmethylsulfonyl fluoride, 0.1 mM leupeptin, 0.1 mM E64] The samples were subjected to three rounds of sonication for 45 s with 10 min of equilibration at 4 °C between sonication steps. The resultant lysate was centrifuged for 90 min at 17,000 × g to clear cellular debris. The supernatant was loaded onto a gravity flow column with amylose resin (pre-equilibrated in cold lysis buffer). The column was then washed with more lysis buffer followed by wash buffer [50 mM Tris pH 7.5, 500 mM NaCl, 2.5% (*v/v*) glycerol]. The MBP-fused peptide was eluted with elution buffer [50 mM Tris pH 7.5, 300 mM NaCl, 2.5% (*v/v*) glycerol, 10 mM D-maltose]. Eluted protein was collected in Amicon Ultra 15 mL centrifugal filters [30 kDa NMWL (Nominal Molecular Weight Limit)] and concentrated by centrifugation at 3,800 × g until the volume had decreased to ~1 mL. The sample was then subjected to a 10-fold buffer exchange by addition of storage buffer [50

mM, 4-(2-hydroxyethyl)-1-piperazineethanesulfonic acid (HEPES), 300 mM NaCl, 2.5% (*v*/*v*) glycerol, pH 7.4] and then further centrifuged to an appropriate concentration. The resultant aliquots were used for all proteolytic digests from which the mass spectrometry (MS) data derive.

Purification of Modified Freyrasin D6E Variant. MBP-tagged and PapB modified freyrasin D6E [referred to as D6E here] was obtained by the methods described above. The resultant isolates (~50 mg/mL) were combined with TEV protease in a 1:100 [TEV Protease : isolate] ratio by mass and were allowed to equilibrate at room temperature for 1 h to remove the MBP tag. As suggested by previous work,[1] some non-canonical proteolysis occurred at varying positions in the leader peptide [N-terminal to the following residues: G1, G(-9), N(-13), Q(-15), G(-20)]. The majority of peptide was cleaved at the G(-20) non-canonical site, one residue downstream of the canonical TEV protease cut site. Free MBP was removed by addition of acetonitrile (MeCN) to 50% (*v*/*v*) followed by freezing at -80 °C for 30 min. The sample was thawed and subjected to centrifugation at 13,000 × g for 20 minutes to remove precipitate. The supernatant was transferred to a new tube and the MeCN was evaporated by SpeedVac for 30 min. The SpeedVac step resulted in the precipitation of additional protein impurities so samples were centrifuged again at 13,000 × g for 20 min. The supernatant, containing a mixture of proteolytically digested D6E peptides, was purified from any remaining contaminants using an Agilent 1200 series HPLC fitted with a 10 × 250 mm Betasil C18 column (Fisher Scientific). A gradient elution was used with solvent A (10 mM Ammonium Bicarbonate in MilliQ water) and solvent B [10 mM Ammonium Bicarbonate in a 80:20 (MeCN : MilliQ water) solvent ratio] according to the following linear gradient combinations: at t=0 min, 10% B; t=5 min, 10% B; t=25, 40% B; t=28 min, 95% B; t=33 min, 95% B; t=38 min, 10% B. Fractions containing D6E processed at the desired position G1 were pooled, dried by SpeedVac, and lyophilized to complete dryness for later experimentation. All fractions containing incompletely processed D6E were collected, pooled, and dried by SpeedVac to remove MeCN and ammonium bicarbonate.

Pooled fractions of incompletely processed D6E were transferred into a chymotrypsin reaction buffer [0.1 M Tris HCl, 10 mM $CaCl_2$, pH 7.8] and combined with 50 µg freshly prepared chymotrypsin. Proteolysis was allowed to proceed at room temperature for 30 min and then the reaction was quenched by the addition of MeCN to 50% (*v*/*v*). Chymotrypsin was removed using the steps described above for MBP and the soluble fraction was purified using the same Betasil C18 column. The primary peptide fragment was the result of chymotrypsin digest C-terminal to Y-1, generating the desired G1 core peptide. This fraction eluted at 16.5 min in the same gradient as above and was collected, dried with SpeedVac to remove acetonitrile, and lyophilized to dryness. Mass of peptide was determined using a 5-digit analytical scale and 1.8 mg total D6E core peptide was collected for 1D and 2D NMR.

MBP-tagged PapB overexpression and purification. *E. coli* BL21(DE3) cells were co-transformed with a pET28 plasmid encoding the MBP-tagged PapB and the pSUF plasmid encoding the Fe-S cluster assembly operon.[2] Cells were grown for 24 h on LB agar plates containing 50 µg/mL kanamycin and 34 µg/mL chloramphenicol at 37 °C. Single colonies were used to inoculate 10 mL of LB containing the same concentration of antibiotics and grown at 37 °C for 16–18 h. This culture was used to inoculate 1 L of LB (5 g/L yeast extract, 10 g/L tryptone and 10 g/L NaCl) supplemented with the same concentration of antibiotics and grown to an optical density at 600 nm (OD_{600}, 1 cm path length) of 0.6 before being placed on ice for 15 min. Protein expression was then induced with the addition of 0.4 mM isopropyl β-D-1-thiogalactopyranoside (IPTG) and supplemented with 100 mg/L of ferrous ammonium sulfate [$Fe(NH_4)_2(SO_4)_2$] and 100 mg/L of cysteine. Expression was allowed to proceed for 12–16 h at 15 °C (at 100 rpm). Cells were harvested by centrifugation at 3,000 × *g* for 20 min, washed with phosphate-buffered saline (PBS; 137 mM NaCl, 2.7 mM KCl, 10 mM Na_2HPO_4, and 1.8 mM KH_2PO_4), and harvested by centrifugation. The cells were flash-frozen and stored at -80 °C.

Protein purification was performed in a Coy anaerobic chamber. All buffers were degassed and stored for 24–48 h in the anaerobic chamber before use. Cells were resuspended in lysis buffer containing 4 mg/mL lysozyme, 2 µM leupeptin, 2 µM benzamidine, and 2 µM E64. Cells were further lysed by sonication (3 ×

45 s with 10 min agitation periods at 4 °C). Insoluble debris was removed by centrifugation at 20,000 × *g* for 40 min at 4 °C. The supernatant was then applied to a lysis-buffer pre-equilibrated amylose resin (NEB; 15 mL of resin per L of initial cell culture). The column was washed with 10 column volumes (CV) of lysis buffer followed by 10 CV of wash buffer (lysis buffer with 400 mM NaCl and lacking Triton X-100). The MBP-tagged proteins were eluted using elution buffer (lysis buffer with 300 mM NaCl, 10 mM maltose, but omitting Triton X-100) until the eluent no longer contained protein detectable with the Bradford reagent. Brown colored fractions were pooled and concentrated using a 30 kDa molecular weight cut-off (MWCO) Amicon Ultra centrifugal filter (EMD Millipore). A buffer exchange with 10× volume of protein storage buffer was performed prior to final concentration, and storage under liquid nitrogen. Protein concentrations were determined using both absorbance at 280 nm (theoretical extinction coefficients were calculated using the ExPASy ProtParam tool; *http://web.expasy.org/protparam/protpar-ref.html*) and a Bradford colorimetric assay. Purity was assessed visually by analysis of Coomassie-stained SDS-PAGE gels (**Figure S1**). All wash, elution, and storage buffers were supplemented with 0.5 mM tris-(2-carboxyethyl)-phosphine (TCEP).

Ferrozine assay for PapB iron quantification. The following aqueous reagents were prepared for ferrozine assay[3]: 8 M guanidine hydrochloride, 2 M HCl, 10 mM ferrozine (3-(2-pridyl)-5,6-diphenyl-1,2,4-triazine-*p,p'*-disulfonic acid monosodium salt hydrate), and 100 mM L-ascorbic acid. To 100 µL of PapB (0–100 µM), 100 µL of 8 M guanidine hydrochloride and 100 µL of 2 M HCl were added and the solution was diluted to 550 µL. Insoluble debris was removed by centrifugation and to 500 µL of the supernatant, 30 µL of the 10 mM ferrozine solution and 30 µL of 100 mM freshly prepared L-ascorbic acid were added. The resulting solution was mixed thoroughly and incubated at room temperature for 30 min. The absorbance of the iron-ferrozine complex was recorded at 562 nm using a Cary 4000 UV-Vis-NIR spectrophotometer (Agilent). The Fe content was determined by comparing this reading to a standard curve that was generated under identical conditions using ferrous ammonium sulfate [$Fe(NH_4)_2(SO_4)_2$] with a concentration range from 0–100 µM.

Methylene blue assay for sulfide quantitation. For the methylene blue assay[4], to a 300 µL of assay solution containing PapB (0–100 µM), 1 mL of 1% (*w/v*) zinc acetate was added followed by 50 µL of 3 M NaOH. This mixture was agitated gently and 250 µL of 0.1% *N, N*-dimethyl-*p*-phenylenediamine (DMPD) monohydrochloride in 5 M HCl and 50 µL of 23 mM $FeCl_3$ in 1.2 M HCl were added. The resulting solution was mixed vigorously for 5 min intervals for a total of 30 min. The samples were then centrifuged at 16,000 × *g* for 5 min at 25 °C. The supernatant was collected and the absorbance at 670 nm was recorded using a Cary 4000 UV-Vis-NIR spectrophotometer (Agilent). The sulfide content was determined by comparing the reading to a standard curve that was generated under identical conditions using a fresh solution of sodium sulfide (Na_2S) in 0.1 M NaOH with a concentration range of 0–100 µM.

In vitro reconstitution of PapB reaction. Reaction mixtures generally included the following components: PapA precursor peptide (50 µM), purified PapB from *E. coli* heterologous expression (5 µM), SAM (1 mM) and sodium dithionite (3 mM) in reaction buffer (50 mM Tris-HCl pH 7.5). The reaction was allowed to proceed for 6–12 h at 25 °C in an anaerobic chamber. In case of the biological reductant system, flavodoxin (5 µM), flavodoxin reductase (5 µM) and NADPH (0.5 mM) was used. Reaction mixtures were desalted via C18 ZipTip (EMD Millipore) per the manufacturer's instructions, and the product was eluted using a saturated solution of sinapinic acid in 70% aq. MeCN. Reactions were monitored using MALDI-TOF-MS.

HPLC analysis. To detect 5'-deoxyadenosine, proteins in the reaction mixture were precipitated by heating at 100 °C for 2 min and the precipitate was separated by ultracentrifugation (15000 × g, 20 min). The supernatant was subjected to HPLC analysis, which was performed by using a linear gradient, at a flow rate of 1 mL/min was used with absorbance detection at 254 nm. Solvent A is water, solvent B is 100 mM K_2HPO_4, pH 6.6 and solvent C is methanol: 0 min, 100% B; 5 min, 100 % B; 12 min, 48 % A, 40 % B, 12

% C; 14 min, 50 % A, 30 % B, 20 % C; 18 min, 30 % A, 10% B, 60% C; 20 min, 100 % B; 25 min 100 % B. The column used was a Betasil LC-18 HPLC column (15 cm × 4.6 mm, 3 μM particle size).

ESI-LC-MS analysis. The compound eluting at 19.5 min was collected, the solvent was removed by speed vac (Thermo Scientific), re-dissolved in Tris-HCl buffer (50 mM, pH 7.5) and subjected to LC-MS analysis, which was performed using a Waters SYNAPT mass spectrometer outfitted with an ACQUITY UPLC, an ACQUITY Bridged Ethyl Hybrid C8 column (2.1 × 50 mm, 1.7 μm particle size, 200 Å; Waters), an ESI ion source, and a quadruple TOF detector. A gradient of 2–100% aq. MeCN with 0.1% formic acid (*v/v*) over 20 min was used. Fragmentation of the sample was performed using a collision-induced dissociation (CID) method. Data analysis was performed using mMass software.

MALDI-TOF-MS analysis. Matrix-assisted laser desorption/ionization time of flight mass spectrometry (MALDI-TOF-MS) was used to identify peptide products based upon their characteristic mass changes upon post-translational modification, protease digestion, or chemical modification. The freyrasin precursor peptide and fragments gave the strongest ion intensities when mixed with a matrix consisting of 20 mg/mL of α-cyano-4-hydroxycinnamic acid (CHCA) and 10 mg/mL 2,5-dihydroxybenzoic acid (DHB) in 60% MeCN with 0.1% formic acid. Freyrasin fragments were most readily ionized in DHB matrix that crystallized around the perimeter of the matrix spot. The samples were ionized using a Bruker Daltonics UltrafleXtreme MALDI-TOF mass spectrometer in reflector/positive mode using the default RP900_4500Da.par method and linear/positive mode using the default LP200_1000Da.par method. For analyzing PapB in vitro reaction mixtures, sinapinic acid (SA) was used as a matrix. Data processing was performed using Bruker FlexAnalysis software.

HR-ESI-MS/MS analysis. Samples for high-resolution electrospray ionization (HR-ESI) were prepared for analysis by proteolytic digest with excess trypsin or thermolysin (as indicated in figure). Samples were next desalted by ZipTip. Next, samples were diluted 1:1 into ESI mix (80% MeCN, 19% H_2O, 1% formic acid). Samples were directly infused into a ThermoFisher Scientific Orbitrap Fusion ESI-MS using an Advion TriVersa Nanomate 100. The MS was calibrated and tuned with Pierce LTQ Velos ESI Positive Ion Calibration Solution (ThermoFisher). The MS was operated using the following parameters: resolution, 100,000; isolation width (MS/MS), 2 m/z; normalized collision energy (MS/MS), 35; activation q value (MS/MS), 0.4; activation time (MS/MS), 30 ms. Fragmentation was performed using collision-induced dissociation (CID) at 35 to 70%. Data analysis was conducted using the Qualbrowser application of Xcalibur software (Thermo-Fisher Scientific).

NMR of freyrasin variant D6E. The sample was prepared by dissolving 1.8 mg (HPLC-purified and lyophilized, see above) in 300 μL of 9:1 H_2O:D_2O (99.96 atom % D; Sigma-Aldrich) supplemented with 3 μL of 1M NaOH (aq). The sample was then neutralized with 4 μL of 1 M HCl (aq). The sample was then sonicated at room temperature for 10 minutes. An additional 4 μL of 1 M HCl (aq) was added in order to improve amide proton signal in the NMR spectra. The sample was loaded into a D_2O-lock Shigemi tube and NMR spectra were recorded on an Agilent VNMRS 750 MHz narrow bore magnet spectrometer equipped with a 5 mm triple resonance (1H-13C-15N) triaxial gradient probe and pulse-shaping capabilities. Samples were held at 25˚C during acquisition. Standard Varian pulse sequences were used for each of the following experiments: 1H, 1H-1H TOCSY (70 ms mixing time), and 1H-1H NOESY (350 ms mixing time). Solvent suppression by presaturation (PRESAT) was employed for 1H, 1H-1H NOESY and 1H-1H TOCSY experiments. Spectra were recorded with VNMRJ 3.2A. Spectra were imported into MestReNova 8.1.1, phased and baseline corrected.

Table S1: ^{1}H Chemical shift values of assigned freyrasin D6E residues. Resonances are labeled based on their position within the indicated amino acid, i.e. H-C_α denotes the alpha carbon proton. Unassigned protons are denoted by "*" and bolded ppm values indicate aromatic proton resonances (for Tyr9, Phe10, and Phe25). These values are in good agreement with that acquired for wt freyrasin.[1]

Residue	NH	H-C_α	H-C_β	H-C_γ	H-C_δ	H-C_ε	H-C_ζ
Gly_1	*	-	-	-	-	-	
Cys_2	8.56	4.78	3.04, 3.09				
Ser_3	8.63	4.39	3.81, 3.92				
Ala_4	8.17	4.13	1.28				
Asn_5	8.29	4.37	2.66, 2.72				
Glu_6	7.86	4.14	1.78, 2.11	3.64			
Ala_7	7.96	4.05	1.13				
Cys_8	7.94	4.42	2.78, 2.83				
Tyr_9	8.55	4.44	3.09, 3.02	-	**6.64**	**6.91**	
Phe_{10}	7.82	4.37	2.86	-	**6.78**	**7.48**	**7.46**
Cys_{11}	8.40	4.27	2.77, 2.02				
Asp_{12}	8.49	4.41	3.77				
Thr_{13}	8.17	4.13	4.00	1.04			
Arg_{14}	7.79	4.25	1.60, 1.71	1.39, 1.43	3.03	*	
Asp_{15}	8.32	4.59	3.61				
Asn_{16}	8.43	4.58	2.53, 2.66				
Cys_{17}	7.91	4.57	2.91				
Lys_{18}	8.41	4.06	1.68	1.25, 1.29	*	*	
Ala_{19}	8.13	4.15	1.25				
Cys_{20}	8.16	4.32	2.68, 2.96				
Asp_{21}	8.60	4.51	3.81				
Ala_{22}	8.38	3.96	1.27				
Ser_{23}	7.70	4.31	3.68				
Asp_{24}	7.84	4.62	3.62				
Phe_{25}	7.91	4.48	2.78, 2.95		**6.69**	**7.45**	**7.42**
Cys_{26}	8.06	4.46	2.66, 2.89				
Ile_{27}	8.23	3.90	1.75	1.03	0.79		
Lys_{28}	8.14	4.12	1.70, 1.77	1.54	*	*	
Ser_{29}	8.30	4.18	3.76, 3.79				
Asp_{30}	8.37	4.68	3.75				
Thr_{31}	7.93	4.29	4.22	1.00			

Overlapping amide regions: Lys_{18}, Cys_{11}, Ala_{22}, Asp_{30}; Ala_4, Thr_{13}, Cys_{20}, Lys_{28}; Cys_8, Thr_{31}, Phe_{25}, Cys_{17}.

Table S2: Oligonucleotide primers used in this study. Primers used to generate point mutations through site-directed mutagenesis (SDM) via primer overlap. Codon used for mutagenesis is in lowercase. An asterisk (*) represents a stop codon and negative values indicate position within the PapA leader peptide counting backwards from Gly1. Vector map for plasmid backbone is shown in **Figure S38**.

Primer	Nucleotide sequence (5' to 3')
PapA_C2A_for	GCGCTTATGGTgccTCAGCCAATGATGCTTGCTATTTCTGT
PapA_C2A_rev	TCATTGGCTGAggcACCATAAGCGCGAATTGGTTCTTTAAC
PapA_C8A_for	CCAATGATGCTgccTATTTCTGTGATACTAGAGATAACTGC
PapA_C8A_rev	TCACAGAAATAggcAGCATCATTGGCTGAGCAACCATAAGC
PapA_C11A_for	CTTGCTATTTCgccGATACTAGAGATAACTGCAAAGCATGT
PapA_C11A_rev	TCTCTAGTATCggcGAAATAGCAAGCATCATTGGCTGAGCA
PapA_C17A_for	CTAGAGATAACgccAAAGCATGTGATGCAAGTGATTTTTGT
PapA_C17A_rev	TCACATGCTTTggcGTTATCTCTAGTATCACAGAAATAGCA
PapA_C20A_for	ACTGCAAAGCAgccGATGCAAGTGATTTTTGTATCAAATCG
PapA_C20A_rev	TCACTTGCATCggcTGCTTTGCAGTTATCTCTAGTATCACA
PapA_C26A_for	CAAGTGATTTTgccATCAAATCGGATACCTAGGCGGCCGCA
PapA_C26A_rev	TCCGATTTGATggcAAAATCACTTGCATCACATGCTTTGCA
PapA_D6A_for	GCTCAGCCAATgccGCTTGCTATTTCTGTGATACTAGAGAT
PapA_D6A_rev	AAATAGCAAGCggcATTGGCTGAGCAACCATAAGCGCGAAT
PapA_D12A_for	GCTATTTCTGTgccACTAGAGATAACTGCAAAGCATGTGAT
PapA_D12A_rev	TTATCTCTAGTggcACAGAAATAGCAAGCATCATTGGCTGA
PapA_D15A_for	GTGATACTAGAgccAACTGCAAAGCATGTGATGCAAGTGAT
PapA_D15A_rev	GCTTTGCAGTTggcTCTAGTATCACAGAAATAGCAAGCATC
PapA_D21A_for	GCAAAGCATGTgccGCAAGTGATTTTTGTATCAAATCGGAT
PapA_D21A_rev	AAATCACTTGCggcACATGCTTTGCAGTTATCTCTAGTATC
PapA_D24A_for	GTGATGCAAGTgccTTTTGTATCAAATCGGATACCTAGGCG
PapA_D24A_rev	TTGATACAAAAggcACTTGCATCACATGCTTTGCAGTTATC
PapA_D30A_for	GTATCAAATCGgccACCTAGGCGGCCGCAGCATAATGCTTA
PapA_D30A_rev	GCCGCCTAGGTggcCGATTTGATACAAAAATCACTTGCATC
PapA_D6E_for	GCTCAGCCAATgaaGCTTGCTATTTCTGTGATACTAGAGAT
PapA_D6E_rev	AAATAGCAAGCttcATTGGCTGAGCAACCATAAGCGCGAAT

PapA_D12E_for	GCTATTTCTGTgaaACTAGAGATAACTGCAAAGCATGTGAT
PapA_D12E_rev	TTATCTCTAGTttcACAGAAATAGCAAGCATCATTGGCTGA
PapA_D15E_for	GTGATACTAGAgaaAACTGCAAAGCATGTGATGCAAGTGAT
PapA_D15E_rev	GCTTTGCAGTTttcTCTAGTATCACAGAAATAGCAAGCATC
PapA_D21E_for	GCAAAGCATGTgaaGCAAGTGATTTTTGTATCAAATCGGAT
PapA_D21E_rev	AAATCACTTGCttcACATGCTTTGCAGTTATCTCTAGTATC
PapA_D24E_for	GTGATGCAAGTgaaTTTTGTATCAAATCGGATACCTAGGCG
PapA_D24E_rev	TTGATACAAAAttcACTTGCATCACATGCTTTGCAGTTATC
PapA_D30E_for	GTATCAAATCGgaaACCTAGGCGGCCGCAGCATAATGCTTA
PapA_D30E_rev	GCCGCCTAGGTttcCGATTTGATACAAAAATCACTTGCATC
PapA_D6N_for	GCTCAGCCAATaacGCTTGCTATTTCTGTGATACTAGAGAT
PapA_D6N_rev	AAATAGCAAGCgttATTGGCTGAGCAACCATAAGCGCGAAT
PapA_D12N_for	GCTATTTCTGTaacACTAGAGATAACTGCAAAGCATGTGAT
PapA_D12N_rev	TTATCTCTAGTgttACAGAAATAGCAAGCATCATTGGCTGA
PapA_D15N_for	GTGATACTAGAaacAACTGCAAAGCATGTGATGCAAGTGAT
PapA_D15N_rev	GCTTTGCAGTTgttTCTAGTATCACAGAAATAGCAAGCATC
PapA_D21N_for	GCAAAGCATGTaacGCAAGTGATTTTTGTATCAAATCGGAT
PapA_D21N_rev	AAATCACTTGCgttACATGCTTTGCAGTTATCTCTAGTATC
PapA_D24N_for	GTGATGCAAGTaacTTTTGTATCAAATCGGATACCTAGGCG
PapA_D24N_rev	TTGATACAAAAgttACTTGCATCACATGCTTTGCAGTTATC
PapA_D30N_for	GTATCAAATCGaacACCTAGGCGGCCGCAGCATAATGCTTA
PapA_D30N_rev	GCCGCCTAGGTgttCGATTTGATACAAAAATCACTTGCATC
PapA_ring1exp_for	TGGTTGCTCAgccGCCAATGATGCTTGCTATTTCTGTGAT
PapA_ring1exp_rev	CATCATTGGCggcTGAGCAACCATAAGCGCGAATTGGTTC
PapA_ring1cont_for	TGGTTGCTCAAATGATGCTTGCTATTTCTGTGATACT
PapA_ring1cont_rev	AAGCATCATTTGAGCAACCATAAGCGCGAATTGGTTC
PapA_C8*_for	CCAATGATGCTtaaTATTTCTGTGATACTAGAGATAACTGC
PapA_C8*_rev	TCACAGAAATAttaAGCATCATTGGCTGAGCAACCATAAGC
PapA_L(-17A)_for	CCGGATCCATGgccAAGCAAATCAATGTTATTGCAGGAGTT
PapA_L(-17A)_rev	TTGATTTGCTTggcCATGGATCCGGATTGGAAGTACAGGTT

PapA_K(-16A)_for	GATCCATGTTGgccCAAATCAATGTTATTGCAGGAGTTAAA
PapA_K(-16A)_rev	ACATTGATTTGggcCAACATGGATCCGGATTGGAAGTACAG
PapA_Q(-15A)_for	CCATGTTGAAGgccATCAATGTTATTGCAGGAGTTAAAGAA
PapA_Q(-15A)_rev	ATAACATTGATggcCTTCAACATGGATCCGGATTGGAAGTA
PapA_(I-14A)_for	TGTTGAAGCAAgccAATGTTATTGCAGGAGTTAAAGAACCA
PapA_(I-14A)_rev	GCAATAACATTggcTTGCTTCAACATGGATCCGGATTGGAA
PapA_(N-13A)_for	TGAAGCAAATCgccGTTATTGCAGGAGTTAAAGAACCAATT
PapA_(N-13A)_rev	CCTGCAATAACggcGATTTGCTTCAACATGGATCCGGATTG
PapA_(V-12A)_for	AGCAAATCAATgccATTGCAGGAGTTAAAGAACCAATTCGC
PapA_(V-12A)_rev	ACTCCTGCAATggcATTGATTTGCTTCAACATGGATCCGGA
PapA_(I-11A)_for	AAATCAATGTTgccGCAGGAGTTAAAGAACCAATTCGCGCT
PapA_(I-11A)_rev	TTAACTCCTGCggcAACATTGATTTGCTTCAACATGGATCC
PapB_T86*_for	ACATTATTGCCtaaGATGCTAACATATCAGATGTTGAAAAA
PapB_T86*_rev	ATGTTAGCATCttaGGCAATAATGTATGCTTCCTTCATATT
PapB_Δ1-85_for	CGGCCACGCGATCGCTGACGTCACAGATGCTAACATATCAGATG
PapB_Δ1-85_rev	CATCTGATATGTTAGCATCTGTGACGTCAGCGATCGCGTGGCCG
PapB_SalI_for	AAGTCGACAATGGCTAATCTGATTCAGGATAGAGAAG
PapB_HindIII_rev	AAAAAGCTTCTAACCAAAAAGGATGCTTCTTTGTTC
PapB_C119A_for	TGGTGCAAGAAgctAACCTTAGATGTACTTACTGTTATGGG
PapB_C119A_rev	CATCTAAGGTTagcTTCTTGCACCATAAATAAGGTCAGAGA
PapB_C123A_for	GTAACCTTAGAgctACTTACTGTTATGGGGAGGAAGGAGAA
PapB_C123A_rev	TAACAGTAAGTagcTCTAAGGTTACATTCTTGCACCATAAA
PapB_C126A_for	GATGTACTTACgctTATGGGGAGGAAGGAGAATATAATCAA
PapB_C126A_rev	TCCTCCCCATAagcGTAAGTACATCTAAGGTTACATTCTTG

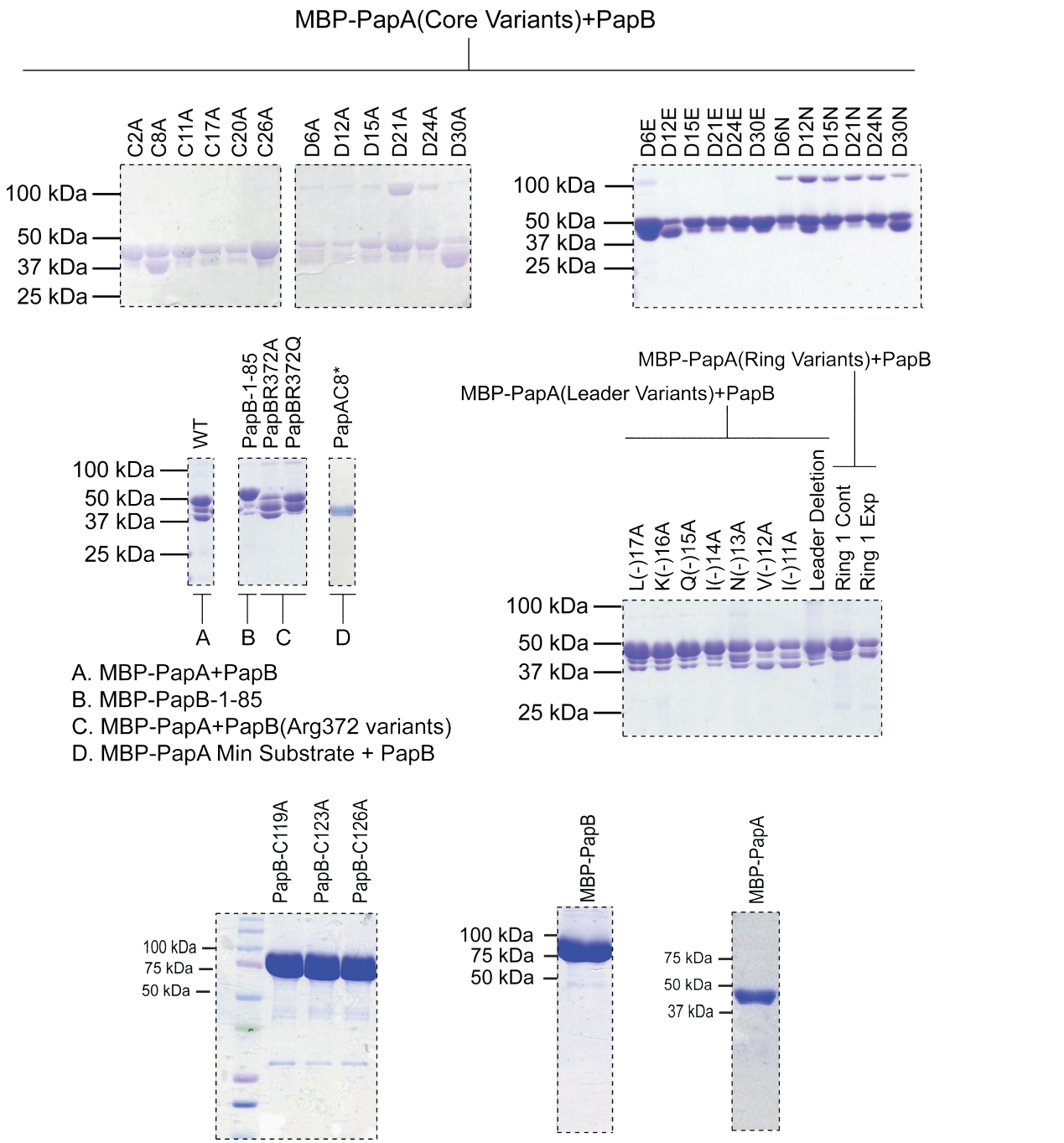

Figure S1: SDS-PAGE analysis of proteins used in this study. MBP-tagged freyrasin variants constructs are visible as the darkest bands ~50 kDa. The band below the MBP-freyrasin fusion (~45 kDa) is proteolyzed MBP, a typical consequence of MBP-peptide fusion overexpression in *E. coli*.

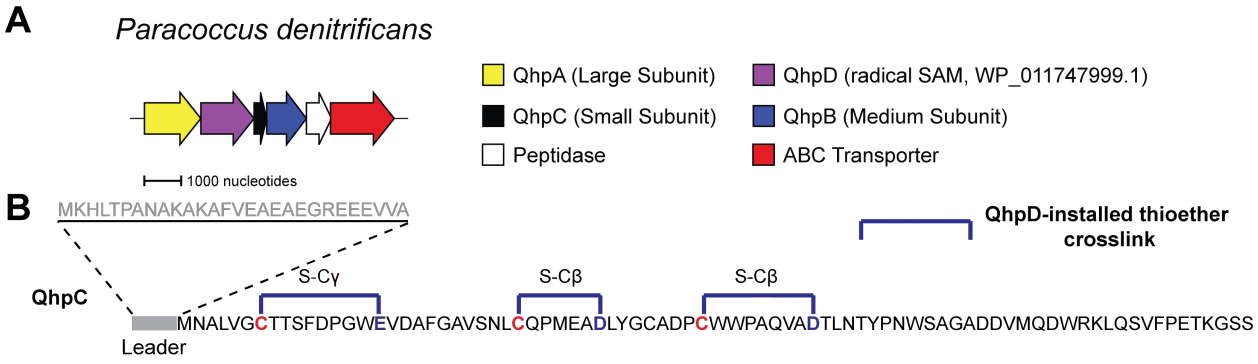

C

```
SDJ52620.1         1 MRRCSASSMRRSGDAMGAL------TLIRHNAHRV-DVDGHAMLMHVPTT     43
                                    |..|      .||..:.::: :||......:|.|.
WP_019688962.1     1 ---------------MANLIQDREDELIHFHPYKLFEVDSKTFFYNVVTN     35

SDJ52620.1        44 SLFELDGVARDVYDLFRRAPAVDPDLMRAELGPRHGPDTLSECLQSFL-A     92
                     ::||:|.:..|:.    .:...:.:.:..:|..|:....:.|.:|:.. |
WP_019688962.1    36 AIFEIDSLIIDIL----HSKGKNEEHVVKDLAERYELSQVREAIQNMKEA     81

SDJ52620.1        93 LDILRNAEAADIPRPVV---KVEEIPLSTIILNVNTGCNLACTYCYKEDL    139
                     ..|..:|..:|:.:..:   ......||::.|.:...|||.|||||.|:.
WP_019688962.1    82 YIIATDANISDVEKMGILDNSQRVFKLSSLTLFMVQECNLRCTYCYGEEG    131

SDJ52620.1       140 TTPAKGQKMGFETAKASFELLLKQAHARDRVNVVFFGGEPLSNMPLIREL    189
                     ....|| ||..|.|:::.:.|::|:...:::|:.|||||||.|.|||:|.
WP_019688962.1   132 EYNQKG-KMTSEIARSAVDFLIQQSGEIEQLNITFFGGEPLLNFPLIQET    180

SDJ52620.1       190 VAYARPRAAELGKAVDFSLTTNATLLTPELVDWFDAHRFALTVSMDGPKA    239
                     |.|...::....|...||:|||.||:||::.::|..|.||:..|:||.:.
WP_019688962.1   181 VQYVHEQSEIHNKKFSFSITTNGTLITPKIKNFFYKHHFAVQTSIDGDEK    230

SDJ52620.1       240 LHDANRKTVGGKGTYDLVARNVRMLLSRYRSRPVGGRVTLTRGVTDVIGI    289
                     .|:.||...||:|:|||:.:....:.:   .|.:|.|.|:|....|:...
WP_019688962.1   231 THNFNRFFKGGQGSYDLLLKRTEEMRN---DRKIGARGTVTPAELDLSKS    277

SDJ52620.1       290 HDHLKNELGFHEVGFGPATSGPIAVFNLDAEALKRAFEDMKTLGRRYVEA    339
                     .|||. :|||.::...|      |:::|..:.....::|..|..::.|.
WP_019688962.1   278 FDHLV-KLGFRKIYLSP------ALYSLSDDHYDTLSKEMVKLVEQFREL    320

SDJ52620.1       340 ACRGENI---GFSNMHQLLTDIAQGTKKAVPCGAGLGMLAVDKDGELHLC    386
                     ..|.:.:   ..||:..:|:.|..|..:...||||....|||..|.|.|
WP_019688962.1   321 LEREDYVTAKKMSNVLGMLSKIHSGGPRIHFCGAGTNAAAVDVRGNLFPC    370

SDJ52620.1       387 HRFVGSNQPTYGNVAKGIDIPKLAGFIETAQDRSAYGCKTCRIRSICAGG    436
                     |||||.::.:.||:.....:.|...|||.:..|:...|..|..:::|.||
WP_019688962.1   371 HRFVGEDECSIGNLFDEDPLSKQYNFIENSTVRNRTTCSKCWAKNLCGGG    420

SDJ52620.1       437 CYHESYARQGDPFAPVWHYCDLMRDWVDFGIESYVRIMQANPSFFRSQLE    486
                     |:.|::|..|:...||...|.:.:::::..|..|:::.|...|....
WP_019688962.1   421 CHQENFAENGNVNQPVGKLCKVTKNFINATINLYLQLTQEQRSILFG---    467

SDJ52620.1       487 PRIARSGTAREVLQ    500

WP_019688962.1   468 --------------    467
```

Figure S2: Quinohemoprotein amine dehydrogenase gene cluster. (A) QHNDH gene cluster from *Paracoccus denitrificans*.[5] (B) Primary sequence of QhpC indicating sites of thioether installation by QhpD. (C) Sequence alignment of QhpD (SDJ52620.1) with PapB (WP_019688962.1).

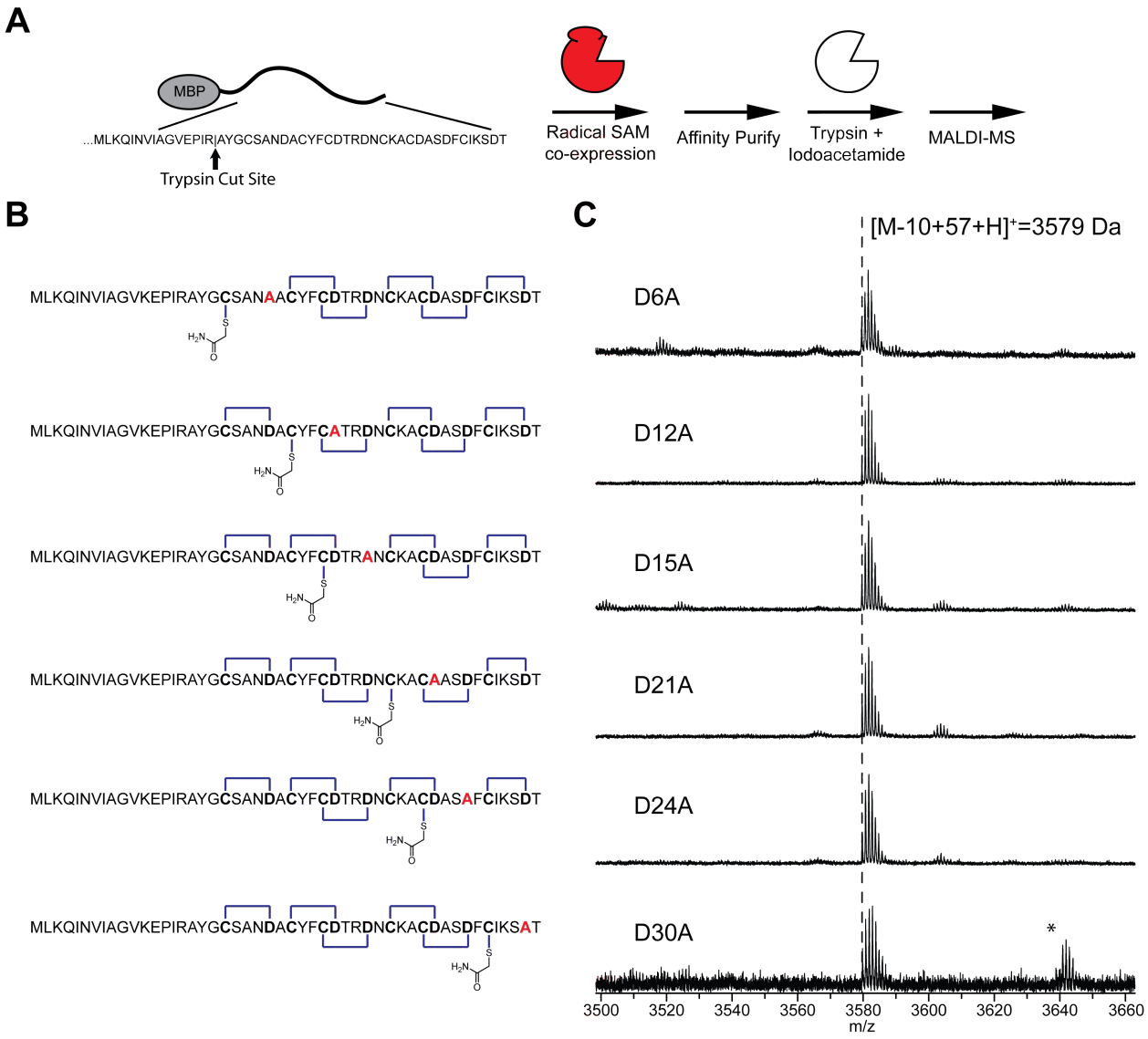

Figure S3: Trypsin digest and IAA labeling of Asp to Ala-substituted freyrasin variants. (A) Overview of experimental procedure. (B) Relevant Asp-Ala sequences and predicted modification structure. (C) Co-expression of all variants with PapB resulted in a variant product 10 Da lighter than the precursor peptide, consistent with the formation of five Cys-Asp linkages. Iodoacetamide treatment of all alanine variants resulted in a mass increase of 57 Da over the purified mass, suggesting the presence of a single free thiol.

*D30A variant has a peak at +114 Da (2 IAA) suggesting the presence of a second free thiol group in the peptide. The extent of proteolysis during expression of D30A, and the isotopic distribution pattern, is consistent with a sub-population of incompletely modified peptide substrate with only four thioether linkages (Fig S1).

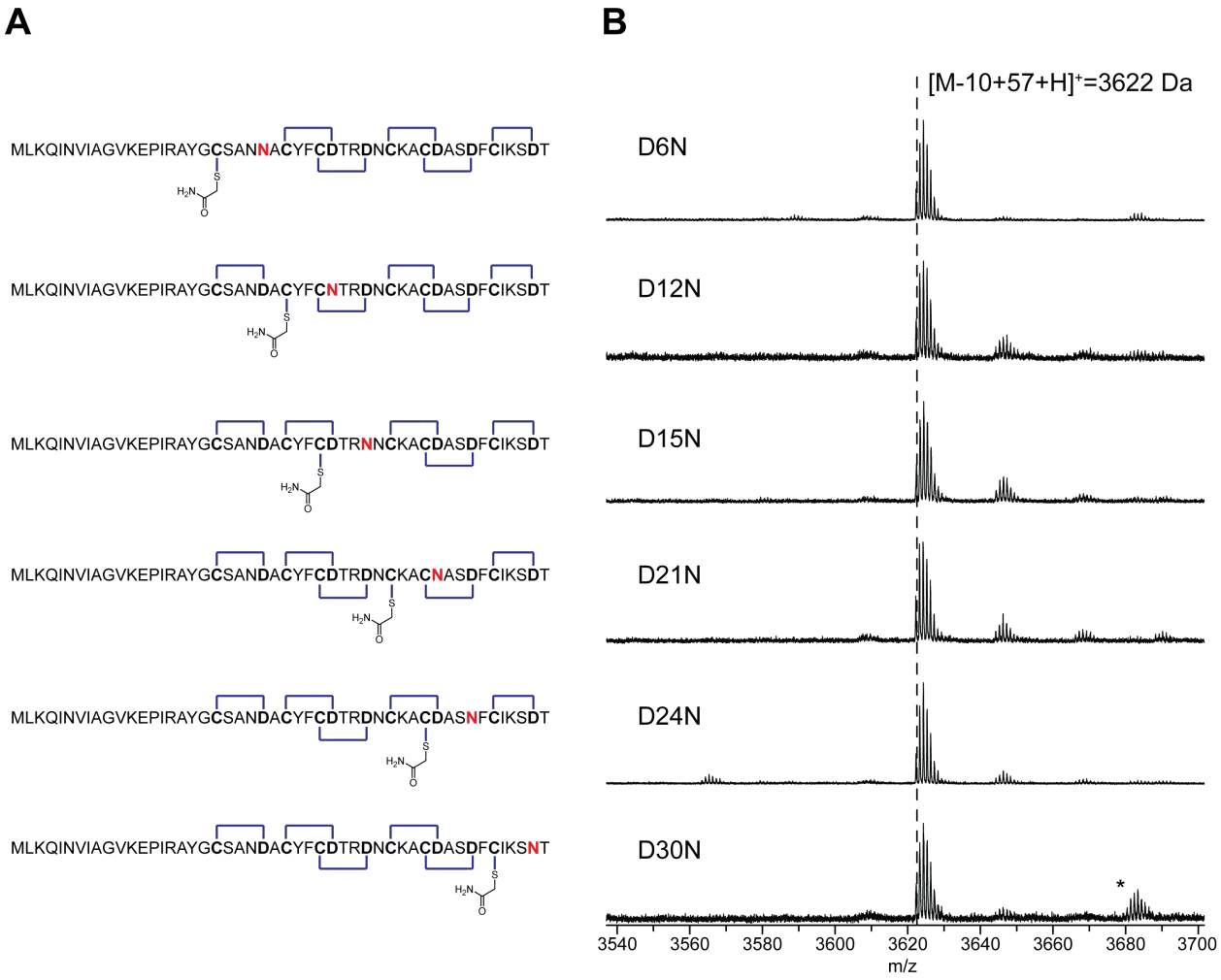

Figure S4: Trypsin digest and IAA labeling of Asp to Asn-substituted freyrasin variants. (A) Relevant Asp-Asn sequences and predicted modification structure. (B) Co-expression of all variants with PapB resulted in a freyrasin product 10 Da lighter than the precursor peptide, consistent with the formation of five Cys-Asp linkages. Iodoacetamide treatment of all asparagine variants resulted in a mass increase of 57 Da over the purified mass, suggesting the presence of a single free thiol.

*D30N variant has a peak at +114 Da indicating the presence of a second free thiol group in the peptide, similar to the results obtained with the D30A variant (Fig. S3).

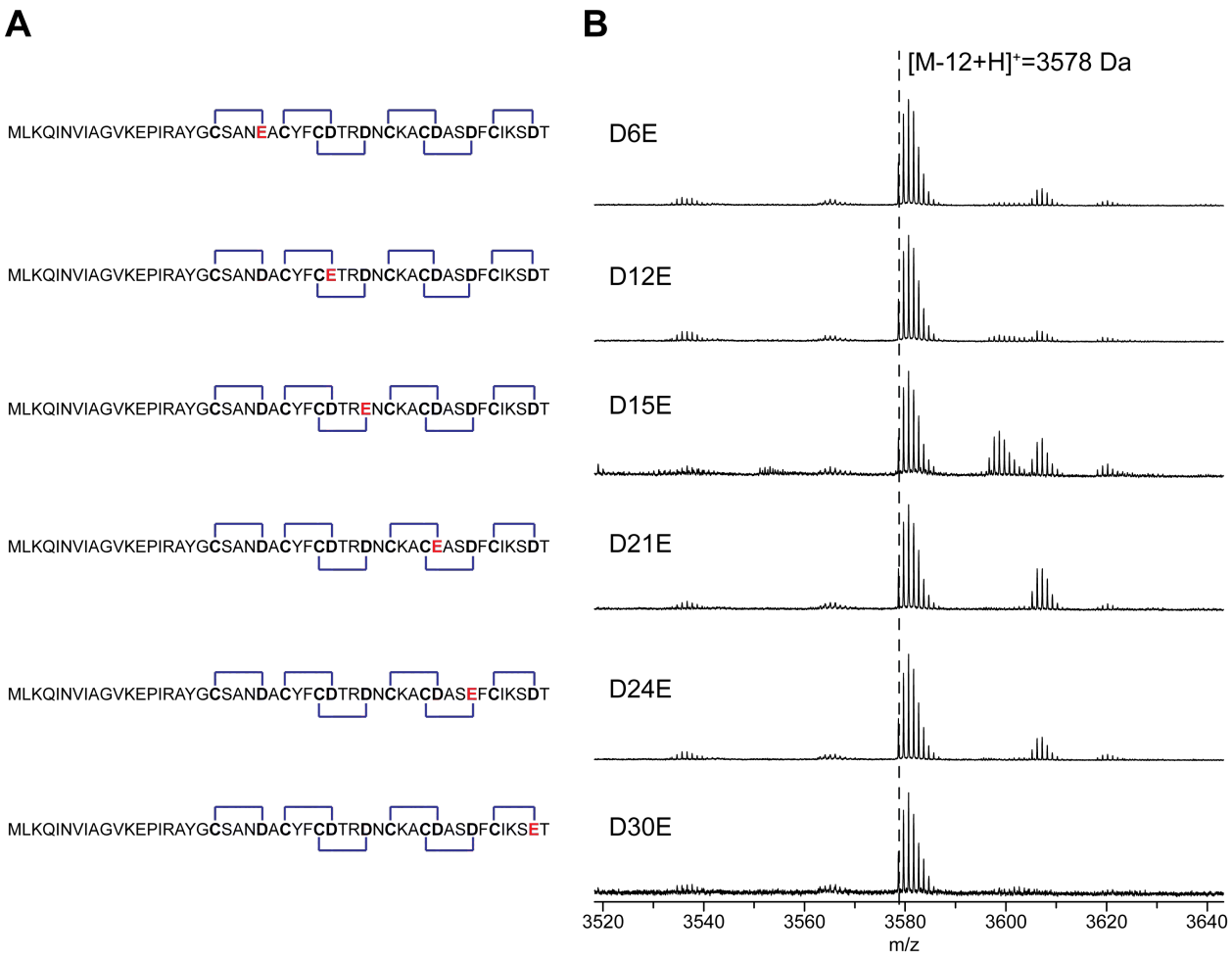

Figure S5: Trypsin digest and IAA labeling of Asp to Glu-substituted freyrasin variants. (A) Relevant Asp-Glu sequences. (B) Co-expression of all variants with PapB resulted in a freyrasin product 12 Da lighter than the precursor peptide, consistent with the formation of six Cys-Asp linkages. All glutamate variants were recalcitrant to iodoacetamide treatment, indicating the lack of a reactive thiol in the products. Spectra obtained by MALDI-MS.

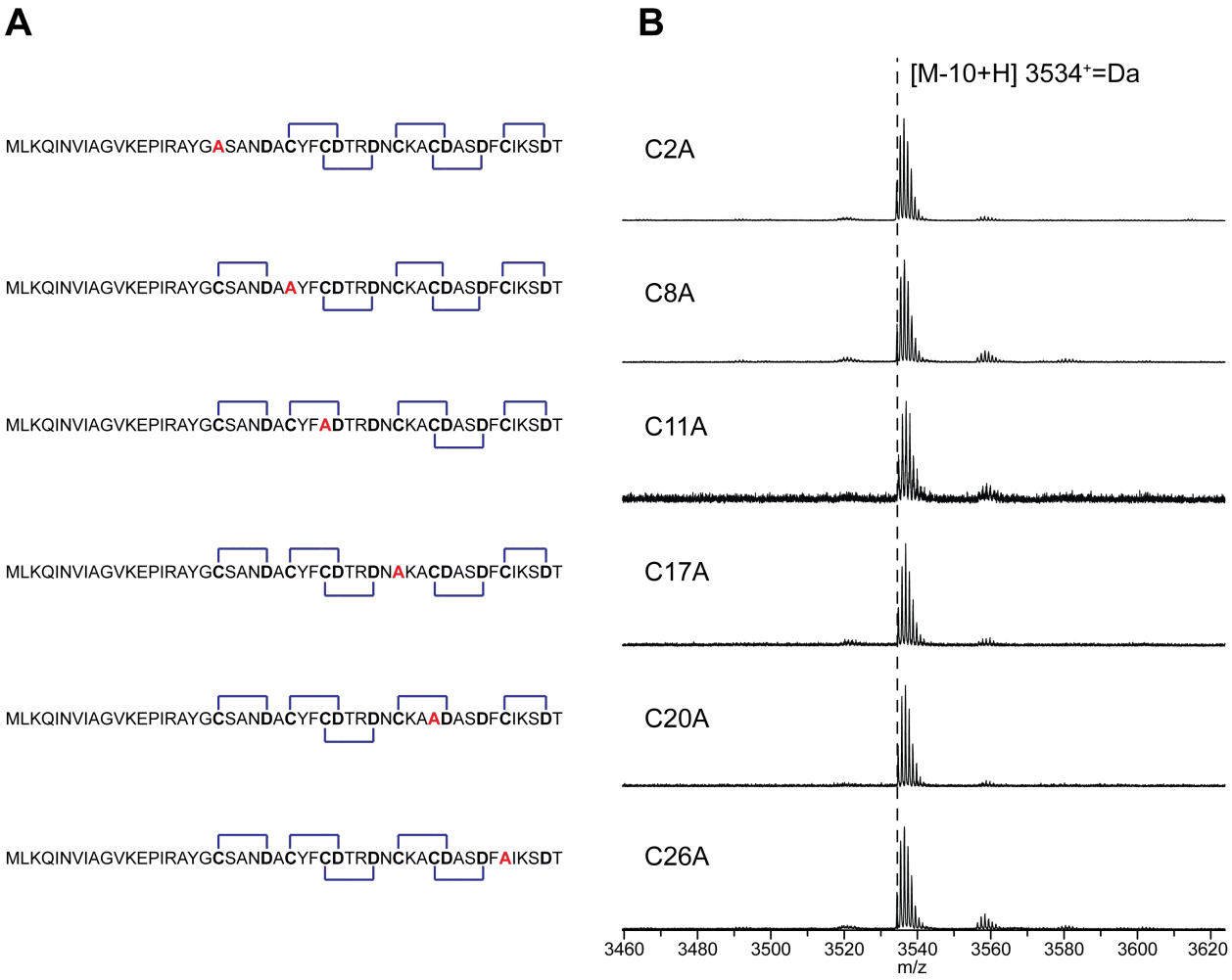

Figure S6: Trypsin digest and IAA labeling of Cys to Ala-substituted freyrasin variants. (A) Relevant Cys-Ala sequences. (B) Co-expression of all variants with PapB resulted in a freyrasin product 10 Da lighter than the precursor peptide, consistent with the formation of five Cys-Asp linkages. All alanine variants were recalcitrant to iodoacetamide treatment, suggesting a lack of free thiol in the molecules. These data are consistent with formation of five thioether bonds in the absence of one of the cysteine residues.

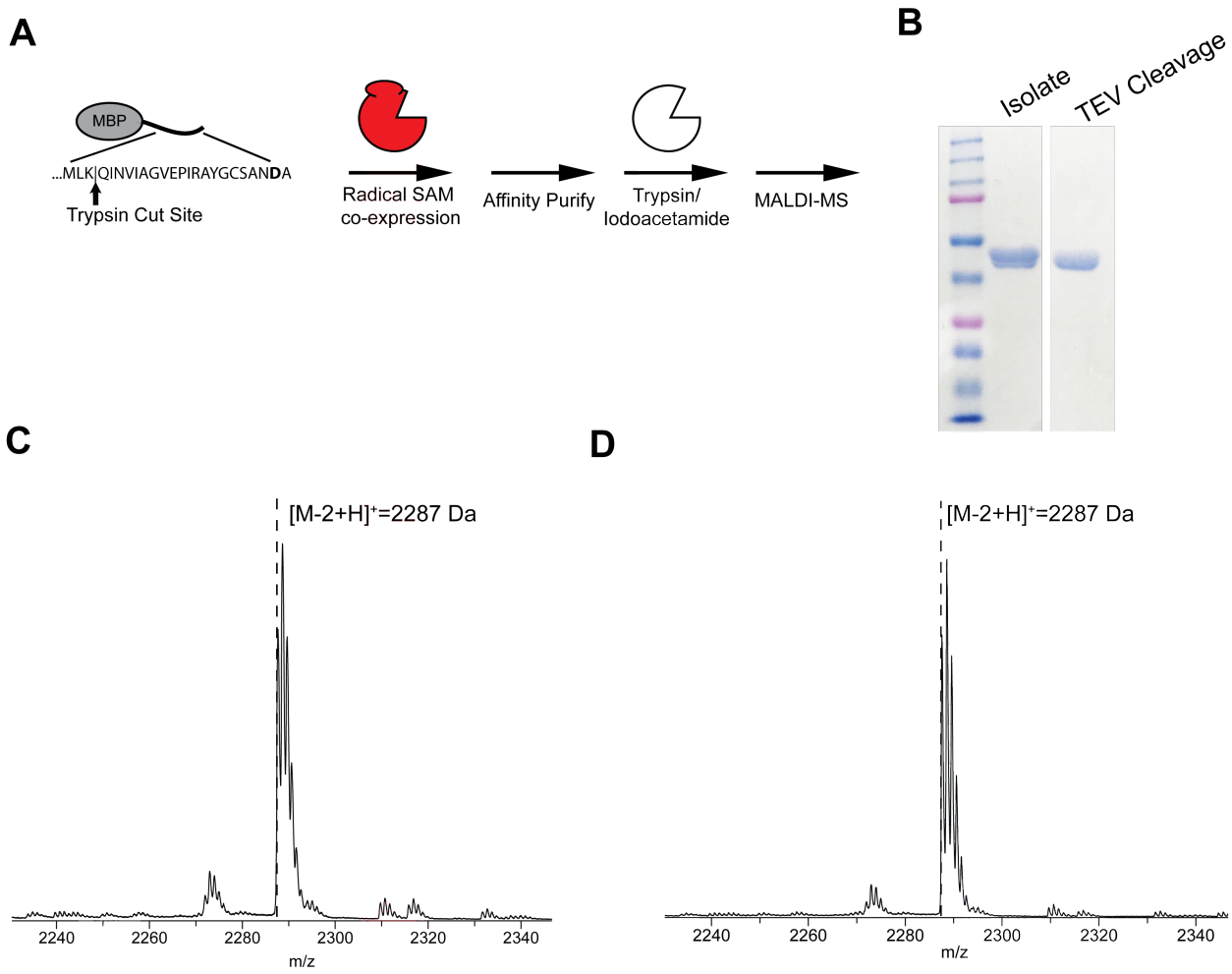

Figure S7: Trypsin digest and IAA labeling of the C8* freyrasin variant. (A) Overview of experimental procedure. (B) SDS-PAGE of modified MBP-PapA C8* isolate (* indicates a stop codon). TEV digest of the protein isolate verified that the purified protein was not empty MBP. (C) Trypsin digest of PapB-modified MBP-PapA C8*. (D) Trypsin digest followed by iodoacetamide treatment of PapB-modified MBP-PapA C8*. Fragment mass (-2 Da relative to unmodified) and resistance to IAA labeling suggests that PapB is able to install a single thioether linkage in this minimal substrate.

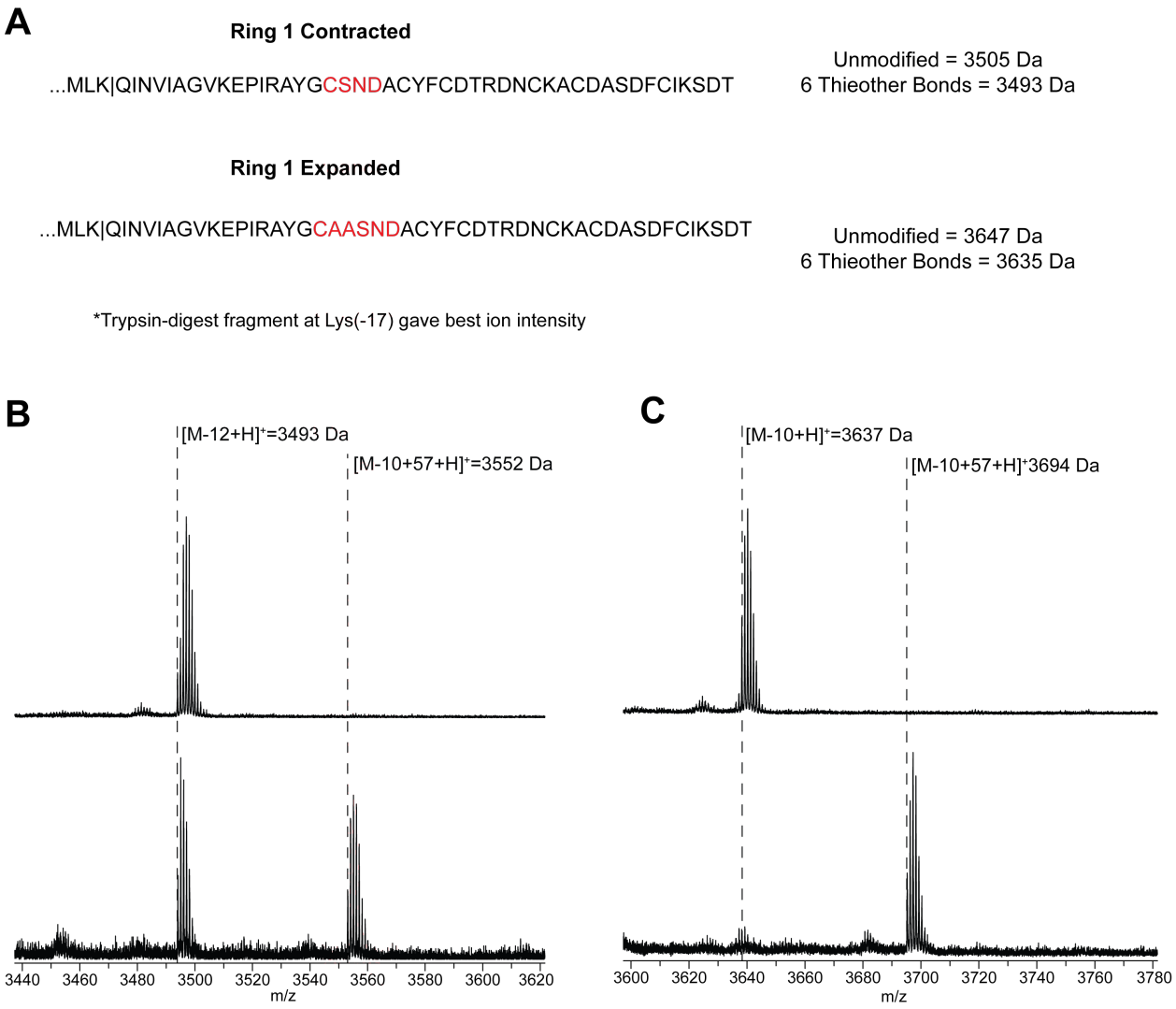

Figure S8: Trypsin digest and IAA labeling of ring 1 expansion and contraction variants. (A) Variant peptide sequences with change to ring 1 emphasized. (B) MALDI-MS of trypsin digest and IAA labeled ring 1 contraction variant. Modest signal for substrate of -12 Da and partial sensitivity to iodoacetamide indicates that only a subpopulation of the variant is fully modified. (C) MALDI-MS of trypsin digest and IAA labeled ring 1 expansion variant. The substrate experiences a mass loss of 10 Da and reacts with one equivalent of iodoacetamide, indicating that one thioether bond fails to form.

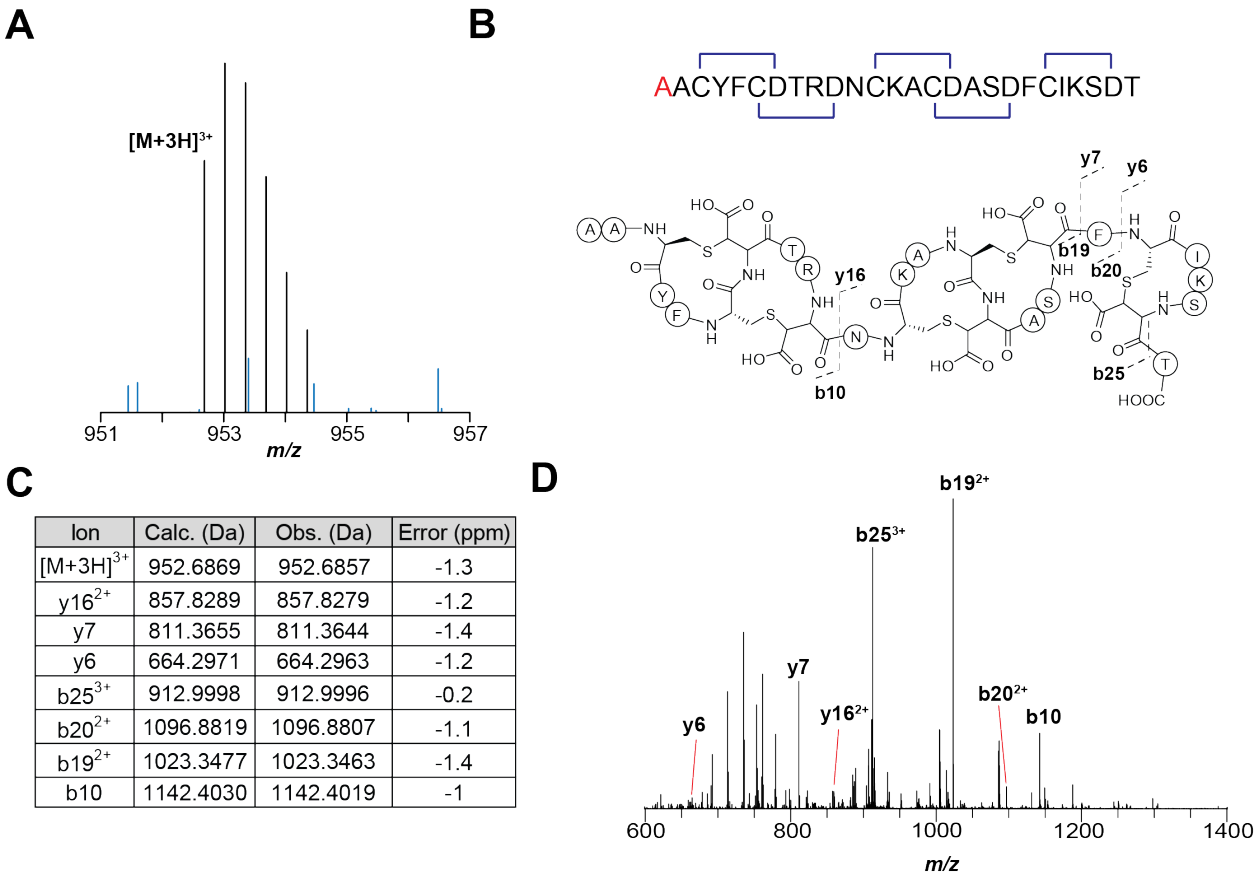

Ion	Calc. (Da)	Obs. (Da)	Error (ppm)
$[M+3H]^{3+}$	952.6869	952.6857	-1.3
$y16^{2+}$	857.8289	857.8279	-1.2
y7	811.3655	811.3644	-1.4
y6	664.2971	664.2963	-1.2
$b25^{3+}$	912.9998	912.9996	-0.2
$b20^{2+}$	1096.8819	1096.8807	-1.1
$b19^{2+}$	1023.3477	1023.3463	-1.4
b10	1142.4030	1142.4019	-1

Figure S9: HR-ESI-MS/MS of freyrasin variant D6A. (A) Molecular ion chosen for fragmentation by collision-induced dissociation (CID). Non-related contaminating peaks are in blue. (B) Proposed structure of freyrasin D6A after thermolysin digest with observed ions annotated. (C) Table of assigned ions. (D) CID spectrum of freyrasin D6A. The limited fragmentation pattern is consistent with previously reported tandem MS of the wild-type molecule.[1]

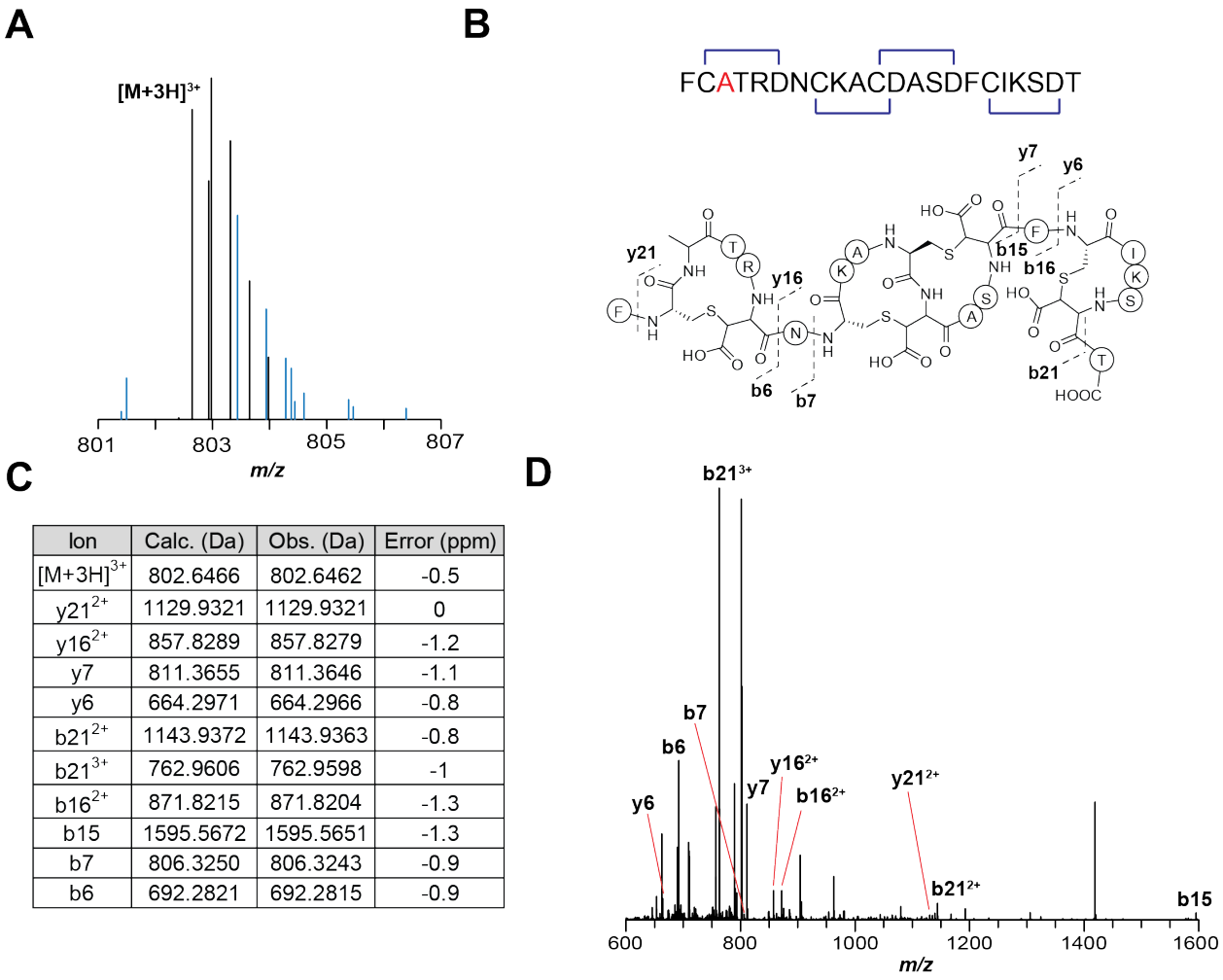

Ion	Calc. (Da)	Obs. (Da)	Error (ppm)
$[M+3H]^{3+}$	802.6466	802.6462	-0.5
$y21^{2+}$	1129.9321	1129.9321	0
$y16^{2+}$	857.8289	857.8279	-1.2
y7	811.3655	811.3646	-1.1
y6	664.2971	664.2966	-0.8
$b21^{2+}$	1143.9372	1143.9363	-0.8
$b21^{3+}$	762.9606	762.9598	-1
$b16^{2+}$	871.8215	871.8204	-1.3
b15	1595.5672	1595.5651	-1.3
b7	806.3250	806.3243	-0.9
b6	692.2821	692.2815	-0.9

Figure S10: HR-ESI-MS/MS of freyrasin variant D12A. (A) Molecular ion chosen for fragmentation by CID. Contaminating ions are in blue. (B) Proposed structure of freyrasin D12A after thermolysin digest. Observed b and y ions are annotated. (C) Table of fragment ion assignments. (D) CID spectrum of freyrasin D12A. The limited fragmentation pattern is consistent with previously reported tandem MS of wild-type freyrasin.

A

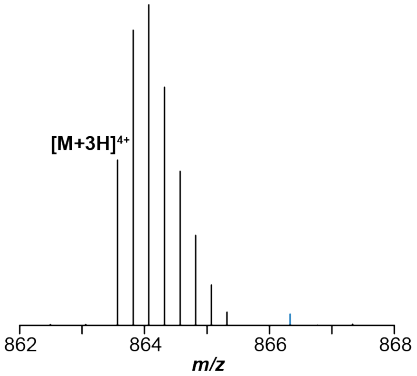

B

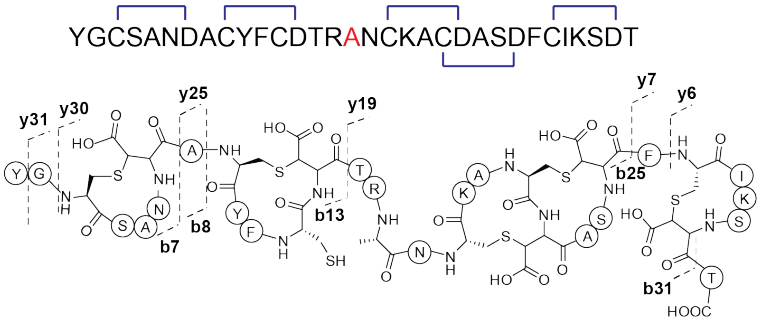

C

Ion	Calc. (Da)	Obs. (Da)	Error (ppm)
$[M+4H]^{4+}$	863.5685	863.5677	-0.9
$y31^{3+}$	1096.7345	1096.7335	-0.9
$y30^{3+}$	1077.7274	1077.7262	-1.1
$y25^{2+}$	1372.0212	1372.0201	-0.8
$y25^{3+}$	915.0165	915.0153	-1.3
$y19^{2+}$	1021.9220	1021.9205	-1.5
$y19^{3+}$	681.6170	681.6163	-1
y7	811.3655	811.3643	-1.5
y6	664.2971	664.2962	-1.4
$b31^{3+}$	1111.4029	1111.4015	-1.3
$b31^{4+}$	833.8040	833.8026	-1.7
$b25^{2+}$	1320.9507	1320.9486	-1.6
$b25^{3+}$	880.9696	880.9683	-1.5
b13	1246.3598	1246.3589	-0.7
b8	780.2617	780.2606	-1.4
b7	709.2246	709.2239	-1

D

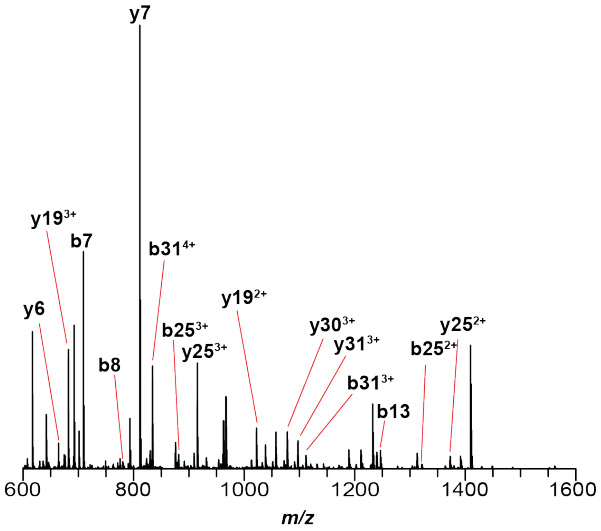

Figure S11: HR-ESI-MS/MS of freyrasin variant D15A. (A) Molecular ion chosen for fragmentation by CID. (B) Proposed structure of freyrasin D15A after thermolysin digest. Observed b and y ions are annotated. (C) Table of CID spectrum ion assignments. (D) CID spectrum of freyrasin D15A. The limited fragmentation pattern is consistent with previously reported tandem MS of wild-type freyrasin.

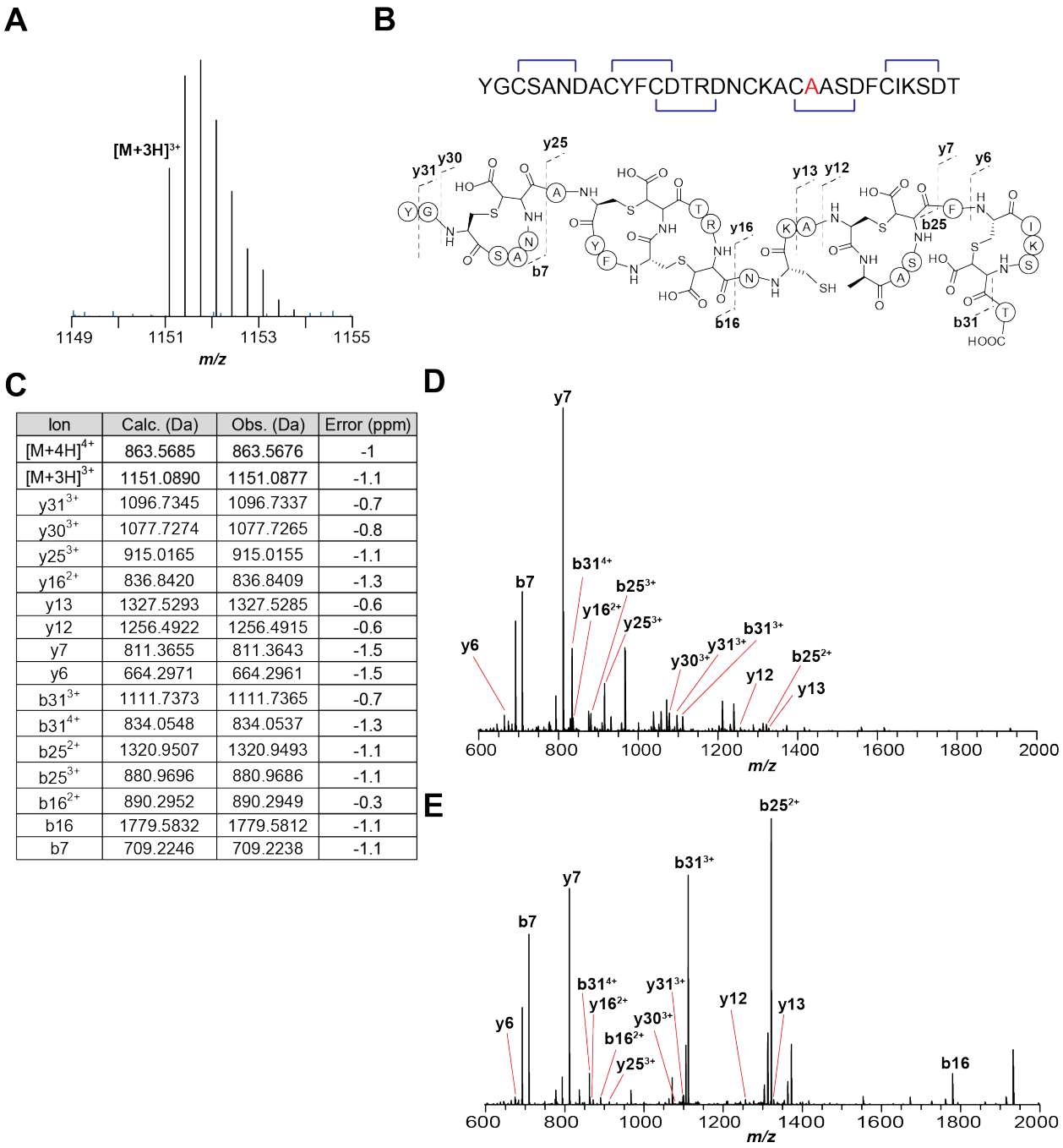

Ion	Calc. (Da)	Obs. (Da)	Error (ppm)
$[M+4H]^{4+}$	863.5685	863.5676	-1
$[M+3H]^{3+}$	1151.0890	1151.0877	-1.1
$y31^{3+}$	1096.7345	1096.7337	-0.7
$y30^{3+}$	1077.7274	1077.7265	-0.8
$y25^{3+}$	915.0165	915.0155	-1.1
$y16^{2+}$	836.8420	836.8409	-1.3
y13	1327.5293	1327.5285	-0.6
y12	1256.4922	1256.4915	-0.6
y7	811.3655	811.3643	-1.5
y6	664.2971	664.2961	-1.5
$b31^{3+}$	1111.7373	1111.7365	-0.7
$b31^{4+}$	834.0548	834.0537	-1.3
$b25^{2+}$	1320.9507	1320.9493	-1.1
$b25^{3+}$	880.9696	880.9686	-1.1
$b16^{2+}$	890.2952	890.2949	-0.3
b16	1779.5832	1779.5812	-1.1
b7	709.2246	709.2238	-1.1

Figure S12: HR-ESI-MS/MS of freyrasin variant D21A. (A) Molecular ion chosen for fragmentation by CID. (B) Proposed structure of freyrasin D21A after thermolysin digest. Observed b and y ions are annotated. (C) Table of CID spectrum ion assignments. (D) CID spectrum of freyrasin D21A $[M+4H]^{4+}$ ion. (E) CID spectrum of freyrasin D21A $[M+3H]^{3+}$ ion. The limited fragmentation pattern is consistent with previously reported tandem MS of wild-type freyrasin.

A

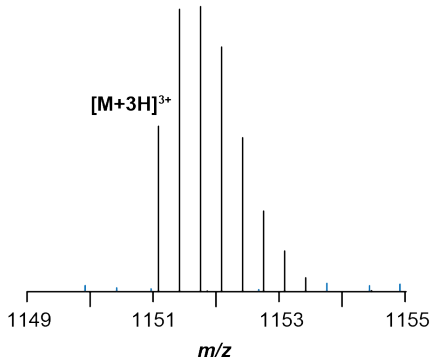

B

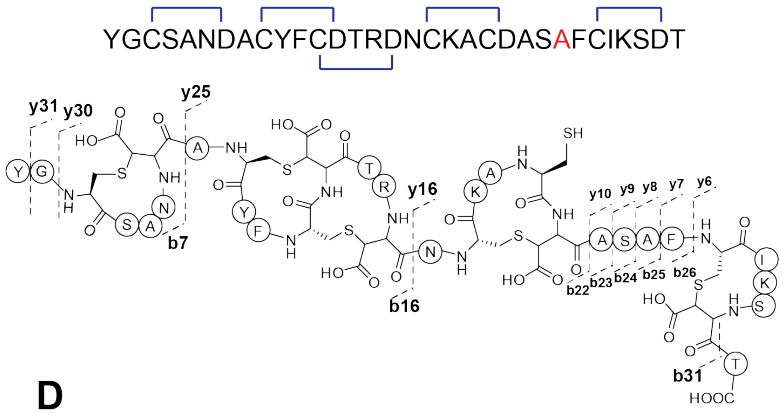

C

Ion	Calc. (Da)	Obs. (Da)	Error (ppm)
$[M+3H]^{3+}$	1151.0890	1151.0878	-1
$y31^{3+}$	1096.7345	1096.7345	0
$y30^{3+}$	1077.7274	1077.7264	-0.9
$y25^{2+}$	1372.0211	1372.0200	-0.8
$y24^{2+}$	1336.5026	1336.5030	0.3
$y16^{2+}$	836.8418	836.8408	-1.2
y16	1672.6764	1672.6746	-1.1
y10	1040.4717	1040.4705	-1.2
y9	969.4346	969.4335	-1.1
y8	882.4026	882.4016	-1.1
y7	811.3655	811.3645	-1.2
y6	664.2971	664.2964	-1.1
$b31^{3+}$	1111.4029	1111.4018	-1
$b26^{2+}$	1394.4849	1394.4836	-0.9
$b25^{2+}$	1320.9507	1320.9499	-0.6
$b24^{2+}$	1285.4322	1285.4313	-0.7
$b23^{2+}$	1241.9161	1241.9154	-0.6
$b22^{2+}$	1206.3976	1206.3965	-0.9
b16	1779.5832	1779.5821	-0.6
b7	709.2246	709.2240	-0.8

D

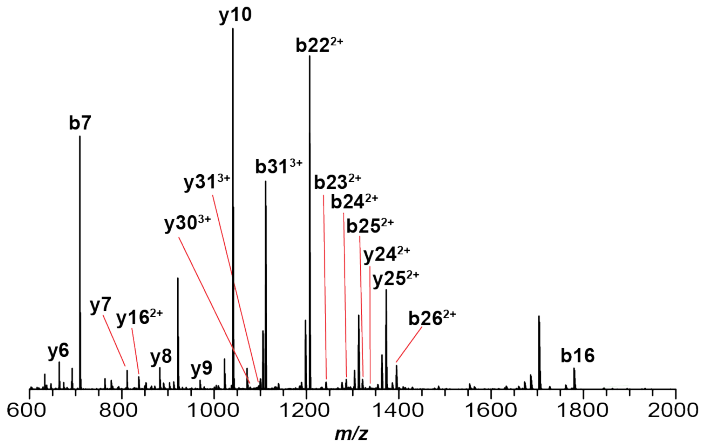

Figure S13: HR-ESI-MS/MS of freyrasin variant D24A. (A) Molecular ion chosen for fragmentation by CID. (B) Proposed structure of freyrasin D24A after thermolysin digest. Observed b and y ions are annotated. (C) Table of CID spectrum ion assignments. (D) CID spectrum of freyrasin D24A.

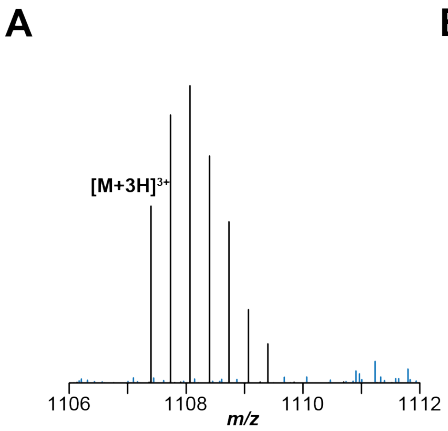

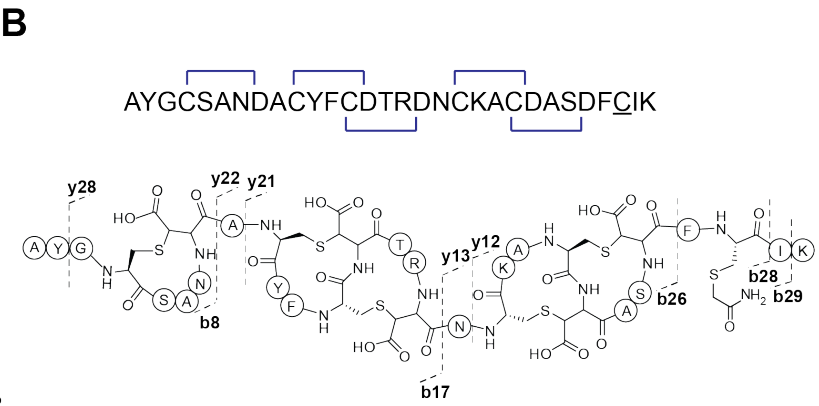

C

Ion	Calc. (Da)	Obs. (Da)	Error (ppm)
$[M+3H]^{3+}$	1107.4029	1107.3993	-3.3
$y28^{2+}$	1543.5505	1543.5437	-4.4
$y28^{3+}$	1029.3694	1029.3650	-4.3
$y22^{2+}$	1270.9735	1270.9690	-3.5
$y21^{2+}$	1235.4549	1235.4517	-2.6
y13	1470.5810	1470.5765	-3.1
$y13^{2+}$	735.7942	735.7919	-3.1
y4	567.2959	567.2943	-2.8
$b29^{2+}$	1587.5479	1587.5425	-3.4
$b28^{2+}$	1531.0059	1531.0004	-3.6
$b26^{2+}$	1377.4564	1377.4514	-3.6
b17	1850.6203	1850.6139	-3.5
b8	780.2617	780.2589	-3.6

C = site of IAA labeling

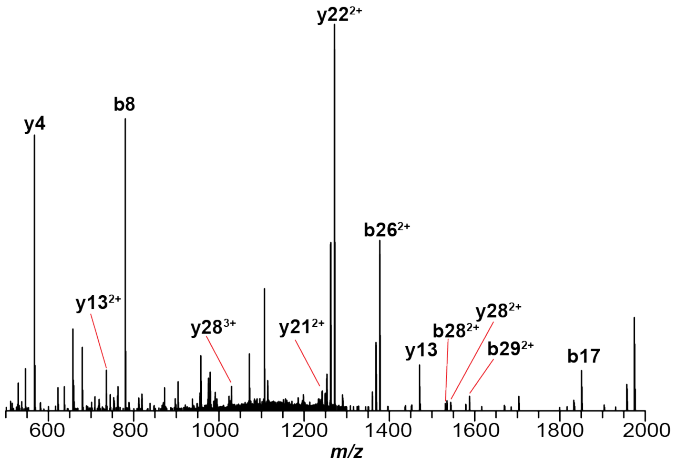

Figure S14: HR-ESI-MS/MS of 1-IAA labeled freyrasin variant D30A. (A) Molecular ion chosen for fragmentation by CID. (B) Proposed structure of freyrasin D30A after trypsin digest and iodoacetamide labeling. As ring 6 is no longer formed, Lys28 (**Figure 1** numbering) became a viable trypsin site, resulting in loss of the C-terminal portion of the peptide. Observed b and y ions are annotated. (C) Table of CID spectrum ion assignments. (D) CID spectrum of freyrasin D30A. The limited fragmentation pattern is consistent with previously reported tandem MS of wild-type freyrasin. A modified protocol was deployed for this and all other samples digested by trypsin wherein the final molecule was labeled by alkylation with IAA before tandem mass spectrometry was performed.

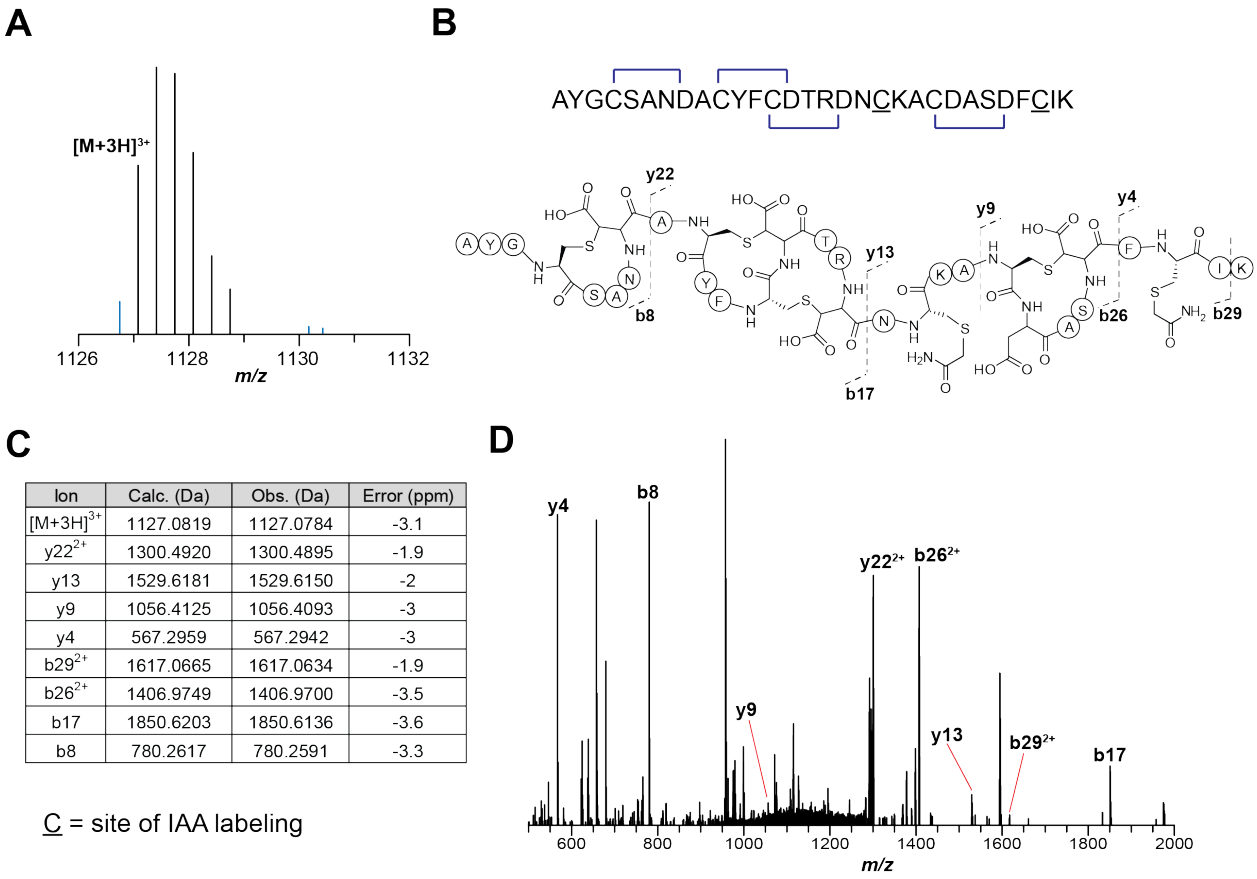

Ion	Calc. (Da)	Obs. (Da)	Error (ppm)
$[M+3H]^{3+}$	1127.0819	1127.0784	-3.1
$y22^{2+}$	1300.4920	1300.4895	-1.9
y13	1529.6181	1529.6150	-2
y9	1056.4125	1056.4093	-3
y4	567.2959	567.2942	-3
$b29^{2+}$	1617.0665	1617.0634	-1.9
$b26^{2+}$	1406.9749	1406.9700	-3.5
b17	1850.6203	1850.6136	-3.6
b8	780.2617	780.2591	-3.3

C = site of IAA labeling

Figure S15: HR-ESI-MS/MS of 2-IAA labeled freyrasin variant D30A. (A) Molecular ion chosen for fragmentation by CID. (B) Proposed structure of freyrasin D30A after trypsin digest and two IAA labeling events. As ring 6 is no longer formed, Lys28 (**Figure 1** numbering) became a viable trypsin site, resulting in loss of the C-terminal portion of the peptide. Observed b and y ions are annotated. (C) Table of CID spectrum ion assignments. (D) CID spectrum of freyrasin D30A. The presence of b and y series ions in ring 4 suggests that it may be the final thioether linkage formed by PapB *in vivo*, further analysis supports this suggestion.

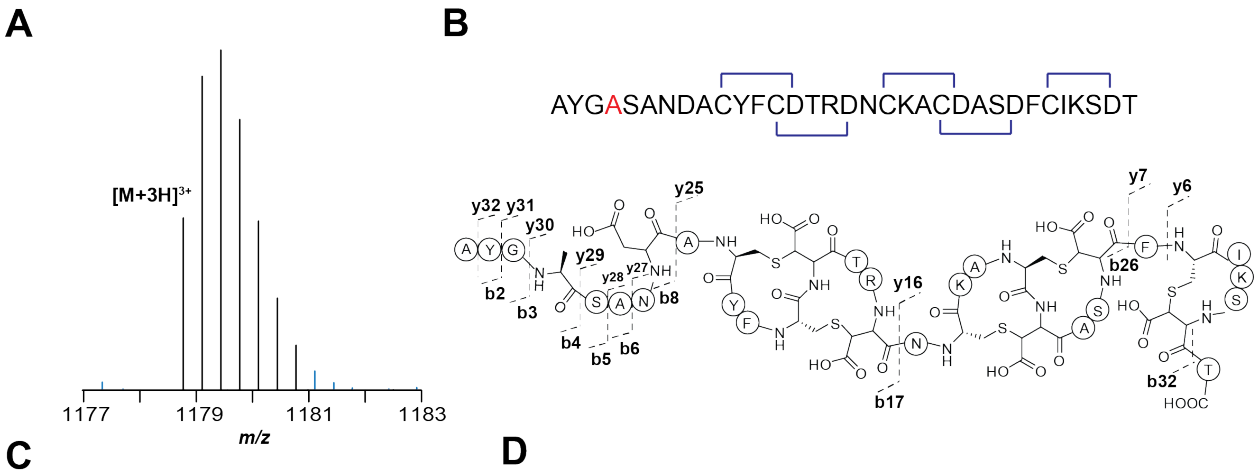

C

Ion	Calc. (Da)	Obs. (Da)	Error (ppm)
$[M+3H]^{3+}$	1178.7739	1178.7701	-3.2
$y32^{3+}$	1155.0949	1155.0915	-2.9
$y31^{2+}$	1650.6070	1650.6017	-3.2
$y31^{3+}$	1100.7404	1100.7369	-3.2
$y30^{2+}$	1622.0963	1622.0916	-2.9
$y30^{3+}$	1081.7333	1081.7304	-2.7
$y29^{2+}$	1586.5777	1586.5691	-5.4
$y28^{2+}$	1543.0617	1543.0572	-2.9
$y27^{2+}$	1507.5432	1507.5387	-3
$y25^{2+}$	1393.0082	1393.0040	-3
y16	1714.6506	1714.6449	-3.3
$y16^{2+}$	857.8289	857.8261	-3.3
y7	811.3655	811.3630	-3.1
y6	664.2971	664.2949	-3.3
$b32^{3+}$	1139.0878	1139.0841	-3.2
$b26^{2+}$	1362.4781	1362.4739	-3.1
b17	1820.6639	1820.6578	-3.4
$b17^{2+}$	910.8356	910.8326	-3.3
b8	750.3053	750.3031	-2.9
b6	521.2354	521.2342	-2.3
b5	450.1983	450.1973	-2.2
b4	363.1663	363.1655	-2.2
b3	292.1292	292.1286	-2.1
b2	235.1077	235.1073	-1.7

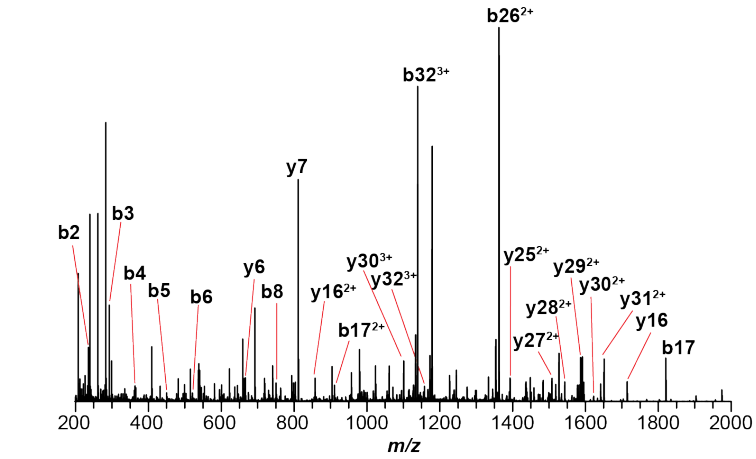

Figure S16: HR-ESI-MS/MS of freyrasin variant C2A. (A) Molecular ion chosen for fragmentation by CID. (B) Proposed structure of freyrasin C2A after trypsin digest. Observed b and y ions are annotated. (C) Table of CID spectrum ion assignments. (D) CID spectrum of freyrasin C2A.

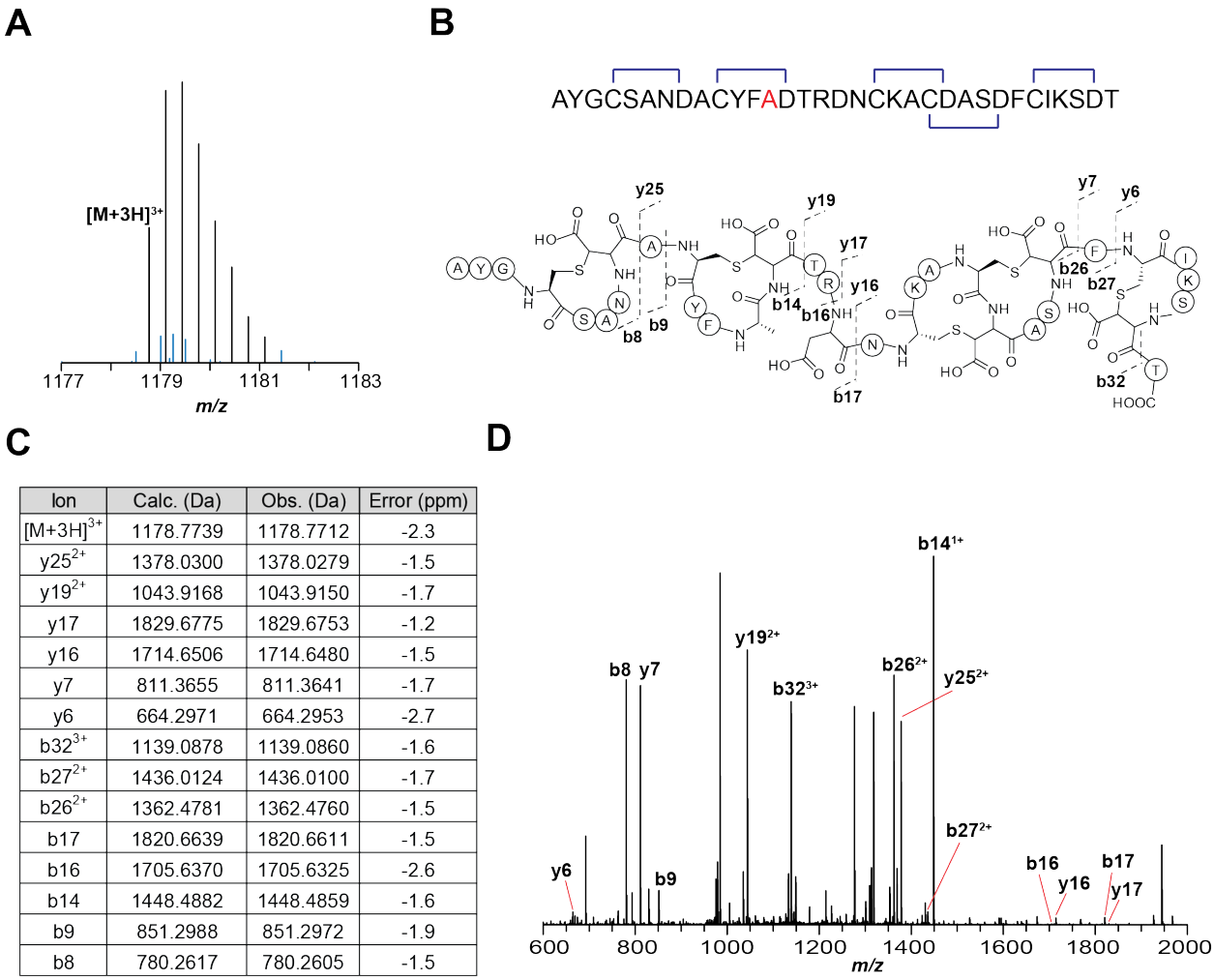

Ion	Calc. (Da)	Obs. (Da)	Error (ppm)
$[M+3H]^{3+}$	1178.7739	1178.7712	-2.3
$y25^{2+}$	1378.0300	1378.0279	-1.5
$y19^{2+}$	1043.9168	1043.9150	-1.7
y17	1829.6775	1829.6753	-1.2
y16	1714.6506	1714.6480	-1.5
y7	811.3655	811.3641	-1.7
y6	664.2971	664.2953	-2.7
$b32^{3+}$	1139.0878	1139.0860	-1.6
$b27^{2+}$	1436.0124	1436.0100	-1.7
$b26^{2+}$	1362.4781	1362.4760	-1.5
b17	1820.6639	1820.6611	-1.5
b16	1705.6370	1705.6325	-2.6
b14	1448.4882	1448.4859	-1.6
b9	851.2988	851.2972	-1.9
b8	780.2617	780.2605	-1.5

Figure S17: HR-ESI-MS/MS of freyrasin variant C11A. (A) Molecular ion chosen for fragmentation by CID. Contaminating peaks are in blue. (B) Proposed structure of freyrasin C11A after trypsin digestion. Observed b and y ions are annotated. (C) Table of CID spectrum ion assignments. (D) CID spectrum of freyrasin C11A. The limited fragmentation pattern is consistent with previously reported tandem MS of wild-type freyrasin.

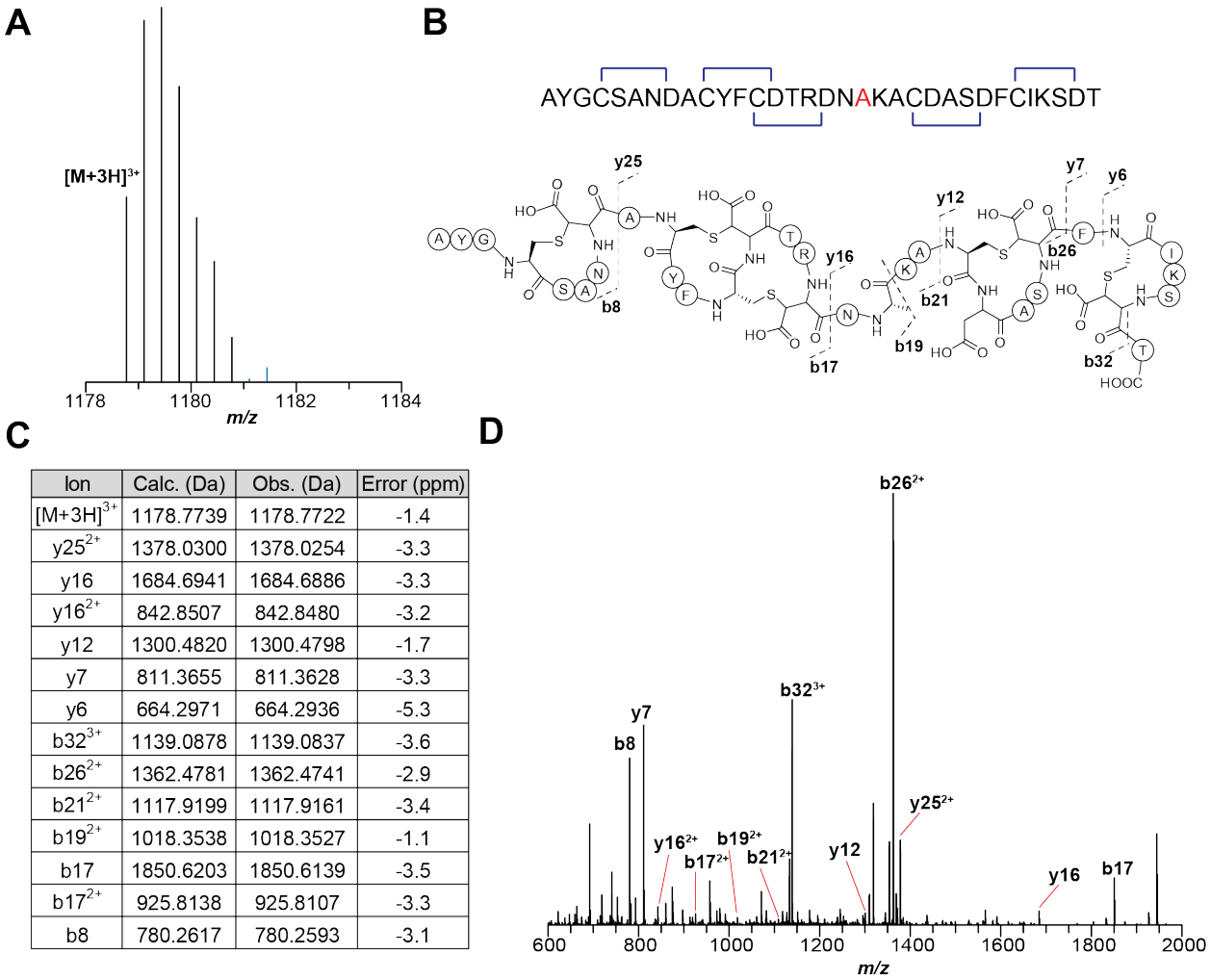

Ion	Calc. (Da)	Obs. (Da)	Error (ppm)
$[M+3H]^{3+}$	1178.7739	1178.7722	-1.4
$y25^{2+}$	1378.0300	1378.0254	-3.3
y16	1684.6941	1684.6886	-3.3
$y16^{2+}$	842.8507	842.8480	-3.2
y12	1300.4820	1300.4798	-1.7
y7	811.3655	811.3628	-3.3
y6	664.2971	664.2936	-5.3
$b32^{3+}$	1139.0878	1139.0837	-3.6
$b26^{2+}$	1362.4781	1362.4741	-2.9
$b21^{2+}$	1117.9199	1117.9161	-3.4
$b19^{2+}$	1018.3538	1018.3527	-1.1
b17	1850.6203	1850.6139	-3.5
$b17^{2+}$	925.8138	925.8107	-3.3
b8	780.2617	780.2593	-3.1

Figure S18: HR-ESI-MS/MS of freyrasin variant C17A. (A) Molecular ion chosen for fragmentation by CID. (B) Proposed structure of freyrasin C17A after trypsin digestion. Observed b and y ions are annotated. (C) Table of CID spectrum ion assignments. (D) CID spectrum of freyrasin C17A. The limited fragmentation pattern is consistent with previously reported tandem MS of wild-type freyrasin.

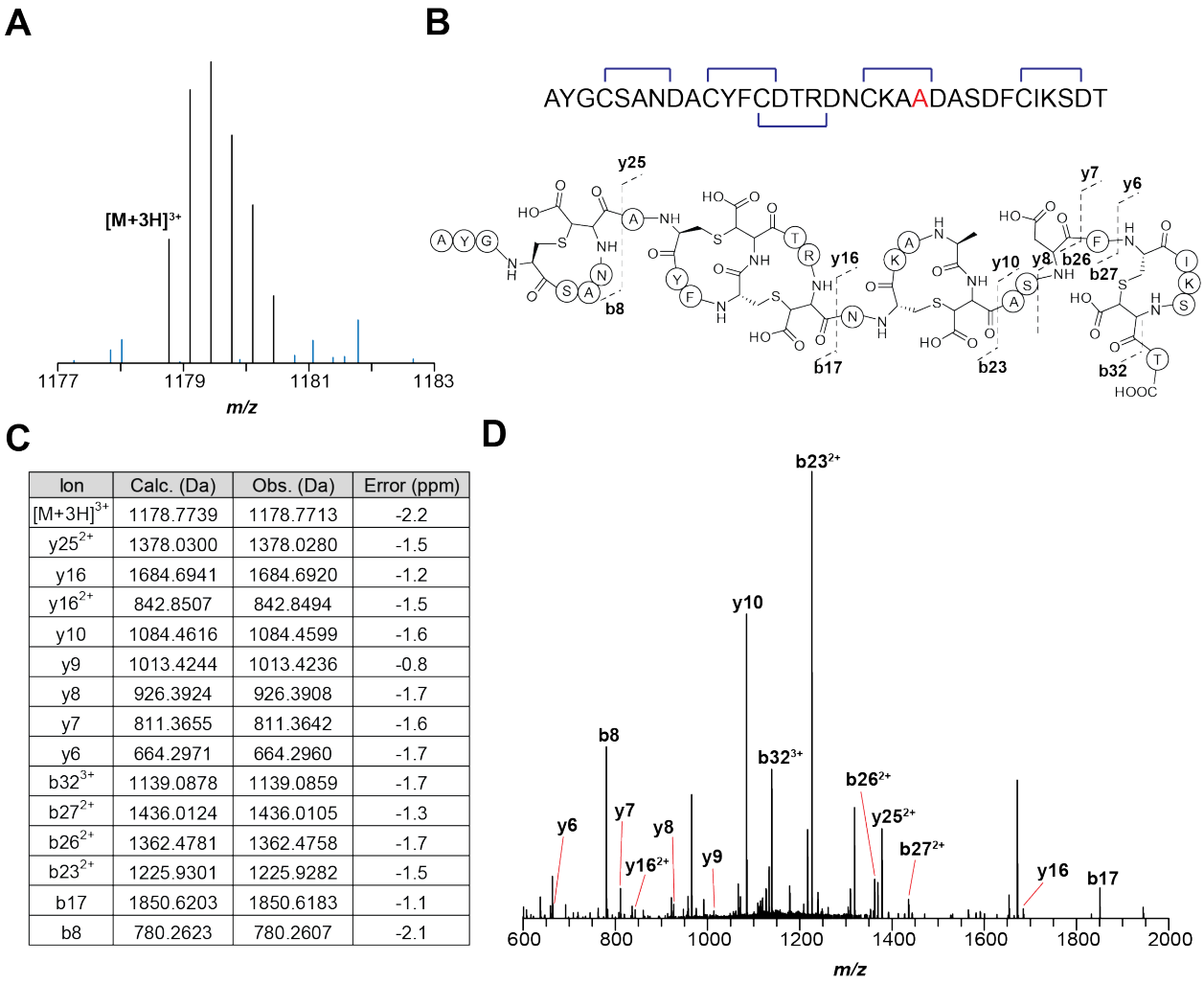

Ion	Calc. (Da)	Obs. (Da)	Error (ppm)
$[M+3H]^{3+}$	1178.7739	1178.7713	-2.2
$y25^{2+}$	1378.0300	1378.0280	-1.5
y16	1684.6941	1684.6920	-1.2
$y16^{2+}$	842.8507	842.8494	-1.5
y10	1084.4616	1084.4599	-1.6
y9	1013.4244	1013.4236	-0.8
y8	926.3924	926.3908	-1.7
y7	811.3655	811.3642	-1.6
y6	664.2971	664.2960	-1.7
$b32^{3+}$	1139.0878	1139.0859	-1.7
$b27^{2+}$	1436.0124	1436.0105	-1.3
$b26^{2+}$	1362.4781	1362.4758	-1.7
$b23^{2+}$	1225.9301	1225.9282	-1.5
b17	1850.6203	1850.6183	-1.1
b8	780.2623	780.2607	-2.1

Figure S19: HR-ESI-MS/MS of freyrasin variant C20A. (A) Molecular ion chosen for fragmentation by CID. (B) Proposed structure of freyrasin C20A after trypsin digestion. Observed b and y ions are annotated. (C) Table of CID spectrum ion assignments. (D) CID spectrum of freyrasin C20A. The limited fragmentation pattern is consistent with previously reported tandem MS of wild-type freyrasin.

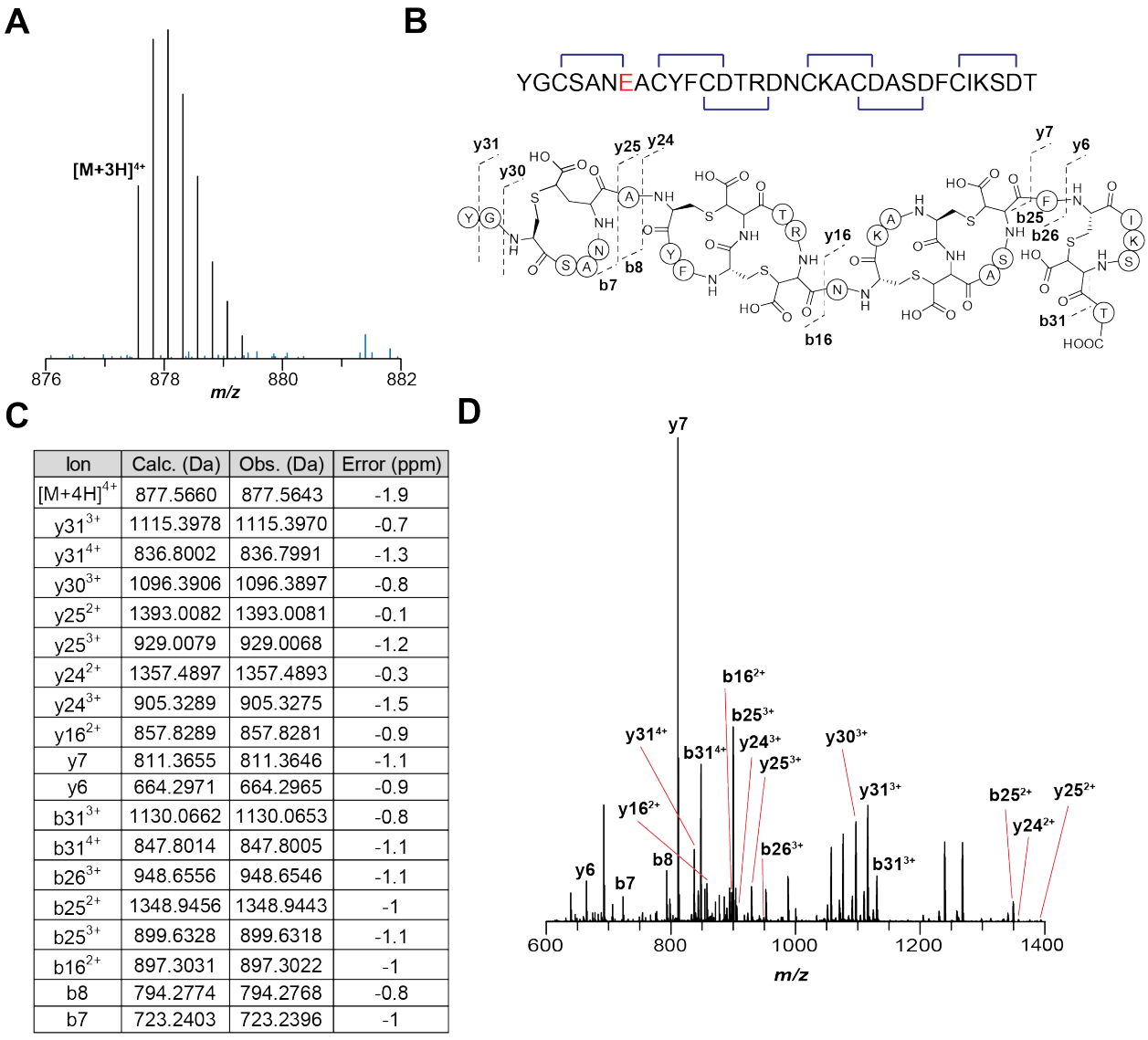

Ion	Calc. (Da)	Obs. (Da)	Error (ppm)
$[M+4H]^{4+}$	877.5660	877.5643	-1.9
$y31^{3+}$	1115.3978	1115.3970	-0.7
$y31^{4+}$	836.8002	836.7991	-1.3
$y30^{3+}$	1096.3906	1096.3897	-0.8
$y25^{2+}$	1393.0082	1393.0081	-0.1
$y25^{3+}$	929.0079	929.0068	-1.2
$y24^{2+}$	1357.4897	1357.4893	-0.3
$y24^{3+}$	905.3289	905.3275	-1.5
$y16^{2+}$	857.8289	857.8281	-0.9
y7	811.3655	811.3646	-1.1
y6	664.2971	664.2965	-0.9
$b31^{3+}$	1130.0662	1130.0653	-0.8
$b31^{4+}$	847.8014	847.8005	-1.1
$b26^{3+}$	948.6556	948.6546	-1.1
$b25^{2+}$	1348.9456	1348.9443	-1
$b25^{3+}$	899.6328	899.6318	-1.1
$b16^{2+}$	897.3031	897.3022	-1
b8	794.2774	794.2768	-0.8
b7	723.2403	723.2396	-1

Figure S20: HR-ESI-MS/MS of freyrasin variant D6E. (A) Molecular ion chosen for fragmentation by CID. (B) Proposed structure of freyrasin D6E after thermolysin digestion. Observed b and y ions are annotated. (C) Table of CID spectrum ion assignments. (D) CID spectrum of freyrasin D6E. The limited fragmentation pattern is consistent with previously reported tandem MS of wild-type freyrasin.

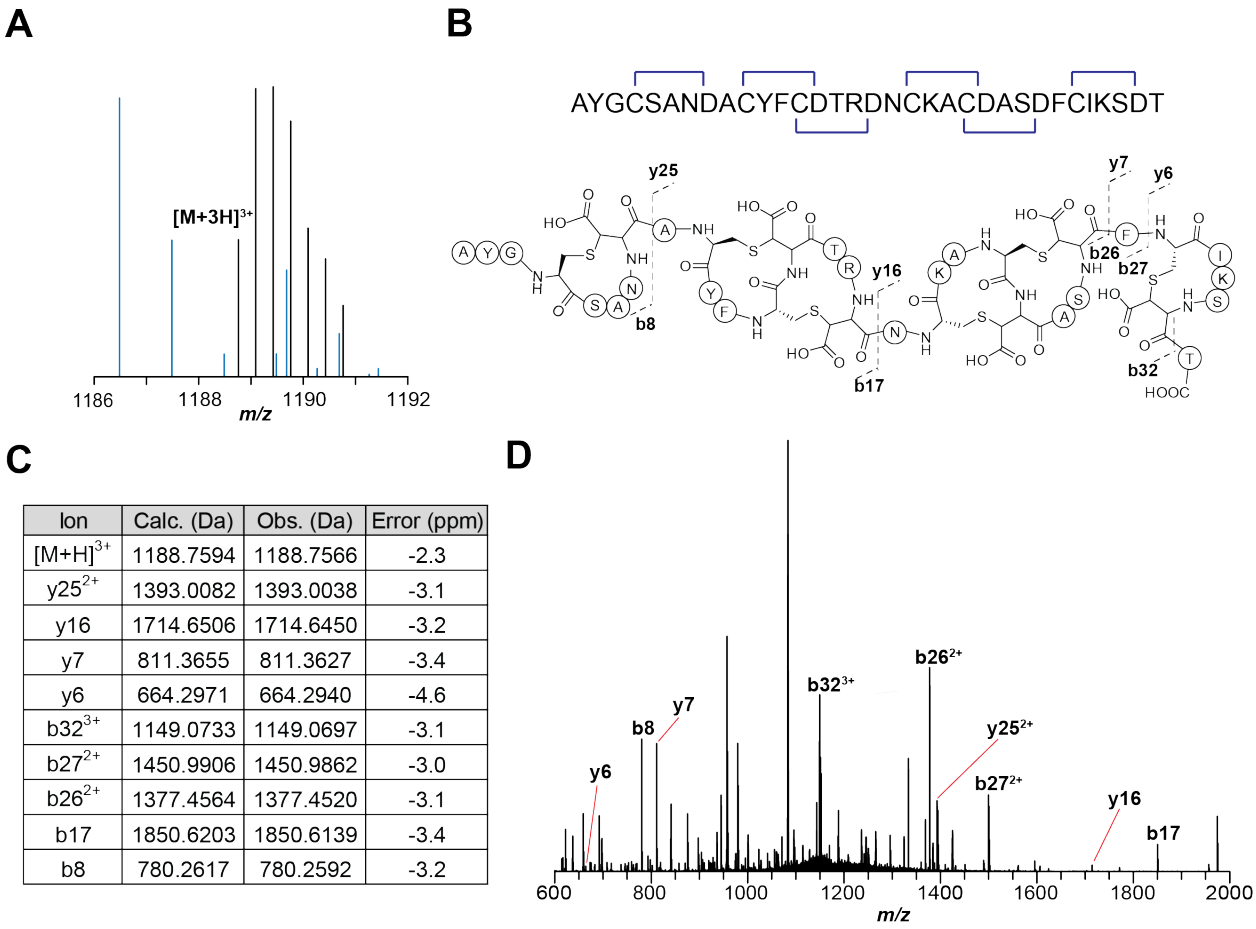

Ion	Calc. (Da)	Obs. (Da)	Error (ppm)
$[M+H]^{3+}$	1188.7594	1188.7566	-2.3
$y25^{2+}$	1393.0082	1393.0038	-3.1
y16	1714.6506	1714.6450	-3.2
y7	811.3655	811.3627	-3.4
y6	664.2971	664.2940	-4.6
$b32^{3+}$	1149.0733	1149.0697	-3.1
$b27^{2+}$	1450.9906	1450.9862	-3.0
$b26^{2+}$	1377.4564	1377.4520	-3.1
b17	1850.6203	1850.6139	-3.4
b8	780.2617	780.2592	-3.2

Figure S21: HR-ESI-MS/MS of freyrasin variant N(-13)A. (A) Molecular ion chosen for fragmentation by CID. Contaminating peaks are in blue. (B) Proposed structure of freyrasin N(-13)A after trypsin digest. Observed b and y ions are annotated. (C) Table of CID spectrum ion assignments. (D) CID spectrum of the freyrasin N(-13)A core. The limited fragmentation pattern is consistent with previously reported tandem MS of wild-type freyrasin. The fully modified species is a low intensity ion and competing species from MBP fragmentation resulted in several unidentifiable peaks.

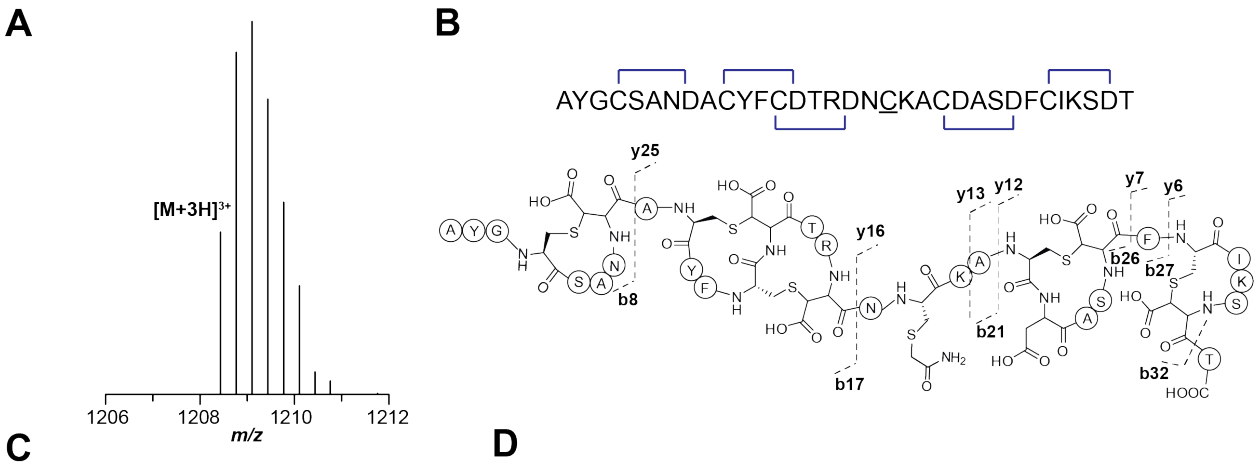

C

Ion	Calc. (Da)	Obs. (Da)	Error (ppm)
$[M+H]^{3+}$	1208.4384	1208.4349	-2.9
$y25^{2+}$	1422.5268	1422.5223	-3.2
y16	1773.6877	1773.6833	-2.5
$y16^{2+}$	887.3475	887.3446	-3.3
y13	1371.5191	1371.5139	-3.8
y12	1300.4820	1300.4783	-2.8
y7	811.3655	811.3630	-3.1
y6	664.2971	664.2949	-3.3
$b32^{3+}$	1168.7523	1168.7478	-3.9
$b27^{2+}$	1480.5091	1480.5044	-3.2
$b26^{2+}$	1406.9749	1406.9701	-3.4
$b21^{2+}$	1162.4166	1162.4125	-3.5
b17	1850.6203	1850.6141	-3.4
b8	780.2617	780.2594	-2.9

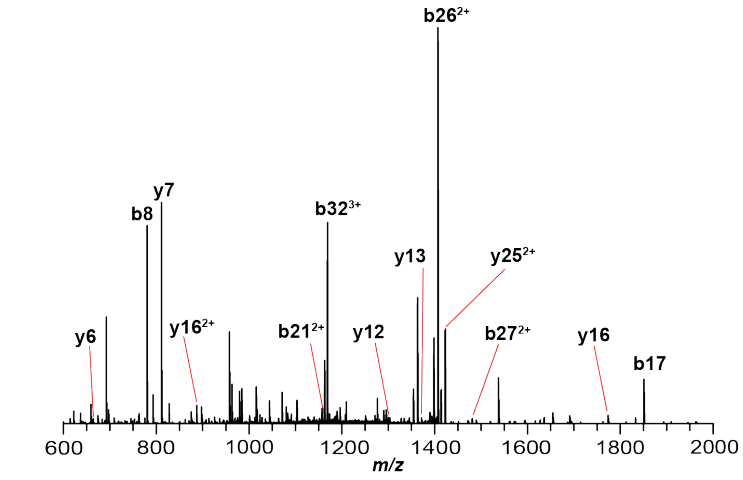

C = site of IAA labeling

Figure S22: HR-ESI-MS/MS of 1-IAA labeled freyrasin variant N(-13)A. (A) Molecular ion chosen for fragmentation by CID. (B) Proposed structure of freyrasin N(-13)A after trypsin digest and one IAA labeling event. Observed b and y ions are annotated. (C) Table of CID spectrum ion assignments. (D) CID spectrum of freyrasin N(-13)A. The presence of b and y series ions in ring 4 suggests that it may be the final thioether linkage formed by PapB *in vivo*.

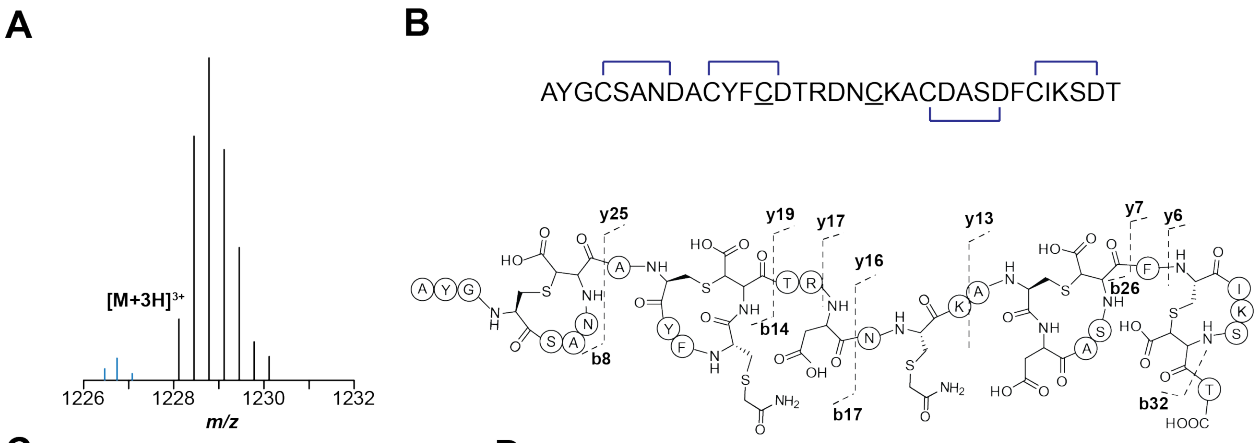

C

Ion	Calc. (Da)	Obs. (Da)	Error (ppm)
$[M+3H]^{3+}$	1228.1175	1228.1136	-3.2
$y25^{2+}$	1452.0453	1452.0408	-3.1
$y19^{2+}$	1073.4353	1073.4320	-3.1
$y17^{2+}$	944.8610	944.8578	-3.4
y16	1773.6877	1773.6826	-2.9
$y16^{2+}$	887.3475	887.3444	-3.5
y13†	1371.5191	1371.5146	-3.3
y7	870.4026	870.3996	-3.4
y7	811.3655	811.3626	-3.6
y6	664.2971	664.2936	-5.3
$b32^{3+}$	1188.4314	1188.4269	-3.8
$b26^{2+}$	1436.4935	1436.4889	-3.2
b17	1909.6574	1909.6520	-2.8
b14	1537.4817	1537.4768	-3.2
b8	780.2617	780.2592	-3.2

C = site of IAA labeling
†Present in CID near baseline
y7 is IAA-labeled ring 6

D

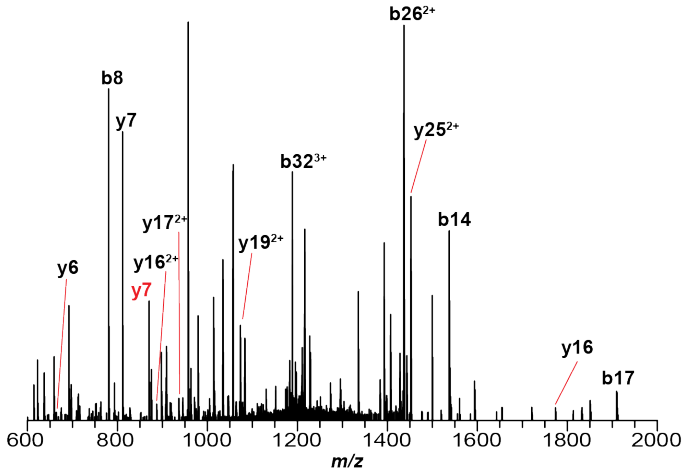

Figure S23: HR-ESI-MS/MS of 2-IAA labeled freyrasin variant N(-13)A. (A) Molecular ion chosen for fragmentation by CID. (B) Proposed structure of freyrasin N-13A after trypsin digest and two IAA labeling events. Observed b and y ions are annotated. (C) Table of CID spectrum ion assignments. (D) CID spectrum of freyrasin N(-13)A. The presence of b and y series ions in ring 3 suggests that it may be the penultimate ring formed by PapB *in vivo*. It is worth noting, however, that $y7^{+}$ has two peaks, one corresponding to a labeled Cys26, suggesting that rings 3 and 6 are both installed prior to ring 4. The doubly-alkylated species is a low abundance ion and competing species from MBP fragmentation results in a number of unidentifiable ions.

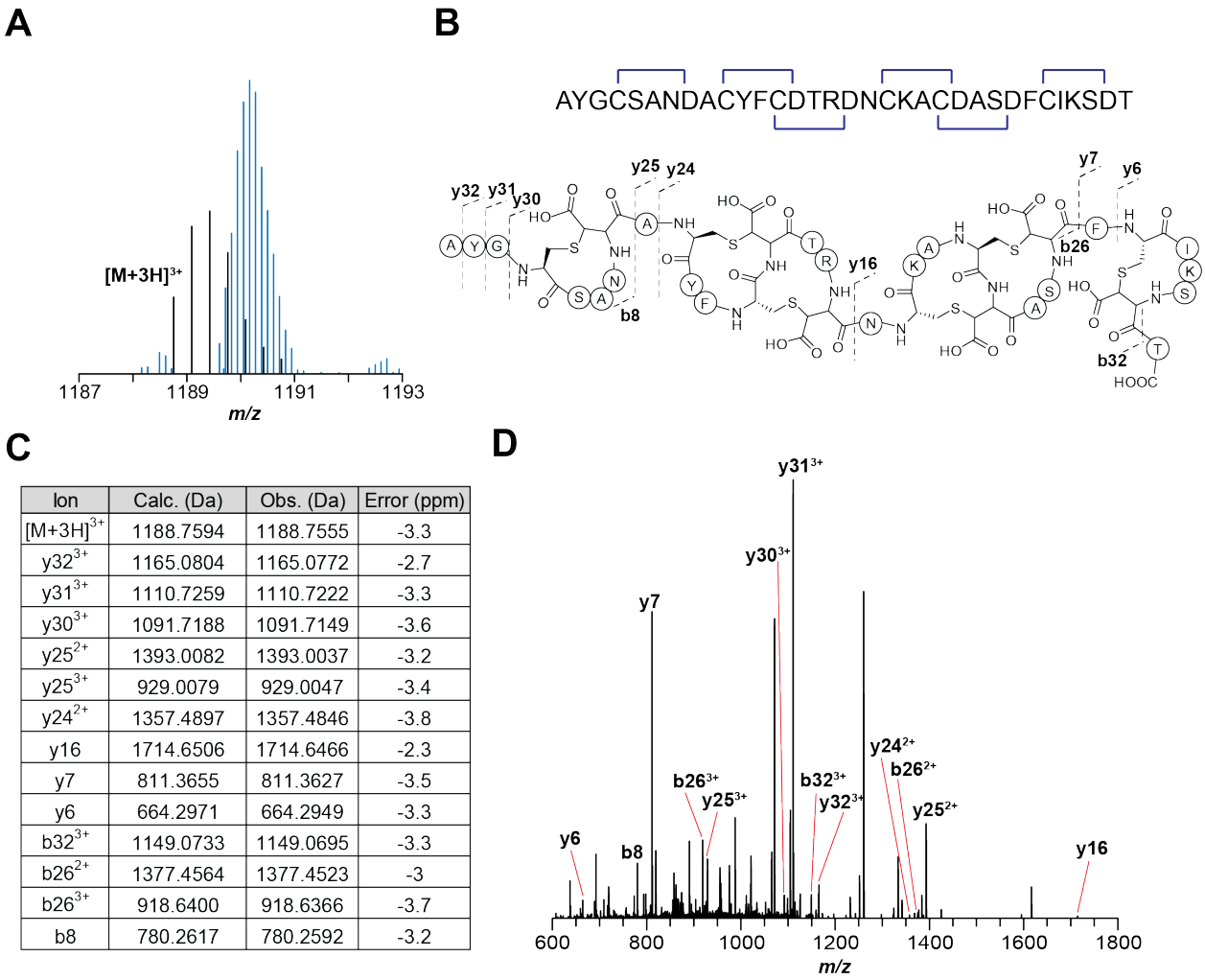

Ion	Calc. (Da)	Obs. (Da)	Error (ppm)
$[M+3H]^{3+}$	1188.7594	1188.7555	-3.3
$y32^{3+}$	1165.0804	1165.0772	-2.7
$y31^{3+}$	1110.7259	1110.7222	-3.3
$y30^{3+}$	1091.7188	1091.7149	-3.6
$y25^{2+}$	1393.0082	1393.0037	-3.2
$y25^{3+}$	929.0079	929.0047	-3.4
$y24^{2+}$	1357.4897	1357.4846	-3.8
y16	1714.6506	1714.6466	-2.3
y7	811.3655	811.3627	-3.5
y6	664.2971	664.2949	-3.3
$b32^{3+}$	1149.0733	1149.0695	-3.3
$b26^{2+}$	1377.4564	1377.4523	-3
$b26^{3+}$	918.6400	918.6366	-3.7
b8	780.2617	780.2592	-3.2

Figure S24: HR-ESI-MS/MS of freyrasin with excised RRE supplied *in trans*. (A) Molecular ion chosen for fragmentation by CID (2+ and 4+ species were insufficient for fragmentation). Contaminating peaks are in blue. (B) Proposed structure of freyrasin after trypsin digest. Observed b and y ions are annotated. (C) Table of CID spectrum ion assignments. (D) CID spectrum of freyrasin. The limited fragmentation pattern is consistent with previously reported tandem MS of wild-type freyrasin. This is consistent with a successful rescue of the RRE-deletion PapB variant by addition of the RRE *in trans*, resulting in thioether installation in the PapA precursor.

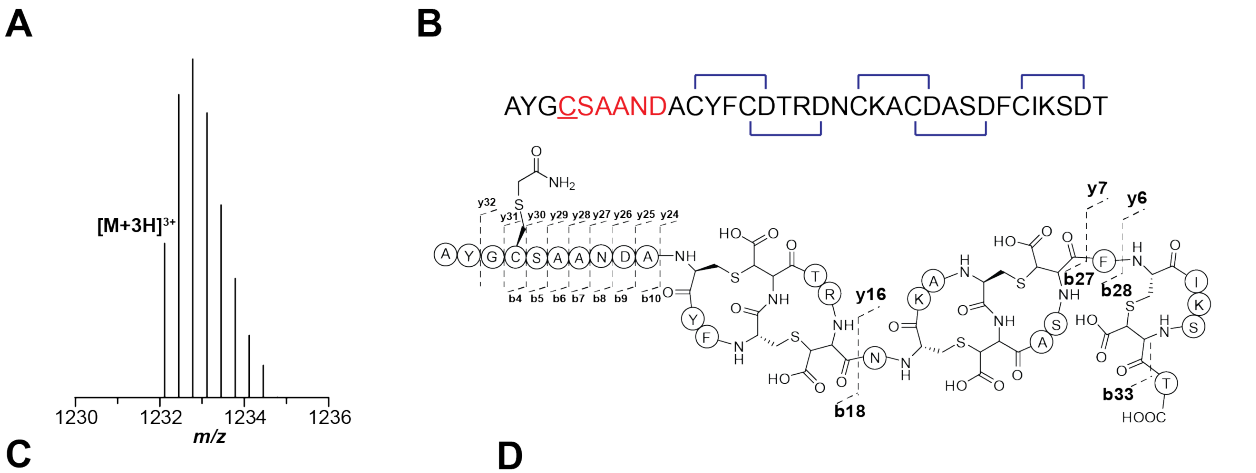

C

Ion	Calc. (Da)	Obs. (Da)	Error (ppm)
$[M+3H]^{3+}$	1232.1175	1232.1149	-2.1
$y32^{2+}$	1730.6223	1730.6163	-3.4
$y32^{3+}$	1154.0840	1154.0796	-3.8
$y31^{3+}$	1135.0768	1135.0694	-6.5
$y30^{2+}$	1622.0963	1622.0908	-3.3
$y29^{2+}$	1578.5803	1578.5743	-3.8
$y28^{2+}$	1543.0617	1543.0563	-3.4
$y27^{2+}$	1507.5432	1507.5306	-8.3
$y26^{2+}$	1450.5217	1450.5173	-3.0
$y25^{2+}$	1393.0082	1393.0035	-3.3
$y24^{2+}$	1357.4897	1357.4854	-3.1
y16	1714.6506	1714.6446	-3.4
$y16^{2+}$	857.8289	857.8261	-3.2
y7	811.3655	811.3628	-3.3
y6	664.2971	664.2948	-3.4
$b33^{3+}$	1192.4314	1192.4271	-3.6
$b28^{2+}$	1516.0277	1516.0227	-3.2
$b27^{2+}$	1442.4935	1442.4889	-3.1
b18	1980.6946	1980.6872	-3.7
$b18^{2+}$	990.8509	990.8474	-3.5
b10	981.3731	981.3697	-3.4
b9	910.3360	910.3328	-3.5
b8	795.3090	795.3064	-3.2
b7	681.2661	681.2641	-2.9
b6	610.2290	610.2273	-2.7
b5†	539.1919	539.1905	-2.5
b4†	452.1598	452.1588	-2.2

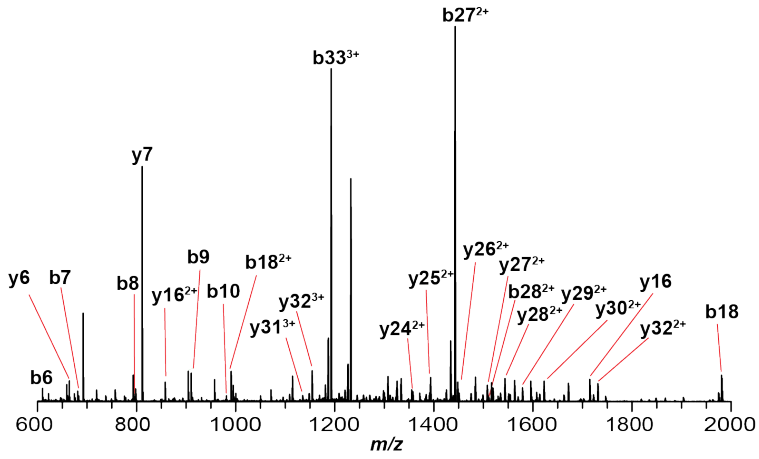

C = site of IAA labeling
†Outside range of displayed spectrum

Figure S25: HR-ESI-MS/MS of 1-IAA labeled freyrasin ring expansion variant. (A) Molecular ion chosen for fragmentation by CID. (B) Proposed structure of the freyrasin ring expansion variant after trypsin digest and one IAA labeling event. Area of text in red represents the expanded Cys-X_4-Asp motif. Observed b and y ions are annotated. (C) Table of CID spectrum ion assignments. (D) CID spectrum of the ring expansion variant.

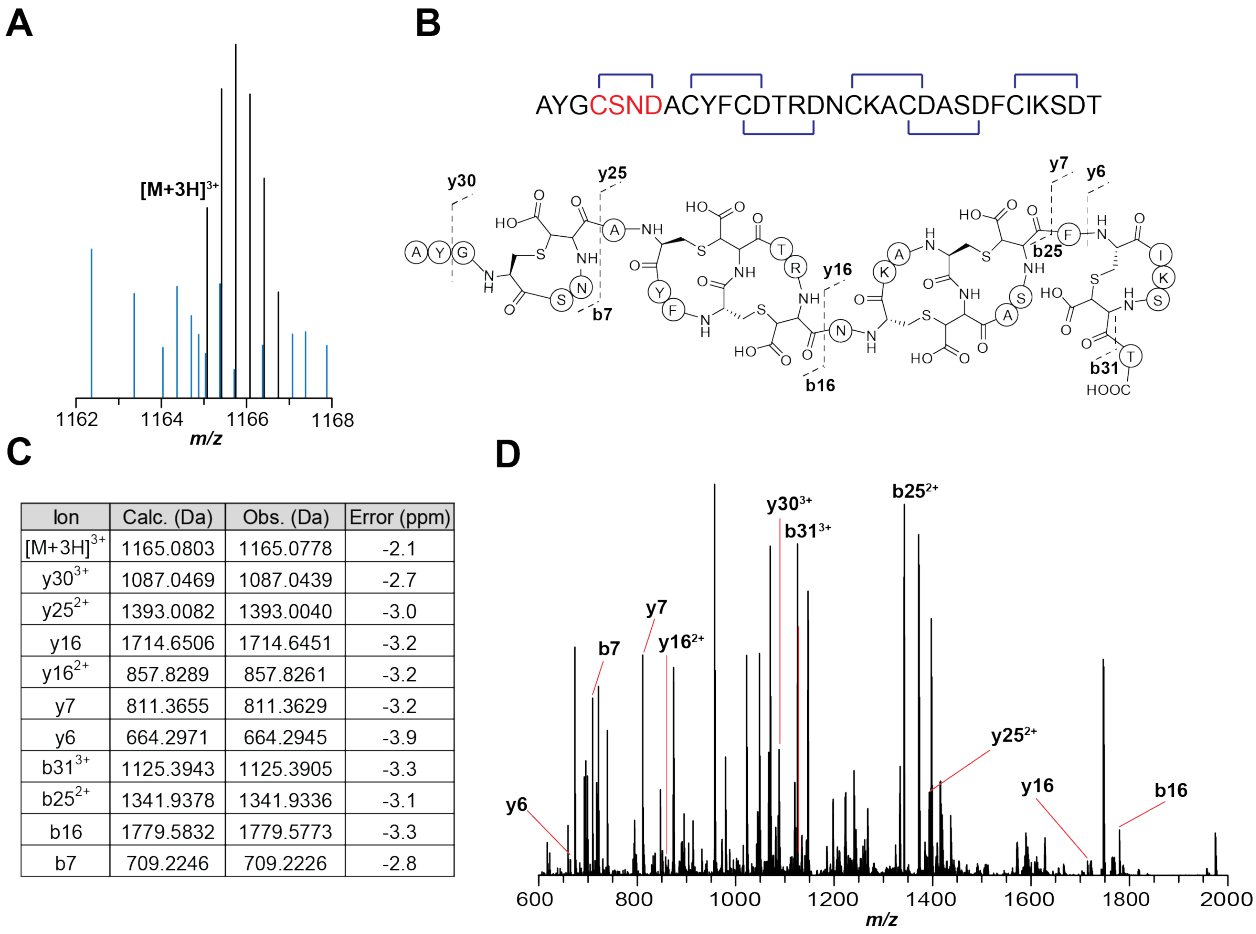

Ion	Calc. (Da)	Obs. (Da)	Error (ppm)
$[M+3H]^{3+}$	1165.0803	1165.0778	-2.1
$y30^{3+}$	1087.0469	1087.0439	-2.7
$y25^{2+}$	1393.0082	1393.0040	-3.0
y16	1714.6506	1714.6451	-3.2
$y16^{2+}$	857.8289	857.8261	-3.2
y7	811.3655	811.3629	-3.2
y6	664.2971	664.2945	-3.9
$b31^{3+}$	1125.3943	1125.3905	-3.3
$b25^{2+}$	1341.9378	1341.9336	-3.1
b16	1779.5832	1779.5773	-3.3
b7	709.2246	709.2226	-2.8

Figure S26: HR-ESI-MS/MS of freyrasin ring contraction variant. (A) Molecular ion chosen for fragmentation by CID. Contaminating peaks are in blue. (B) Proposed structure of the freyrasin ring contraction variant after trypsin digest. Area of text in red represents the contracted Cys-X_2-Asp motif. Observed b and y ions are annotated. (C) Table of CID spectrum ion assignments. (D) CID spectrum of the ring expansion variant. The limited observation of b and y ions surrounding the thioether rings of freyrasin is consistent with previously reported tandem MS of the wild-type molecule. The singly-alkylated species did not produce adequate fragmentation for inclusion. The fully-modified species is a low abundance ion and competing species from MBP fragment peaks results in a large number of high abundance unidentifiable peaks in the CID.

Figure S27: 1H-1H TOCSY correlations and assignments of freyrasin D6E. Amino acids were identified by a combination of their known TOCSY correlation patterns and similarity to a previously reported WT freyrasin 1H-1H TOCSY spectrum.[1] Amino acid residue sequence was assigned based on NH-NH NOESY correlations (see **Figure S27**).

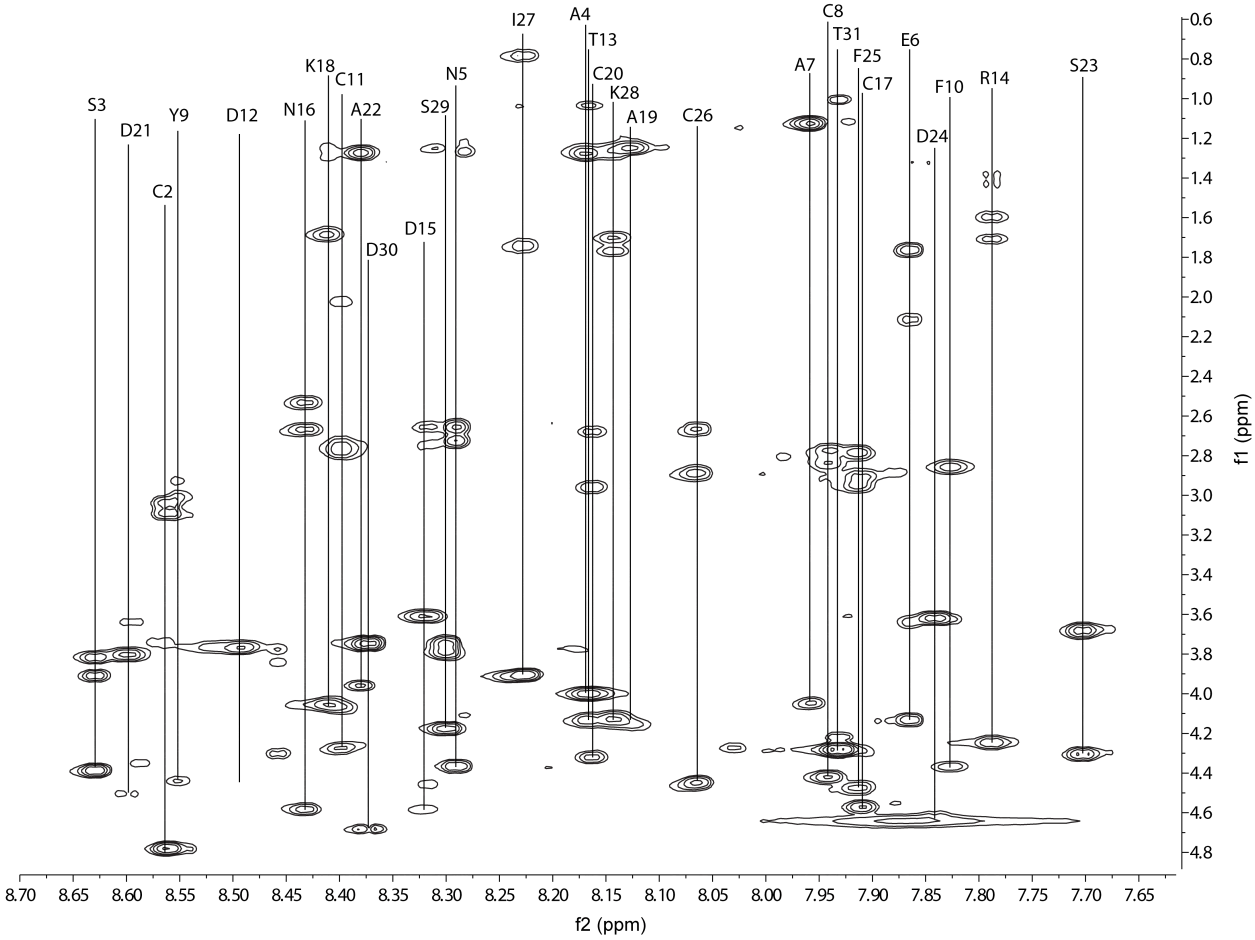

Figure S28: Amide NOESY correlations of freyrasin variant D6E. (A) Contacts from residues 1-15. (B) Contacts from residues 15-31. Amino acids are assigned based on their amide proton chemical shifts along the diagonal, and neighboring residue correlations are labelled off diagonal. Residues that did not generate NOESY correlations were assigned based on the known precursor peptide primary sequence, process of elimination, side chain proton correlations and similarity to the previously reported spectrum for WT freyrasin.[1]

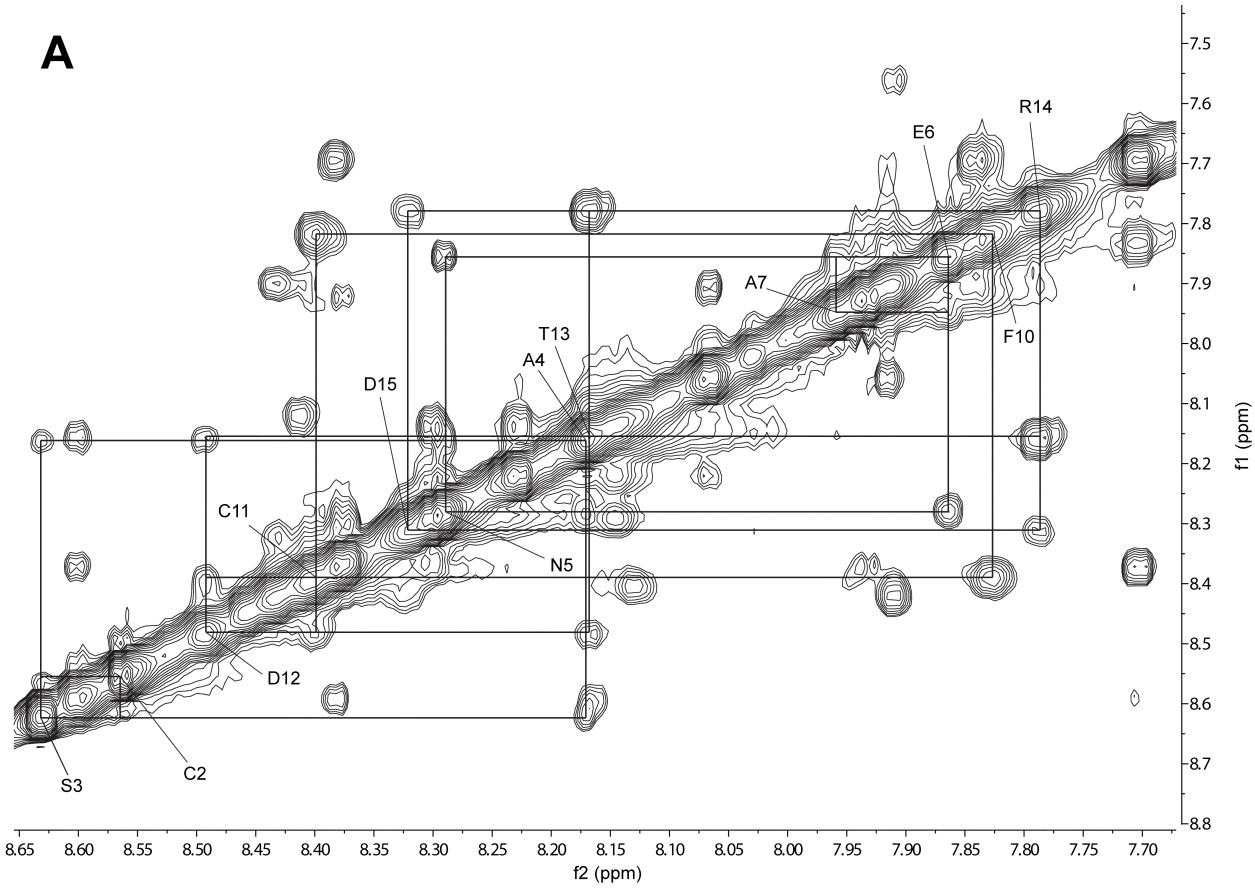

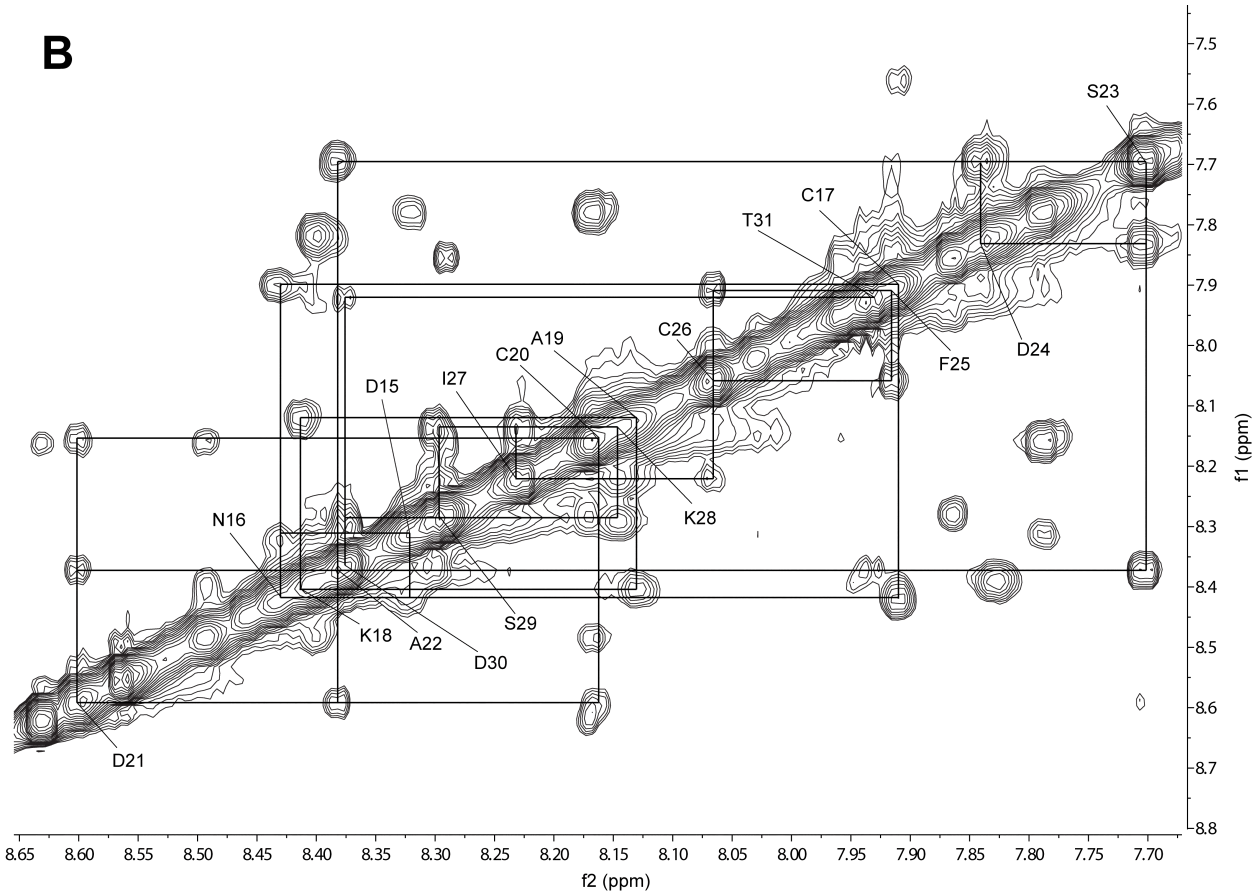
B
S23
C17
T31
C26
A19
C20
D15
I27
F25
D24
K28
N16
S29
K18
A22
D30
D21
f1 (ppm)
f2 (ppm)

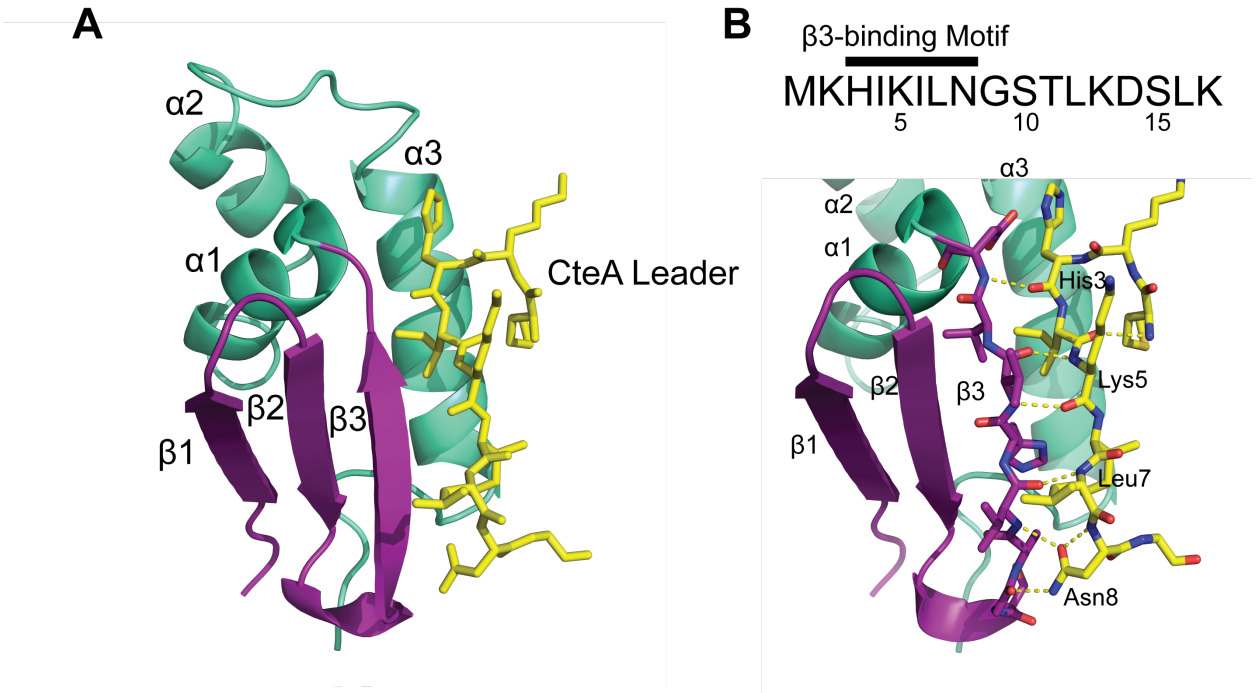

Figure S29: Crystal structure of CteB RRE in complex with CteA leader peptide.[6] (A) Interaction of the CteA leader peptide with the β3 and α3 motifs of the CteB RRE (PDB code: 5WGG). (B) Stick model indicating points of contact between the CteA leader peptide and the β3 sheet of the CteB RRE. In this case, the leader Asn8 is within polar contact distance of backbone amides in Gly21 and Val23 of CteB. This Asn is also conserved in PapA, as indicated in **Figure 4** (albeit at position 6).

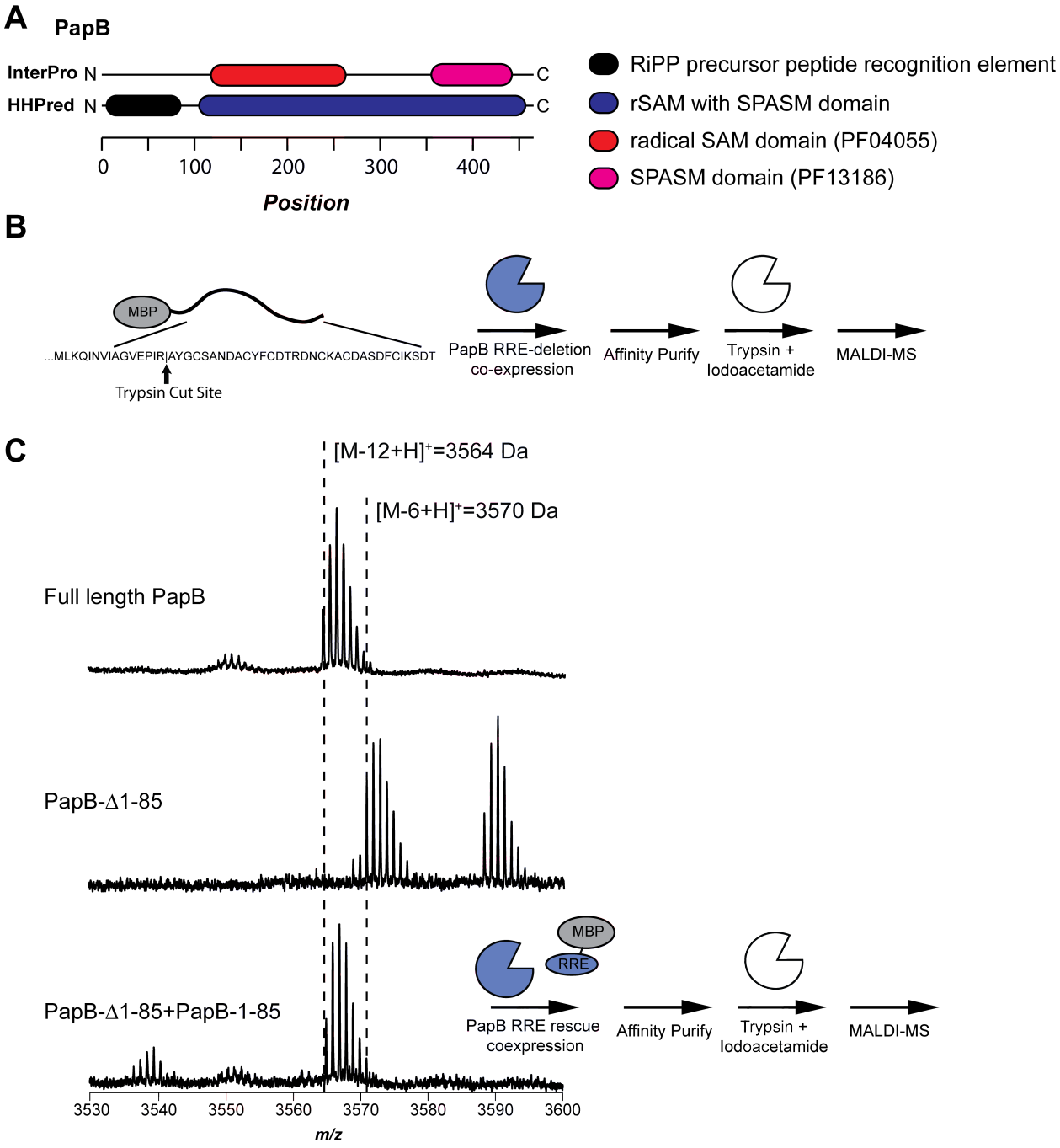

Figure S30: RRE-deleted PapB and rescue with MBP-PapB-RRE. (A) Domain structure of PapB as predicted by HHpred and InterPro.[7,8] (B) Protocol for generation of PapA core for MALDI-TOF-MS analysis. (C) MALDI-TOF-MS analysis of core peptide after coexpression with the RRE-deleted PapB (residues 86-467). Mass loss of 6 Da is consistent with the formation of 3 disulfide linkages and a lack of thioether formation in the core. When the RRE (PapB residues 1-85) was supplied *in trans*, the core peptide mass was equivalent to reactions that received full length PapB. The structure of the rescued core was verified by high-resolution and tandem MS (**Figure S24**). The *m/z* 3589 Da species is an unknown contaminant.

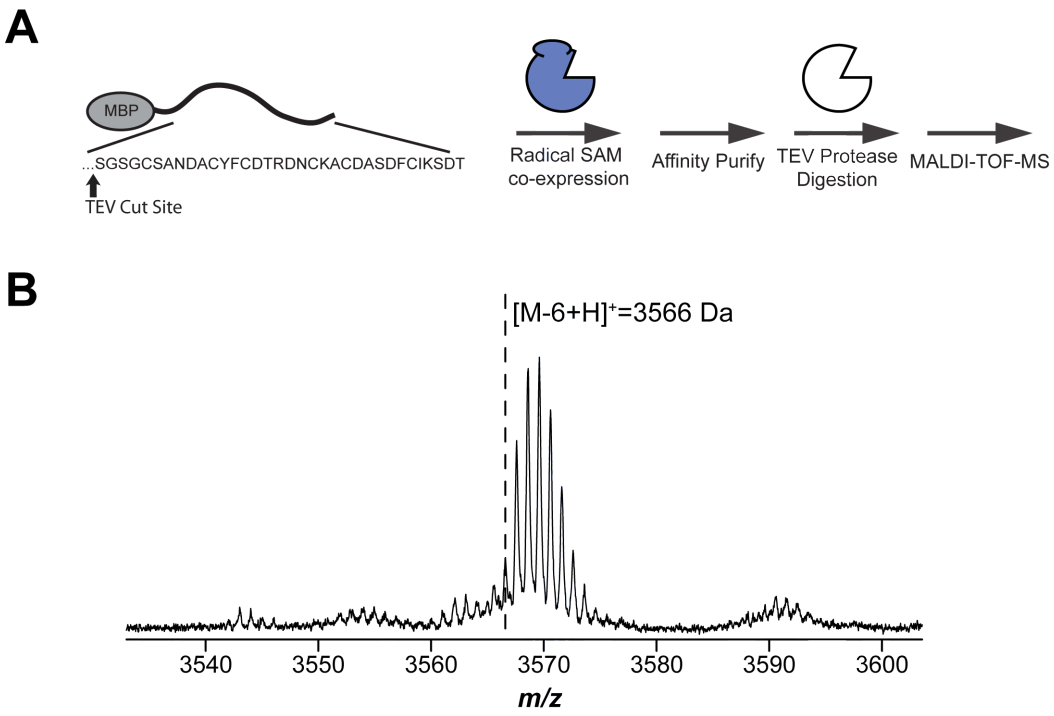

Figure S31: PapA leader deletion and co-expression with PapB. (A) Protocol for generation of PapA core for MALDI-TOF-MS analysis. (B) After TEV protease cleavage, the resultant peptide displayed a mass loss of 6 Da, consistent with the formation of 3 disulfide bonds.

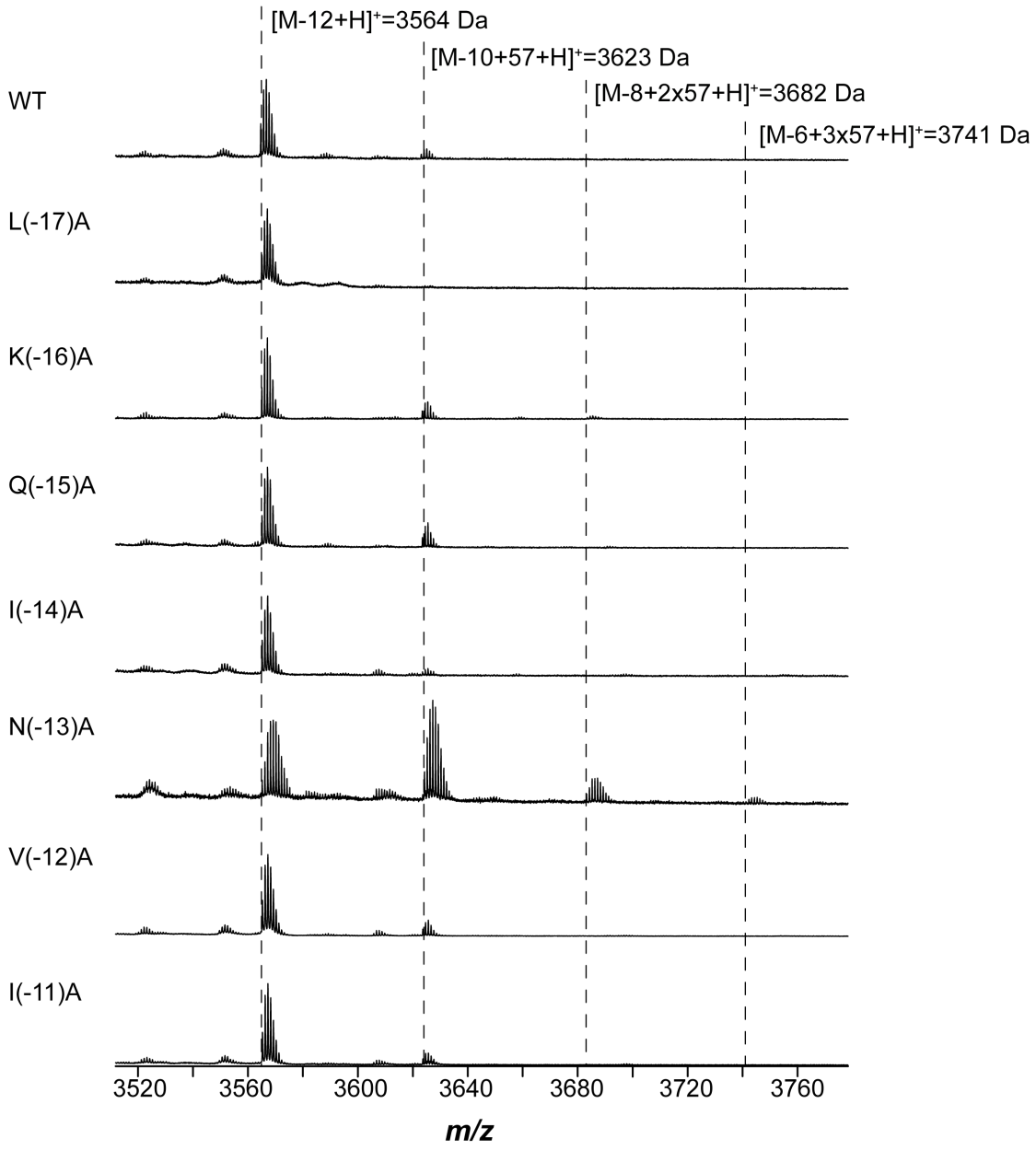

Figure S32: Iodoacetamide labeling of PapA leader Ala scan coexpression. Coexpression of MBP-PapA with PapB in a leader peptide Ala scan. The MBP-tagged PapA variants were purified and treated with trypsin followed by alkylation with IAA (+57 Da per label). Consistent with the isotopic pattern of the N(-13)A variant, the population is heavily labeled by IAA indicating a lack processing this variant.

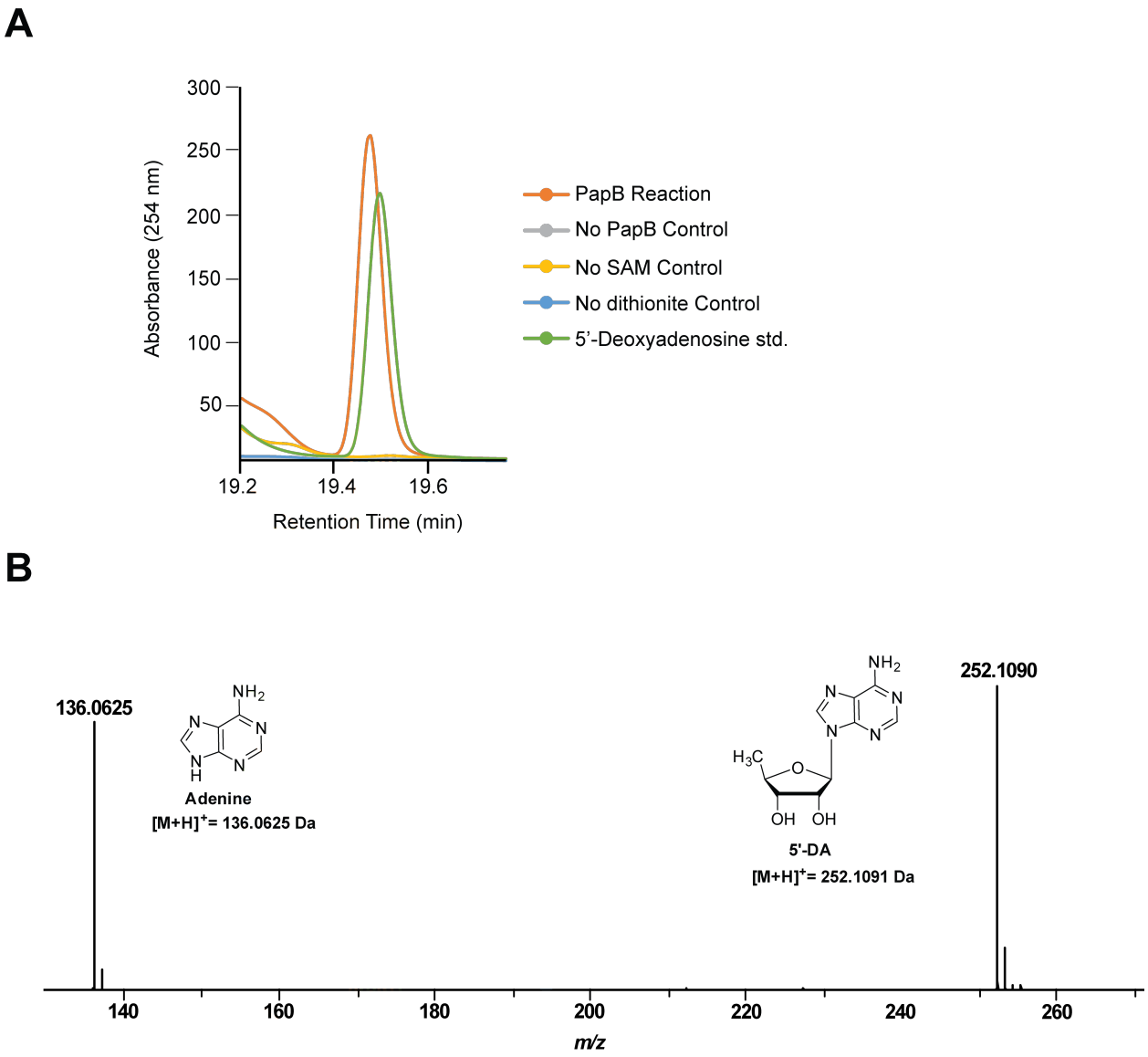

Figure S33: Detection of 5'-DA in the PapB reaction mixture by HRMS (A) PapB *in vitro* reaction mixtures HPLC analysis. Orange trace: full PapB reaction mixture (PapA substrate + PapB + *S*-adenosylmethionine (SAM) + dithionite); Grey trace: reaction mixture devoid of PapB; Yellow trace: reaction mixture devoid of SAM; Blue trace: reaction mixture devoid of dithionite; Green trace: 5'-deoxydenosine standard sample (std). Formation of 5'-DA was observed only in the full reaction mixture (retention time 19.5 min), which co-eluted with an authentic sample of 5'-DA. (B) The compound eluting at 19.5 min was analyzed by HRMS. The compound was confirmed as 5'-DA (calc. mass 252.1091 Da; obsv. mass 252.1090 Da; error, 0.3 ppm). Adenine was also observed, which resulted from fragmentation of the N-glycosyl bond (calc. mass 136.0625 Da; obsv. mass 136.0625 Da; error, 0 ppm).

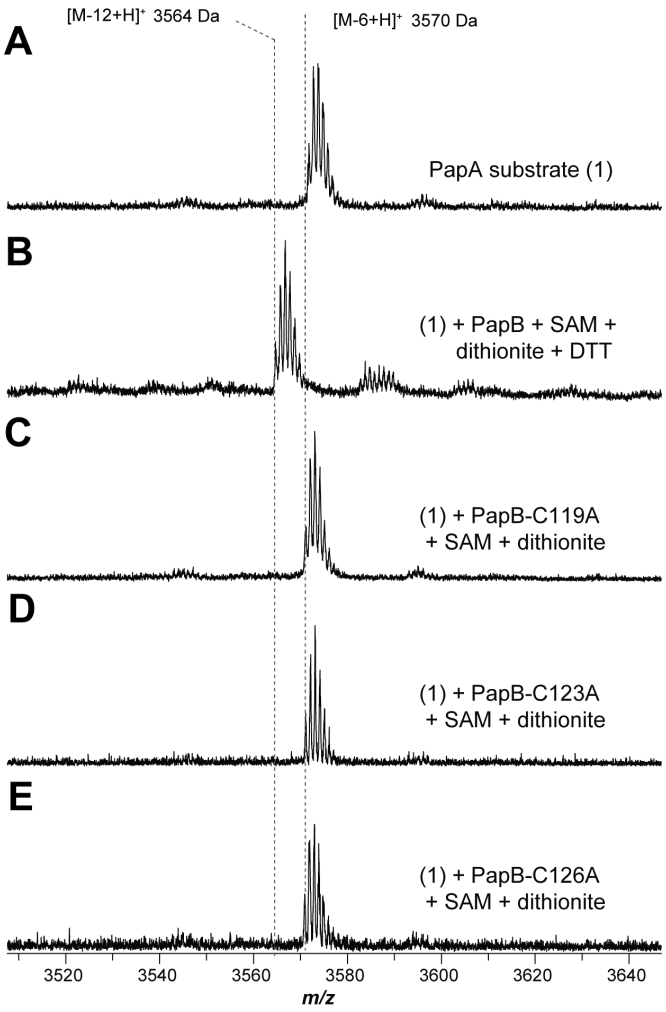

Figure S34: MALDI-TOF-MS analysis of the Cys variants of PapB. (A) Mass spectrum of the PapA peptide, *m/z* 3570 Da. Mass loss of 6 Da is consistent with three disulfide bond formation as reported previously.[1] (B) Mass spectrum of the peptide after reaction with the full array of reactants, *m/z* 3564 Da (DTT=dithiothreitol). This is consistent with the formation of six thioether bonds (loss of 12 Da from the unmodified peptide)[1] (C) Identical to panel B except PapB-C119A variant was used (D) Identical to panel B except PapB-C123A variant was used (E) Identical to panel B except PapB-C126A variant was used. No modification was observed on substituting cysteines in the [4Fe-4S] cluster binding motif in PapB with Ala.

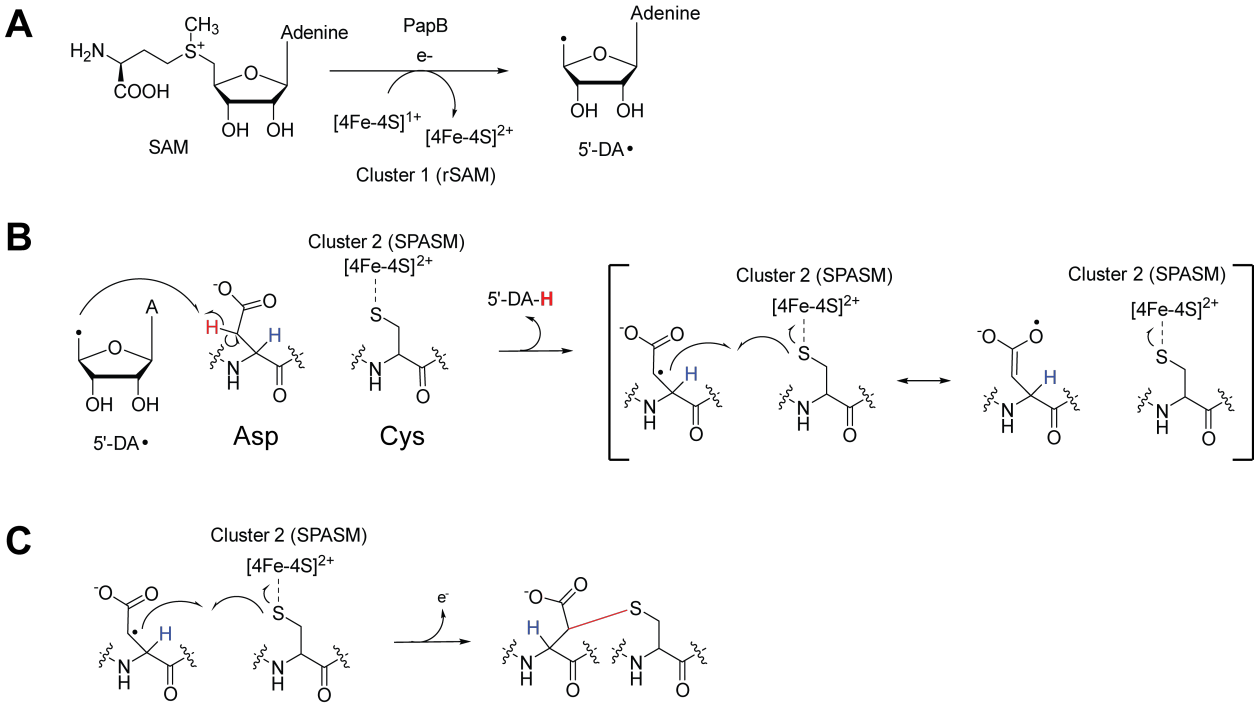

Figure S35: Proposed mechanism for PapB. (A) [4Fe-4S]-mediated reductive cleavage of SAM to generate the 5'-DA radical. (B) The resultant 5'-DA radical is proposed to abstract hydrogen from the acceptor site on the peptide (in this case, from the β-carbon of Asp), generating a radical on the peptide substrate. The sulfur of the Cys donor is proposed to be coordinated by a SPASM [4Fe-4S] auxiliary cluster and (C) directed to combine with the radical on the acceptor residue to form a thioether linkage. The order of events in this mechanism remain under investigation.

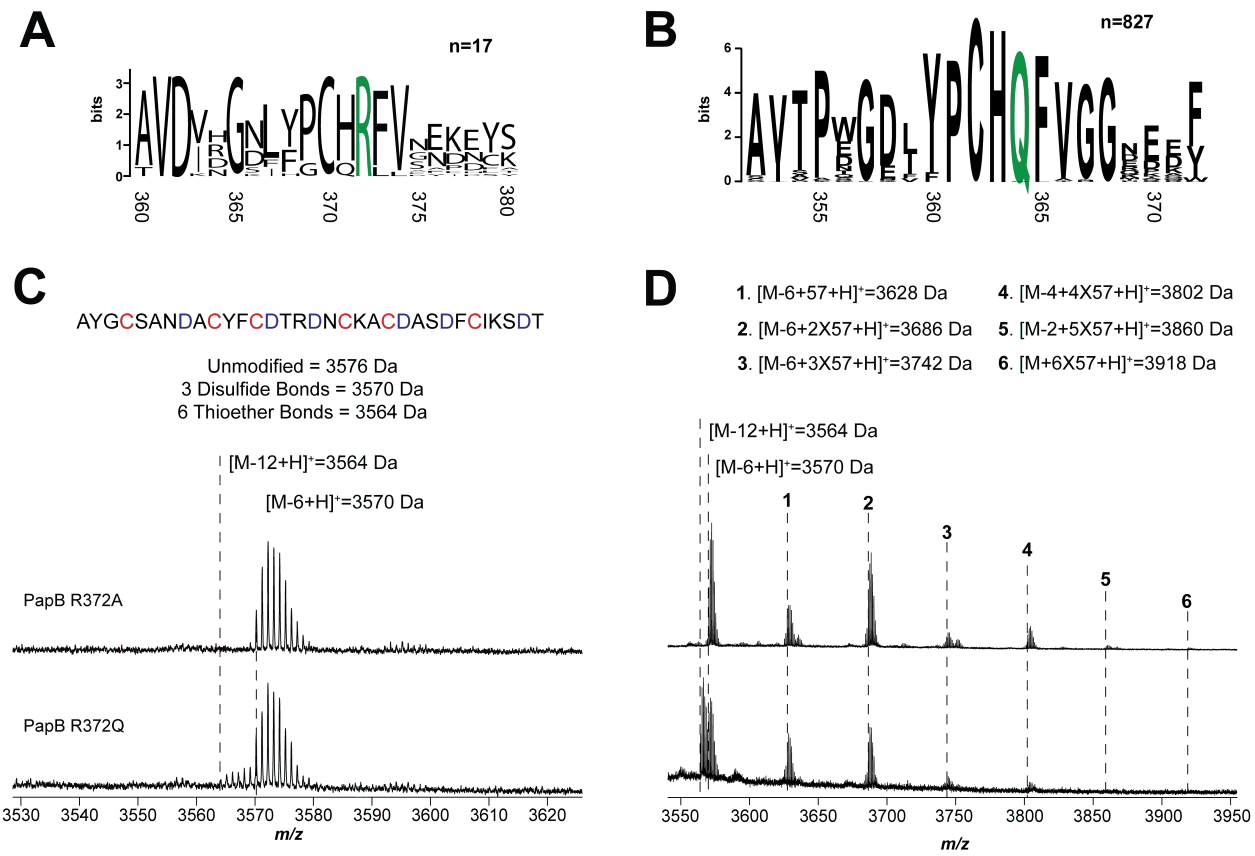

Figure S36: Mutagenesis of PapB-Arg372. (A) Sequence logo generated from multiple sequence alignment of 17 Cys-X_3-Asp-modifying ranthisynthases. Arg372 is 100% conserved. (B) Sequence logo generated from alignment of 827 (non-identical) thermocellin-like maturases. The active site Gln is 99.5% conserved. Numbering is based on the primary sequence of CteB.[6] (C) Trypsin digest of PapA after expression with PapB containing substitutions at Arg372. PapB-R372A and -R372D were unable to modify PapA and a mass loss of 6 Da was observed, consistent with the formation of three disulfide bonds. PapB-R372Q modified PapA with low efficiency. (D) IAA labeling indicates the presence of extensive free thiols when PapA is co-expressed with the Arg372 variants (top, R372A; bottom, R372Q).

Figure S37: Alignment of rSAM proteins with SPASM domains. (A) Partial sequence alignment of PapB with two structurally characterized proteins with a SPASM domain, anSME (PDB code: 4K37) and CteB (PDB code: 5WGG). anSME has 4 Cys residues coordinated to auxiliary cluster 1 in the SPASM domain (TIGR04085). CteB and PapB each have 3 Cys, indicating the presence of an open coordination site for the precursor substrate Cys in auxiliary cluster 1. (B) Domain architecture diagram of the above proteins as determined by InterPro.[8] CteB (5WGG) and PapB contain an N-terminal RRE domain, which causes the start of the rSAM domain (PF04055) to begin around residue 100.

A

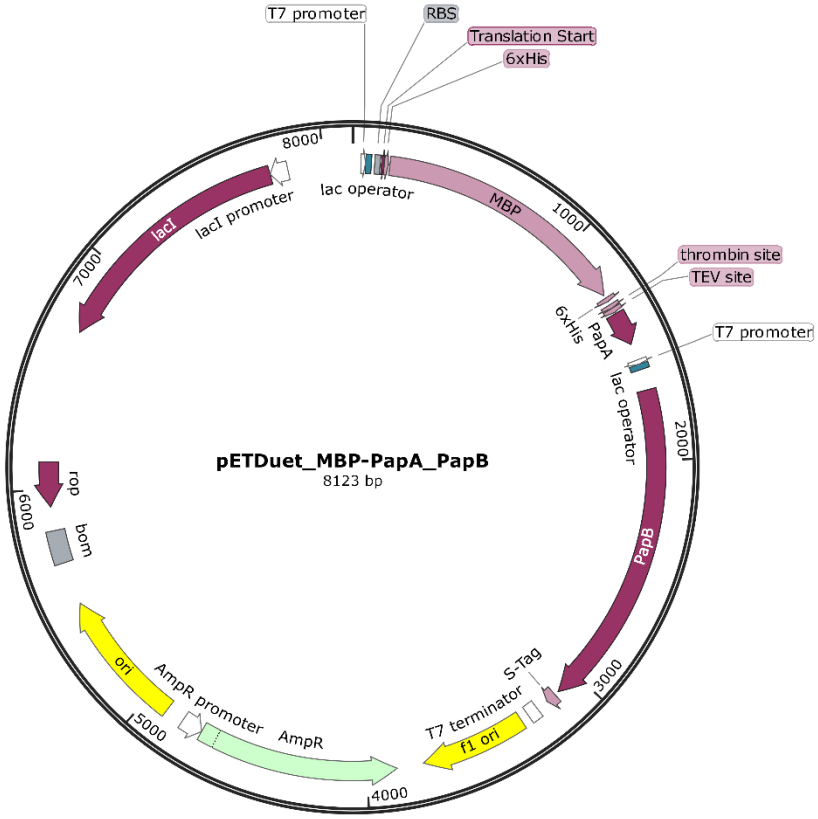

B

CGTAGAGGATCGAGATCGATCTCGATCCCGCGAAATTAATACGACTCACTATAGGGGAATTGTGAGCGGATAACAATTCCCCTCTAGAAATAATTTTGTTTAACTTTAAGA
AGGAGATATACCATGGGCAGCAGCCATCACCATCATCACCACAGCCAGAAAATCGAAGAAGGTAAACTGGTAATCTGGATTAACGGCGATAAAGGCTATAACGGTCTCGCT
GAAGTCGGTAAGAAATTCGAGAAAGATACCGGAATTAAAGTCACCGTTGAGCATCCGGATAAACTGGAAGAGAAATTCCCACAGGTTGCGGCAACTGGCGATGGCCCTGAC
ATTATCTTCTGGGCACACGACCGCTTTGGTGGCTACGCTCAATCTGGCCTGTTGGCTGAAATCACCCCGGACAAAGCGTTCCAGGACAAGCTGTATCCGTTTACCTGGGAT
GCCGTACGTTACAACGGCAAGCTGATTGCTTACCCGATCGCTGTTGAAGCGTTATCGCTGATTTATAACAAAGACCTGCTGCCGAACCCGCCAAAAACCTGGGAAGAGATC
CCGGCGCTGGATAAAGAACTGAAAGCGAAAGGTAAGAGCGCGCTGATGTTCAACCTGCAAGAACCGTACTTCACCTGGCCGCTGATTGCTGCTGACGGGGGTTATGCGTTC
AAGTATGAAAACGGCAAGTACGACATTAAAGACGTGGGCGTGGATAACGCTGGCGCGAAAGCGGGTCTGACCTTCCTGGTTGACCTGATTAAAAACAAACACATGAATGCA
GACACCGATTACTCCATCGCAGAAGCTGCCTTTAATAAAGGCGAAACAGCGATGACCATCAACGGCCCGTGGGCATGGTCCAACATCGACACCAGCAAAGTGAATTATGGT
GTAACGGTACTGCCGACCTTCAAGGGTCAACCATCCAAACCGTTCGTTGGCGTGCTGAGCGCAGGTATTAACGCCGCCAGTCCGAACAAAGAGCTGGCGAAAGAGTTCCTC
GAAAACTATCTGCTGACTGATGAAGGTCTGGAAGCGGTTAATAAAGACAAACCGCTGGGTGCCGTAGCGCTGAAGTCTTACGAGGAAGAGTTGGCGAAAGATCCACGTATT
GCCGCCACCATGGAAAACGCCCAGAAAGGTGAAATCATGCCGAACATCCCGCAGATGTCCGCTTTCTGGTATGCCGTGCGTACTGCGGTGATCAACGCCGCCAGCGGTCGT
CAGACTGTCGATGAAGCCCTGAAAGACGCGCAGACTAATTCGAGCTCCCACCATCACCATCACCACGCGTCGAATGTACCGCTGGTTCCGCGTGGATCTGAGAACCTGTAC
TTCCAATCCGGATCCATGTTGAAGCAAATCAATGTTATTGCAGGAGTTAAAGAACCAATTCGCGCTTATGGTTGCTCAGCCAATGATGCTTGCTATTTCTGTGATACTAGA
GATAACTGCAAAGCATGTGATGCAAGTGATTTTTGTATCAAATCGGATACCTAGGCGGCCGCAGCATAATGCTTAAGTCGAACAGAAAGTAATCGTATTGTACACGGCCGC
ATAATCGAAATTAATACGACTCACTATAGGGGAATTGTGAGCGGATAACAATTCCCCATCTTAGTATATTAGTTAAGTATAAGAAGGAGATATACATATGGCAGATCTCAA
TTGGATATCGGCCGGCCACGCGATCGCTGACGTCATGGCTAATCTGATTCAGGATAGAGAAGATGAACTCATTCATTTCCACCCTTATAAATTGTTTGAAGTTGACTCAAA
AACCTTCTTTTATAACGTTGTAACGAATGCCATATTTGAGATTGACTCATTAATTATCGATATTCTACATAGTAAAGGCAAAAACGAGGAGCACGTTGTTAAGGATTTAGC
CGAGCGTTATGAATTATCACAGGTAAGAGAAGCCATCCAAAATATGAAGGAAGCATACATTATTGCCACAGATGCTAACATATCAGATGTTGAAAAAATGGGGATACTTGA
TAACTCGCAAAGAGTCTTCAAATTATCCTCTCTGACCTTATTTATGGTGCAAGAATGTAACCTTAGATGTACTTACTGTTATGGGGAGGAAGGAGAATATAATCAAAAAGG
GAAAATGACTTCAGAGATTGCTAGATCTGCCGTAGACTTTCTGATCCAACAATCGGGTGAAATAGAGCAATTGAATATCACCTTTTTCGGCGGTGAACCCTTGTTAAATTT
CCCTCTCATACAAGAGACGGTACAGTATGTTCATGAGCAATCCGAAATTCATAATAAGAAATTTTCTTTTTCAATAACGACAAATGGTACACTTATCACTCCTAAAATCAA
AAACTTTTTTTACAAACATCATTTTGCGGTGCAGACCAGCATAGATGGTGATGAAAAAACGCATAATTTCAATCGTTTTTTTAAAGGTGGACAAGGATCCTACGATTTACT
CTTGAAGCGTACAGAAGAAATGAGAAATGATCGTAAAATAGGCGCGCGCGGTACAGTAACTCCTGCAGAGCTTGACCTTTCTAAATCTTTTGATCATTTAGTGAAACTGGG
GTTCAGAAAAATATATTTATCTCCAGCACTTTATTCCCTATCGGACGATCATTACGATACTTTATCCAAAGAAATGGTTAAACTCGTAGAGCAATTCCGAGAGTTACTGGA
ACGTGAAGACTATGTTACAGCCAAAAAAATGTCCAATGTCCTTGGCATGCTTAGTAAAATTCATTCTGGCGGTCCTAGAATCCACTTTTGTGGAGCGGGTACGAATGCGGC
CGCTGTTGATGTTAGGGGAAATTTGTTCCCTTGCCATCGTTTTGTAGGCGAGGATGAATGCTCTATTGGCAATCTATTTGATGAAGATCCATTGAGCAAACAGTATAATTT
CATTGAGAATTCAACAGTAAGAAATAGAACCACCTGTTCAAAGTGTTGGGCCAAAAATCTTTGTGGTGGTGGATGCCATCAAGAGAACTTCGCGGAGAACGGAAATGTCAA
TCAACCTGTCGGTAAACTTTGCAAAGTAACTAAGAATTTCATTAACGCTACTATAAATTTATACCTCCAACTTACCCAGGAACAAAGAAGCATCCTTTTTGGTTAGGGTAC
CCTCGAGTCTGGTAAAGAAACCGCTGCTGCGAAATTTGAACGCCAGCACATGGACTCGTCTACTAGCGCAGCTTAATTAACCTAGGCTGCTGCCACCGCTGAGCAATAACT
AGCATAACCCCTTGGGGCCTCTAAACGGGTCTTGAGGGGTTTTTTGCTGAAAGGAGGAACTATATCCGGATTGGCGAATGGGACGCGCCCTGTAGCGGCGCATTAAGCGCG
GCGGGTGTGGTGGTTACGCGCAGCGTGACCGCTACACTTGCCAGCGCCCTAGCGCCCGCTCCTTTCGCTTTCTTCCCTTCCTTTCTCGCCACGTTCGCCGGCTTTCCCCGT
CAAGCTCTAAATCGGGGGCTCCCTTTAGGGTTCCGATTTAGTGCTTTACGGCACCTCGACCCCAAAAAACTTGATTAGGGTGATGGTTCACGTAGTGGGCCATCGCCCTGA

TAGACGGTTTTTCGCCCTTTGACGTTGGAGTCCACGTTCTTTAATAGTGGACTCTTGTTCCAAACTGGAACAACACTCAACCCTATCTCGGTCTATTCTTTTGATTTATAA
GGGATTTTGCCGATTTCGGCCTATTGGTTAAAAAATGAGCTGATTTAACAAAAATTTAACGCGAATTTTAACAAAATATTAACGTTTACAATTTCTGGCGGCACGATGGCA
TGAGATTATCAAAAAGGATCTTCACCTAGATCCTTTTAAATTAAAAATGAAGTTTTAAATCAATCTAAAGTATATATGAGTAAACTTGGTCTGACAGTTACCAATGCTTAA
TCAGTGAGGCACCTATCTCAGCGATCTGTCTATTTCGTTCATCCATAGTTGCCTGACTCCCCGTCGTGTAGATAACTACGATACGGGAGGGCTTACCATCTGGCCCCAGTG
CTGCAATGATACCGCGAGACCCACGCTCACCGGCTCCAGATTTATCAGCAATAAACCAGCCAGCCGGAAGGGCCGAGCGCAGAAGTGGTCCTGCAACTTTATCCGCCTCCA
TCCAGTCTATTAATTGTTGCCGGGAAGCTAGAGTAAGTAGTTCGCCAGTTAATAGTTTGCGCAACGTTGTTGCCATTGCTACAGGCATCGTGGTGTCACGCTCGTCGTTTG
GTATGGCTTCATTCAGCTCCGGTTCCCAACGATCAAGGCGAGTTACATGATCCCCCATGTTGTGCAAAAAAGCGGTTAGCTCCTTCGGTCCTCCGATCGTTGTCAGAAGTA
AGTTGGCCGCAGTGTTATCACTCATGGTTATGGCAGCACTGCATAATTCTCTTACTGTCATGCCATCCGTAAGATGCTTTTCTGTGACTGGTGAGTACTCAACCAAGTCAT
TCTGAGAATAGTGTATGCGGCGACCGAGTTGCTCTTGCCCGGCGTCAATACGGGATAATACCGCGCCACATAGCAGAACTTTAAAAGTGCTCATCATTGGAAAACGTTCTT
CGGGGCGAAAACTCTCAAGGATCTTACCGCTGTTGAGATCCAGTTCGATGTAACCCACTCGTGCACCCAACTGATCTTCAGCATCTTTTACTTTCACCAGCGTTTCTGGGT
GAGCAAAAACAGGAAGGCAAAATGCCGCAAAAAAGGGAATAAGGGCGACACGGAAATGTTGAATACTCATACTCTTCCTTTTTCAATCATGATTGAAGCATTTATCAGGGT
TATTGTCTCATGAGCGGATACATATTTGAATGTATTTAGAAAAATAAACAAATAGGTCATGACCAAAATCCCTTAACGTGAGTTTTCGTTCCACTGAGCGTCAGACCCCGT
AGAAAAGATCAAAGGATCTTCTTGAGATCCTTTTTTTCTGCGCGTAATCTGCTGCTTGCAAACAAAAAAACCACCGCTACCAGCGGTGGTTTGTTTGCCGGATCAAGAGCT
ACCAACTCTTTTTCCGAAGGTAACTGGCTTCAGCAGAGCGCAGATACCAAATACTGTCCTTCTAGTGTAGCCGTAGTTAGGCCACCACTTCAAGAACTCTGTAGCACCGCC
TACATACCTCGCTCTGCTAATCCTGTTACCAGTGGCTGCTGCCAGTGGCGATAAGTCGTGTCTTACCGGGTTGGACTCAAGACGATAGTTACCGGATAAGGCGCAGCGGTC
GGGCTGAACGGGGGGTTCGTGCACACAGCCCAGCTTGGAGCGAACGACCTACACCGAACTGAGATACCTACAGCGTGAGCTATGAGAAAGCGCCACGCTTCCCGAAGGGAG
AAAGGCGGACAGGTATCCGGTAAGCGGCAGGGTCGGAACAGGAGAGCGCACGAGGGAGCTTCCAGGGGGAAACGCCTGGTATCTTTATAGTCCTGTCGGGTTTCGCCACCT
CTGACTTGAGCGTCGATTTTTGTGATGCTCGTCAGGGGGGCGGAGCCTATGGAAAAACGCCAGCAACGCGGCCTTTTTACGGTTCCTGGCCTTTTGCTGGCCTTTTGCTCA
CATGTTCTTTCCTGCGTTATCCCCTGATTCTGTGGATAACCGTATTACCGCCTTTGAGTGAGCTGATACCGCTCGCCGCAGCCGAACGACCGAGCGCAGCGAGTCAGTGAG
CGAGGAAGCGGAAGAGCGCCTGATGCGGTATTTTCTCCTTACGCATCTGTGCGGTATTTCACACCGCATATATGGTGCACTCTCAGTACAATCTGCTCTGATGCCGCATAG
TTAAGCCAGTATACACTCCGCTATCGCTACGTGACTGGGTCATGGCTGCGCCCCGACACCCGCCAACACCCGCTGACGCGCCCTGACGGGCTTGTCTGCTCCCGGCATCCG
CTTACAGACAAGCTGTGACCGTCTCCGGGAGCTGCATGTGTCAGAGGTTTTCACCGTCATCACCGAAACGCGCGAGGCAGCTGCGGTAAAGCTCATCAGCGTGGTCGTGAA
GCGATTCACAGATGTCTGCCTGTTCATCCGCGTCCAGCTCGTTGAGTTTCTCCAGAAGCGTTAATGTCTGGCTTCTGATAAAGCGGGCCATGTTAAGGGCGGTTTTTTCCT
GTTTGGTCACTGATGCCTCCGTGTAAGGGGGATTTCTGTTCATGGGGGTAATGATACCGATGAAACGAGAGAGGATGCTCACGATACGGGTTACTGATGATGAACATGCCC
GGTTACTGGAACGTTGTGAGGGTAAACAACTGGCGGTATGGATGCGGCGGGACCAGAGAAAAATCACTCAGGGTCAATGCCAGCGCTTCGTTAATACAGATGTAGGTGTTC
CACAGGGTAGCCAGCAGCATCCTGCGATGCAGATCCGGAACATAATGGTGCAGGGCGCTGACTTCCGCGTTTCCAGACTTTACGAAACACGGAAACCGAAGACCATTCATG
TTGTTGCTCAGGTCGCAGACGTTTTGCAGCAGCAGTCGCTTCACGTTCGCTCGCGTATCGGTGATTCATTCTGCTAACCAGTAAGGCAACCCCGCCAGCCTAGCCGGGTCC
TCAACGACAGGAGCACGATCATGCTAGTCATGCCCCGCGCCCACCGGAAGGAGCTGACTGGGTTGAAGGCTCTCAAGGGCATCGGTCGAGATCCCGGTGCCTAATGAGTGA
GCTAACTTACATTAATTGCGTTGCGCTCACTGCCCGCTTTCCAGTCGGGAAACCTGTCGTGCCAGCTGCATTAATGAATCGGCCAACGCGCGGGGAGAGGCGGTTTGCGTA
TTGGGCGCCAGGGTGGTTTTTCTTTTCACCAGTGAGACGGGCAACAGCTGATTGCCCTTCACCGCCTGGCCCTGAGAGAGTTGCAGCAAGCGGTCCACGCTGGTTTGCCCC
AGCAGGCGAAAATCCTGTTTGATGGTGGTTAACGGCGGGATATAACATGAGCTGTCTTCGGTATCGTCGTATCCCACTACCGAGATGTCCGCACCAACGCGCAGCCCGGAC
TCGGTAATGGCGCGCATTGCGCCCAGCGCCATCTGATCGTTGGCAACCAGCATCGCAGTGGGAACGATGCCCTCATTCAGCATTTGCATGGTTTGTTGAAAACCGGACATG
GCACTCCAGTCGCCTTCCCGTTCCGCTATCGGCTGAATTTGATTGCGAGTGAGATATTTATGCCAGCCAGCCAGACGCAGACGCGCCGAGACAGAACTTAATGGGCCCGCT
AACAGCGCGATTTGCTGGTGACCCAATGCGACCAGATGCTCCACGCCCAGTCGCGTACCGTCTTCATGGGAGAAAATAATACTGTTGATGGGTGTCTGGTCAGAGACATCA
AGAAATAACGCCGGAACATTAGTGCAGGCAGCTTCCACAGCAATGGCATCCTGGTCATCCAGCGGATAGTTAATGATCAGCCCACTGACGCGTTGCGCGAGAAGATTGTGC
ACCGCCGCTTTACAGGCTTCGACGCCGCTTCGTTCTACCATCGACACCACCACGCTGGCACCCAGTTGATCGGCGCGAGATTTAATCGCCGCGACAATTTGCGACGGCGCG
TGCAGGGCCAGACTGGAGGTGGCAACGCCAATCAGCAACGACTGTTTGCCCGCCAGTTGTTGTGCCACGCGGTTGGGAATGTAATTCAGCTCCGCCATCGCCGCTTCCACT
TTTTCCCGCGTTTTCGCAGAAACGTGGCTGGCCTGGTTCACCACGCGGGAAACGGTCTGATAAGAGACACCGGCATACTCTGCGACATCGTATAACGTTACTGGTTTCACA
TTCACCACCCTGAATTGACTCTCTTCCGGGCGCTATCATGCCATACCGCGAAAGGTTTTGCGCCATTCGATGGTGTCCGGGATCTCGACGCTCTCCCTTATGCGACTCCTG
CATTAGGAAGCAGCCCAGTAGTAGGTTGAGGCCGTTGAGCACCGCCGCCGCAAGGAATGGTGCATGCAAGGAGATGGCGCCCAACAGTCCCCCGGCCACGGGGCCTGCCAC
CATACCCACGCCGAAACAAGCGCTCATGAGCCCGAAGTGGCGAGCCCGATCTTCCCCATCGGTGATGTCGGCGATATAGGCGCCAGCAACCGCACCTGTGGCGCCGGTGAT
GCCGGCCACGATGCGTCCGG

Figure S38: Co-expression plasmid map and sequence. (A) Plasmid map of parent expression vector for freyrasin (B) Nucleotide sequence for entire plasmid. (Point mutations relevant to variants are indicated in **Table S2**).

Supporting References:

(1) Hudson, G. A.; Burkhart, B. J.; DiCaprio, A. J.; Schwalen, C. J.; Kille, B.; Pogorelov, T. V.; Mitchell, D. A. Bioinformatic Mapping of Radical S-Adenosylmethionine-Dependent Ribosomally Synthesized and Post-Translationally Modified Peptides Identifies New Cα, Cβ, and Cγ-Linked Thioether-Containing Peptides. *J. Am. Chem. Soc.* **2019**, 141, 8228–8238.
(2) Jang, S.; Imlay, J. A. Hydrogen Peroxide Inactivates the Escherichia Coli Isc Iron-Sulphur Assembly System, and OxyR Induces the Suf System to Compensate. *Mol. Microbiol.* **2010**, *78*, 1448–1467.
(3) Hidalgo, E.; Bollinger, J. M.; Bradley, T. M.; Walsh, C. T.; Demple, B. Binuclear [2Fe-2S] Clusters in the Escherichia Coli SoxR Protein and Role of the Metal Centers in Transcription. *J. Biol. Chem.* **1995**, *270*, 20908–20914.
(4) Brumby, P. E.; Miller, R. W.; Massey, V. The Content and Possible Catalytic Significance of Labile Sulfide in Some Metalloflavoproteins. *J. Biol. Chem.* **1965**, *240*, 2222–2228.
(5) Nakai, T.; Ito, H.; Kobayashi, K.; Takahashi, Y.; Hori, H.; Tsubaki, M.; Tanizawa, K.; Okajima, T. The Radical S-Adenosyl-L-Methionine Enzyme QhpD Catalyzes Sequential Formation of Intra-Protein Sulfur-to-Methylene Carbon Thioether Bonds. *J. Biol. Chem.* **2015**, *290*, 11144–11166.
(6) Grove, T. L.; Himes, P. M.; Hwang, S.; Yumerefendi, H.; Bonanno, J. B.; Kuhlman, B.; Almo, S. C.; Bowers, A. A. Structural Insights into Thioether Bond Formation in the Biosynthesis of Sactipeptides. *J. Am. Chem. Soc.* **2017**, *139*, 11734–11744.
(7) Söding, J.; Biegert, A.; Lupas, A. N. The HHpred Interactive Server for Protein Homology Detection and Structure Prediction. *Nucleic Acids Res.* **2005**, *33*, W244–W248.
(8) Mitchell, A. L.; Attwood, T. K.; Babbitt, P. C.; Blum, M.; Bork, P.; Bridge, A.; Brown, S. D.; Chang, H.-Y.; El-Gebali, S.; Fraser, M. I.; Gough, J.; Haft, D. R.; Huang, H.; Letunic, I.; Lopez, R.; Luciani, A.; Madeira, F.; Marchler-Bauer, A.; Mi, H.; Natale, D. A.; Necci, M.; Nuka, G.; Orengo, C.; Pandurangan, A. P.; Paysan-Sillitoe, I.; Sutton, G. G.; Thanki, N.; Thomas, P. D.; Tosatto, S. C. E.; Yong, S. Y.; Finn, R. D. InterPro in 2019: Improving Coverage, Classification and Access to Protein Sequence Annotations. *Nucleic Acids Res.* **2019**, *47*, D351–D360.